IRE Transactions on AUDIO

VOLUME AU-3 JULY-AUGUST, 1955 NUMBER 4

editorial	PGA Comes of Age	*Winston E. Kock*	Page 87
news	PGA Award Recipients		Page 88
	Tapescript Committee Activities		Page 89
	PGA Chapter Activities		Page 89
	PGA Committee Membership		Page 90
technical papers	A Multi-Loop, Self-Balancing Power Amplifier	*J. Ross Macdonald*	Page 92
	Properties of Junction Transistors	*R. J. Kircher*	Page 107
	Low Distortion Operation of Some Miniature Dual Triodes	*Julius Z. Knapp*	Page 125
biographies	Authors in this Issue		Page 133

PUBLISHED BY THE

Professional Group on Audio

IRE PROFESSIONAL GROUP ON AUDIO

The Professional Group on Audio is an organization, within the framework of the IRE, of members with principal professional interest in Audio Technology. All members of the IRE are eligible for membership in the Group and will receive all Group publications upon payment of an annual assessment of $2.00.

IRE TRANSACTIONS on AUDIO

Published by the Institute of Radio Engineers, Inc., for the Professional Group on Audio at 1 East 79th Street, New York 21, New York. Responsibility for the contents rests upon the authors, and not upon the IRE, the Group, or its members. Individual copies available for sale to IRE-PGA members at $1.15; to IRE members at $1.75; and to nonmembers at $3.45.

WINSTON E. KOCK

PGA Comes of Age

As the first of the IRE Professional Groups to enter its fifth year, the PGA now stands a strong, mature organization with many of the pitfalls of early growth behind it. The IRE TRANSACTIONS ON AUDIO has become a topflight journal, with letterpress format and photographic reproduction equal in quality to the IRE PROCEEDINGS. With 2,500 members receiving the TRANSACTIONS, its circulation and reading audience should satisfy even the most illustrious authors in this field.

PGA participation in the general spring IRE Convention program in New York has become an established procedure and includes invited sessions featuring well-known scientists in the audio field, and technical sessions at which the latest developments are reported. This year the plan is to extend activity to include a fall program at the National Electronics Conference in Chicago. Interest in audio is further fostered by programs sponsored by a growing number of PGA chapters, the latest in San Francisco.

Perhaps the most certain mark of maturity is the newly established series of PGA awards. PGA financial structure recently has shown itself to be sufficiently strong to take the step of rewarding, each year, deserving authors for their meritorious contributions. These awards, described more fully elsewhere in this issue, are three in number, and in addition to a suitable certificate, include the amount of $100 or $200, as the case may be. Their purpose is intended not only to honor the authors, but to enhance the prestige of the IRE TRANSACTIONS ON AUDIO as a publication medium in which outstanding authors will be encouraged to publish their contributions.

All PGA members have an obligation to encourage young engineers and scientists to enter the audio profession to carry on the high standards of which America now can be justly proud. It is believed that such obligation can be met, at least in part, by maintaining a strong IRE, with its sections and student chapters, and particularly a strong PGA, with active chapters in larger cities throughout the country.

—WINSTON E. KOCK, *Chairman*

PGA Chapter News

PGA AWARD RECIPIENTS

THE IRE-PGA Administrative Committee recently approved an awards plan as described on page 21 of the March-April 1955 issue of the IRE TRANSACTIONS on AUDIO. The titles and amounts of these awards have since been decided upon as: PGA Award—$100; PGA Senior Award—$100; PGA Achievement Award—$200.

This year's recipient of the PGA Achievement Award was Benjamin B. Bauer who has published many papers on audio and has contributed unstintingly in developing the PGA's present state of maturity. Since 1948 he has been Vice-President of Shure Brothers, Inc., where he began in 1936. Mr. Bauer is a graduate of Pratt Institute, and holds the E.E. degree from the University of Cincinnati. He is a Fellow of both the Acoustical Society of America and the Audio Engineering Society. At present he is an Associate Editor of the *Journal of the Acoustical Society of America*.

In accepting the Achievement Award, Mr. Bauer said:

"I am honored to have been selected as the first recipient of the IRE-PGA Achievement Award, and I accept this award with the realization that the job of the Awards Committee was an extremely difficult one in making the selection. Many others have contributed importantly through scientific, literary, and organizational efforts and how is one to measure with accuracy the contributions of one man against those of another? Fortunately, there will be future PGA Achievement Awards, and I trust that whatever inequity might have been created by making the initial choice in my favor will be amended in due course of time.

"Those of us who have served the PGA in various ways—as members of committees, as officers, or as participants in technical sessions—have found it to be a stimulating and rewarding experience. I especially treasure the friendships and the comradeship developed in this association as one of the important values beyond the measure of any conventional yardstick. In a very real sense I can say that the Professional Group on Audio has done much more for me than I have done for it.

"I would like to prevail upon all the IRE members interested in Audio to join the Group and to participate in its work: You too will find it stimulating and rewarding. Young members, and especially students, should weigh this matter carefully. The PGA is interested in encouraging young men to become skilled in Audio technology, as witnessed by the early adoption of its policy to admit student members into the PGA, and the recent creation of the PGA Award for members under 30 years of age. Unfortunately, not enough young engineers are entering this field. Acoustics can hardly hold its own in attracting young men against the competition of atomic energy, computers, solid state devices and other disciplines which lately have become the subject of spectacular publicity. One of the important tasks confronting the PGA, in my opinion, is expansion of its activities among students for the purpose of encouragement and motivation of those with adequate mental and emotional equipment to enter the world of sound.

"Weighing both of these factors, Mr. Chairman, it became evident to me that it would be most satisfying if I were permitted to turn my award to some purpose connected with the work of the PGA among Student Members. Therefore, I am asking you to accept the proceeds of this award as my contribution to the PGA, with the recommendation that it be used for the above purpose in any manner agreeable to the Administrative Committee and to the IRE. I suggest that a suitable way is the creation of a fund, which could be augmented from time to time by PGA proper, and used for annual Student Awards, for meritorious papers on subjects connected with Audio technology.

"It has been a pleasure and a privilege to work with you."

Kenneth W. Goff received the PGA Award for his paper, "The Development of a Variable Time Delay," which was presented at the 1953 IRE Convention.

Mr. Goff holds the B.S. degree in electrical engineering from the West Virginia University, and the S.M. and Sc.D. degrees from the Massachusetts Institute of Technology. After graduating from M.I.T. in 1954, he joined the staff of Bolt Beranek and Newman, Inc., continuing his work in acoustic instrumentation.

In accepting the Award, Mr. Goff said:

"I would like to express my sincere appreciation to the Professional Group on Audio for the selection of my paper, "The Development of a Variable Time Delay" for the 1955 award to an author under 30 years of age. I consider this award to represent not only a real honor, but also a challenge to me, and I hope that my future work and publications will live up to the expectations of the Award Committee.

"I understand that this year inaugurates the award as an annual event in the Professional Group on Audio. By making this award a part of their many activities, the PGA exhibits an interest in the contributions that can be made by young people to the growth and development of the field of Audio. The tremendous challenge of the unsolved problems in the field of Audio, together with the opportunities for organization and individual

recognition made possible by the PGA, combine to present a very attractive picture to those of us who are just beginning our work in electrical engineering."

TAPESCRIPT COMMITTEE ACTIVITIES

According to the Chairman, Andrew B. Jacobsen of the Phoenix Laboratory of Motorola, Inc., in Phoenix, Arizona, the use of tapescripts by various IRE organizations has expanded considerably just recently. More than 75 copies, divided rather evenly between student chapters, IRE sections, and Audio chapters, have been distributed since March, 1954. The peak of tapescript activity appears to occur in April, and this year many request for material could not be filled due to lack of additional copies.

The best way to utilize tapescripts for local presentation is to have a moderator, prepare a short discussion of the subject, and then follow this with the tapescript. The moderator should be available and qualified to answer questions that come up. It is of utmost importance that those presenting a tapescript run through the material from a purely mechanical standpoint, to make sure they have both the copies expected and technical equipment to reproduce sound and picture.

Tapescripts are loaned by the IRE-PGA Tapescripts Committee. The only cost is the return postage on the material. Program chairmen should request the tapescript in advance in order to review the material and work up his program in accordance with it.

Technical standards for tapescripts are: Sound on $7\frac{1}{2}$" per second, $\frac{1}{4}$" tape, full track on 7" reels. The slides are 2"×2" cardboard mounts, double 35mm. Some of the papers have $3\frac{1}{4}$"×4" slides. These are used in a few cases where only one copy is available.

The Tapescript Committee recorded all of the audio sessions at the March 1955 IRE National Convention. This material has been previewed for possible tapescript use and it is expected that several tapescripts will be available from this source. Those who may be interested in using it should contact the Chairman of the Tapescripts Committee for titles and availability.

The following tapescripts are available:

Phonograph Reproduction, B. B. Bauer, Shure Brothers, Inc. Grooves and needles, fidelity and efficiency, pickup arms, and recording-reproducing characteristics are some of the subjects discussed in this one-hour recorded paper.

An Experimental Co-Channel Television Booster Station Using Crossed Polarization, John H. DeWitt, Jr., WSM, Nashville, Tenn. The special receiving and transmitting antennas and equipment developed to improve fringe and reception by co-channel booster methods are discussed. A report on an experimental installation at Lawrenceburg, Tenn. is given.

Method for Time or Frequency Compression-Expansion of Speech, Grant Fairbanks, W. L. Everitt, and R. P. Jaeger, University of Illinois.

Magnetic Recording, Marvin Camras, Armour Research Foundation, Illinois Institute of Technology. Discusses fundamentals of wire and tapes; heads; bias, circuits; equalization; present problems; and future developments. Thirty minutes.

Push-Pull Single Ended Audio Amplifier, Arnold Peterson and D. B. Sinclair, General Radio Company. A convention paper presented by Dr. Peterson, Twenty-five minutes; $3\frac{1}{4}\times4$ slides.

Sound Survey Meter, Arnold Peterson, General Radio Company. A convention paper, twenty minutes, $3\frac{1}{4}\times4$ slides.

Microphones for High Intensity and High Frequencies, John K. Hilliard, Altec Lansing Company. A convention paper; twenty minutes, $3\frac{1}{4}\times4$ slides.

The Ideo-Synchronizer, J. M. Henry and E. R. Moore, Boston Bell. A humorous satire on technical writings, specifications, and engineering. Good for mixed audience. Twelve minutes.

How Much Distortion Can You Hear, Officers of Cincinnati Chapter IRE-PGA. A special tape recording (with commentary) of signals in randomized paired comparisons, containing various measured amounts of harmonic and inter-modulation distortion to be played over a low-distortion reproducing system. A sample test form and typical data will be provided. Approximately 30 minutes.

PGA CHAPTER ACTIVITIES

Boston, Massachusetts

On April 14, John S. Boyers of the National Company presented a paper, "The Past, Present, and Future of Magnetic Recording."

Cincinnati, Ohio

The limitations imposed on the audio reproduction system by the various components used was demonstrated at a "How Many Dollars Can You Hear?" meeting staged by H. F. Gladstein on April 26. Loudspeakers, power amplifier, and phonograph pickups with suitable preamplifier-compensators were arranged for interchangeable connection. The components used covered a broad price and performance range, the performance not always being in direct proportion to the cost of the equipment.

On May 17 a binaural audio demonstration was presented by Messrs. Haehnle, Kay, and Jenkins. At this meeting classical and non-classical program material was interestingly presented through successive monaural, binaural, and combined binaural channels.

Cleveland, Ohio

At the last meeting of the Spring season, on April 21, R. B. Goldman of Philco Corp. presented the paper, "High-Frequency Electro-Static Speaker." He discussed recent developments in this field, including the use of

push-pull transducers to eliminate nonlinearity inherent in single-ended units.

The officers elected for 1955–56 are: Chairman—E. R. Wagenhals; Vice-Chairman—C. P. Germano; Secretary—J. Golfarb.

The Cleveland Chapter, in cooperation with RCA, Livingston, Audio-Video, Webcor, and others, was instrumental in the preparation of forty stereophonic broadcasts over seven radio and television stations. The winter program as a whole received the AFTRA Award.

Los Angeles, California

John K. Hilliard reports that this year the Wescon Show and IRE Convention will be held in San Francisco on August 24, 25, and 26. The Los Angeles Chapter is in the process of organizing at present and Mr. Hilliard hopes to give a further report later.

Twin Cities, Minnesota

On April 5, F. K. Harvey of Bell Telephone Laboratories presented a paper, "Analog Between Microwaves and Sound Waves." He described arrays of rigid conducting elements that are capable of focusing both microwaves and sound waves, and showed how the principles involved were being used in microwave lens antennas and in a sound diffusing lens for loudspeakers.

Washington, D. C.

The Washington Chapter now has a membership of over 100. The last meeting of the 1955 season was held on April 19. Mr. Arthur Jansen from the Jansen Laboratories of Cambridge, Massachusetts, presented a paper, "A New Electro-Static Loudspeaker."

The officers elected for 1955–56 are: Chairman—Irving Levine; Vice-Chairman—George Sugar; Secretary—Richard Knodle.

1955-56 IRE—PGA COMMITTEE MEMBERSHIP

ADMINISTRATIVE COMMITTEE

W. E. Kock, *Choirman*
(until 3/31/58)
Bell Telephone Labs., Inc.
Murray Hill, N. J.

M. S. Corrington, *Vice-Chairman*
(until 3/31/58)
RCA Victor Division
Camden, N. J.

B. B. Bauer, *Secretary-Treasurer*
Shure Brothers, Inc.
225 West Huron Street
Chicago, Ill.

MEMBERS

Walter Goodale (until 3/31/57)
Bell Telephone Labs., Inc.
Murray Hill, N. J.

J. A. Kessler (until 3/31/56)
Acoustics Laboratory
Mass. Inst. of Tech.
Cambridge 39, Mass.

Daniel W. Martin (until 3/31/57)
Baldwin Piano Company
1801 Gilbert Avenue
Cincinnati 2, Ohio

Andrew B. Jacobsen (until 3/31/58)
Motorola, Incorporated
3102 North 56th Street
Phoenix, Ariz.

Frank G. Lennert (until 3/31/56)
Ampex Electric Corporation
935 Charter Street
Redwood City, Calif.

Arnold Peterson (until 3/31/56)
General Radio Co.
275 Massachusetts Ave.
Cambridge 39, Mass.

Frank Slaymaker (until 3/31/57)
Stromberg-Carlson Co.
1225 Clifford Avenue
Rochester 21, N. Y.

AWARDS COMMITTEE

Daniel W. Martin, *Chairman*
Baldwin Piano Company
1801 Gilbert Avenue
Cincinnati 2, Ohio

MEMBERS

A. B. Bereskin
University of Cincinnati
Cincinnati 21, Ohio

J. A. Kessler
Acoustics Lab., Mass. Inst. Tech.
Cambridge, Mass.

Hugh Knowles
Industrial Research Products, Inc.
9400 Belmont Ave., Franklin Pk., Ill.

EDITORIAL COMMITTEE

Prof. Alexander B. Bereskin, *Chairman*
Electrical Engineering Dept.
University of Cincinnati
Cincinnati, Ohio

MEMBERS

B. B. Bauer (until 1957)
Shure Brothers, Inc.
225 West Huron Street
Chicago 10, Ill.

J. A. Kessler (until 1956)
Acoustics Lab., Mass. Inst. Tech.
Cambridge, Mass.

J. Ross Macdonald (until 1958)
Texas Instruments, Inc.
6000 Lemmon Avenue
Dallas 9, Texas

Daniel W. Martin (until 1956)
Baldwin Piano Company
1801 Gilbert Avenue
Cincinnati 2, Ohio

Albert Preisman (until 1957)
Capitol Radio Engineering Inst.
16th and Park Road, N. W.
Washington 10, D. C.

NOMINATING COMMITTEE

Marvin Camras, *Chairman*
Armour Research Foundation
35 West 33rd Street
Chicago 16, Ill.

MEMBERS

B. B. Bauer
Shure Brothers, Inc.
225 West Huron Street
Chicago 10, Ill.

Murlan S. Corrington
RCA Victor Division
Camden, N. J.

Arnold Peterson
General Radio Company
275 Massachusetts Ave.
Cambridge 39, Mass.

Frank Slaymaker
Stromberg-Carlson Co.
1225 Clifford Ave.
Rochester 21, N. Y.

PROGRAM COMMITTEE

Philip B. Williams, *Chairman*
Jensen Manufacturing Company
6601 South Laramie Avenue
Chicago 38, Ill.

REGIONAL PROGRAM CHAIRMEN

East Coast
Michel Copel
156 Olive Street
Huntington, Long Island
New York

Midwest
Herbert H. Heller
Bird Electronic Corporation
1800 East 38th Street
Cleveland 14, Ohio

West Coast
John K. Hilliard
Altec Lansing Corporation
9356 Santa Monica Boulevard
Beverly Hills, Calif.

BYLAWS COMMITTEE

M. S. Corrington, *Chairman*
RCA Victor Division
Camden, N. J.

CHAPTERS COMMITTEE

R. E. Troxel, *Chairman*
Shure Brothers, Inc.
225 West Huron Street
Chicago 10, Ill.

FINANCE COMMITTEE

B. B. Bauer, *Chairman*
Shure Brothers, Inc.
225 West Huron Street
Chicago 10, Ill.

TAPESCRIPTS COMMITTEE

Andrew B. Jacobsen, *Chairman*
Motorola, Incorporated
3102 N. 56th St., Phoenix, Ariz.

TELLERS COMMITTEE

Marvin Camras, *Chairman*
Armour Research Foundation
35 West 33rd St.
Chicago 16, Ill.

WAYS & MEANS COMMITTEE

Michel Copel, *Chairman*
156 Olive St.
Huntington, N. Y.

A Multi-Loop, Self-Balancing Power Amplifier*

J. R. MACDONALD†

Summary—A multi-loop, push-pull power amplifier of exceptional characteristics is described. It employs special circuits to maintain accurate push-pull signal balance throughout and to hold the static or steady-state dc cathode currents of the output tubes equal. A pair of 807 tubes are used in class AB_2 to yield 65w average power output at less than 1 per cent intermodulation distortion with 30 db of over-all negative feedback. Using local positive voltage feedback in addition, the intermodulation distortion is 0.1 per cent at 45w and less than 0.2 per cent at 60w. At full power output, the —0.5 db points occur at 19.8 cps and 22.4 kcps. The rise time of the amplifier is 3 μs, and its transient response and recovery from overload approach the ideal. There are no peaks at the ends of the response curve. A noise level of —106 db referred to 60w output is attained. Extensive measurements of amplifier characteristics under various conditions are described.

INTRODUCTION

A POWER AMPLIFIER is generally required to supply maximum power output at minimum distortion over a specified bandwidth. In addition, cost and complexity must be relatively low for most commercial applications, and power efficiency should be as high as practical. The design and construction of the present amplifier was begun four years ago. By designing the amplifier without stringent cost and complexity restrictions, it was felt that out-of-the-ordinary characteristics might be attained. Some of the means of achieving such characteristics might then be directly applicable to simpler, lower-cost amplifiers; all of them, it was felt, might yield a useful perspective on what kind of a system could be achieved for a given level of cost and complexity.

The amplifier has been operating in substantially its present form for two years. Since it is a developmental unit, it is not really completed, however. Its complexity and corresponding flexibility are such that it is expected that its present form will not remain completely static.

The initial design goals of the amplifier were as follows:

1. Push-pull operation with a pair of automatically balanced output triodes operating with fixed or automatic bias.
2. A gain of the order of 30 db, and a frequency response variable by no more than one db between 10 and 30,000 cps.
3. A distortion not exceeding 1 per cent intermodulation at maximum power output.
4. Excellent transient response at all levels.
5. "Undistorted" maximum power output over substantially the entire working frequency range.
6. Negligible noise and hum.

All the above goals have been met or exceeded by the amplifier in its present state.

* Manuscript received, February 21, 1955. Paper delivered at Dallas IRE Section, October 21, 1954; Houston IRE Section, March 22, 1955.

† Texas Instruments, Inc., Dallas, Tex.

SIMPLIFIED BLOCK DIAGRAM

Since the complete amplifier is rather complex, it will prove convenient to analyze it section by section. The simplified block diagram of Fig. 1 shows that there are three gain stages. The first stage is a special phase inverter with automatic dynamic balancing. This stage is followed by cathode followers included to extend the frequency response and to serve as low-impedance sources for feedback voltage. Next come the only capacitors in the direct signal path. The gain stage A_2 also incorporates dynamic self-balancing. It is direct-coupled to special drivers of about two ohms output impedance which are directly connected to the output tube grids. Over-all feedback which is an adjustable combination of negative voltage and positive or negative current signals is taken from the secondary of the output transformer and returned to the input. The feedback circuit is shown symbolically in Fig. 1. Since 30 db or more of over-all negative voltage feedback is used from output to input, the frequency response requirements of the various stages and of the output transformer are rather stringent.

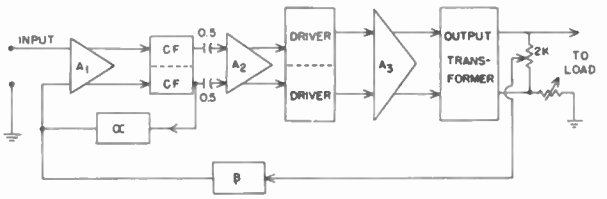

Fig. 1—Simplified block diagram of the amplifier.

PHASE-INVERTER AMPLIFIER STAGE

The initial design of the amplifier employed a cross-coupled phase inverter[1] with the over-all negative feedback returned to one input grid and the other used for the input signal. Although this circuit was found to be satisfactory from inversion and frequency response standpoints, its in-phase response was too high for good operation with a large amount of feedback. When feedback and input signals are applied separately to the two grids of such a circuit, it is desirable that their amplified difference appear at one output plate and the same signal shifted by 180 degrees appear at the other plate. Such behavior was not found.

When feedback signals representing 20 or 30 db of over-all feedback are employed, the difference between the input and the feedback signals is 10 per cent or less, a small difference compared to the magnitude of the individual signals. If the circuit does not have good in-phase (common-mode) rejection, the two large, practically equal, input signals may produce in-phase output signals as large or larger than their out-of-phase

[1] J. N. van Scoyoc, "A cross-coupled input and phase-inverter circuit," *Radio News*, vol. 40, p. 6; November, 1948.

amplified differences. The output will then consist of only two large, almost equal in-phase signals. The difference between them will represent the desired signal. This matter of in-phase response of push-pull amplifiers has been discussed in some detail by Offner.[2] The effectiveness of the over-all feedback is, of course, entirely dependent upon the precision with which this difference between input and feedback signals is produced, and the presence of a common-mode signal in the phase inverter output definitely degrades performance.

In a push-pull amplifier with appreciable common-mode signal at the outputs of the phase inverter, the in-phase signal may be amplified by the rest of the amplifier and at the worst can cause strong overloading of succeeding stages. Such signals, of course, will not pass through to the secondary of the output transformer because of its in-phase discrimination.[3] Even if the in-phase signals do not cause overloading, however, their presence anywhere in the amplifier can produce increased intermodulation. Therefore, it is of considerable importance to ensure that the outputs of any phase-inverter used with appreciable feedback contain only a negligible amount of common-mode signal.

The unconventional self-balancing phase inverter finally used in the amplifier is shown in Fig. 2. The basic idea for a simplified version of this circuit was suggested to the author by L. C. Labarthe.[4] Since then, it has been found that the same idea has been developed independently.[5] The function of the circuit is as follows. A signal at either input grid produces an amplified output across the cathode of the corresponding cathode follower. The two 100K resistors between the cathode follower outputs are closely matched. If the cathode follower outputs are accurately 180 degrees out-of-phase, no signal will appear at the junction of the resistors. Should any in-phase components be present at the cathode follower outputs, however, an error signal will appear at this junction. This error signal then passes through the cathode-follower voltage divider V_a to the constant-resistance tube V_b.[6] The error signal then finally appears at the plate of V_b where it drives the cathodes of the input double triode in such phase that the error signal at the outputs is itself greatly reduced. It will be seen that the circuit itself therefore uses a kind of negative feedback which has been called "active-error feedback."[7]

Experimentally, it is found that the out-of-phase to in-phase amplification ratio of this circuit is between 10^3 and 10^4. At all frequencies from zero up to more than 500kc, the output signals remain closely 180 degrees out-of-phase, and even with 30 or 40 db feedback no common mode output signal is detectable. Such behavior is largely independent of tube ageing effects since it is produced by feedback. In addition, another important advantage of the circuit is that all even harmonics act like in-phase signals and are themselves automatically greatly reduced in amplitude at output.

The cathode-follower outputs of the phase-inverter-amplifier drive two feedback loops and the succeeding stage. We shall defer until later discussion of all such feedback loops to the input. The 0.5 μf isolating capacitors have about 400v across them. They are, therefore, low-leakage oil-filled units. Their capacity to ground is minimized by mounting them on porcelain stand-off insulators inside the amplifier chassis. The shielding shown in Fig. 2 requires some comment. It will be seen that the shields are also driven by the cathode followers. Such driven shields can do much to extend the very-high-frequency response of the input amplifier stage by reducing its output capacity to ground. The capacity from each plate circuit to its shield is of no importance because the shield is driven by a voltage practically identical to that at the plate.[8] The decoupling networks for the -380v and $+400$v supplies shown in Fig. 2 are not necessary to eliminate motor boating; it was found that their addition markedly decreased the intermodulation distortion of this stage.

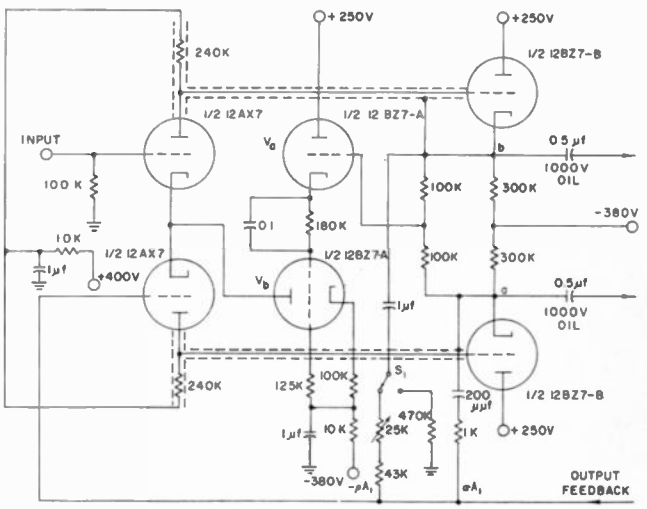

Fig. 2—Phase-inverter amplifier stage circuit.

Driver Amplifier Stage

The driver amplifier stage of Fig. 3 (next page) is quite similar to the input phase-inverter-amplifier stage except it operates with a push-pull input. A dynamic balancing circuit is here employed to accomplish three objectives: stabilization of the average value of the bias voltages applied to the grids of the output tubes; production of stable, accurately push-pull driver signal voltages; and elimination of even-order harmonic distortion in the driver outputs.

[2] F. F. Offner, "Balanced amplifiers," Proc. IRE, vol. 35, pp. 306–310; March, 1947.

[3] The in-phase discrimination may be poor at high frequencies because of capacitative coupling between primary and secondary unless electrostatic shielding is employed.

[4] Private communication in 1951.

[5] E. M. I. Laboratories, "Balanced output amplifiers of highly stable and accurate balance," *Electronic Engrg.*, vol. 18, p. 189; June, 1946.

[6] G. E. Valley and H. Wallman, "Vacuum Tube Amplifiers," McGraw-Hill Book Co., Inc., New York, N. Y., p. 432; 1948.

[7] J. R. Macdonald, "Active-error feedback and its application to a specific driver circuit," Proc. IRE, vol. 43, pp. 808–813; July, 1955.

[8] J. R. Macdonald, "An ac cathode-follower circuit of very high input impedance," *Rev. Sci. Instr.*, vol. 25, pp. 144–147; February, 1954.

The present amplifier incorporates a direct-coupled static balance circuit which acts to keep the average values of the cathode currents of the two output tubes equal. This function, which will be discussed in detail later, is accomplished by means of a closed feedback loop which holds the grid bias voltages of the output tubes to the correct values. The dc and ultra-low-frequency bias correction signals are injected into the grids of the driver amplifiers through frequency-sensitive networks at the points marked *SB* in Fig. 3. These signals are themselves accurately push-pull; therefore, after amplification in the driver amplifier stage, they have no effect on the average value of the output tube grid bias voltages.

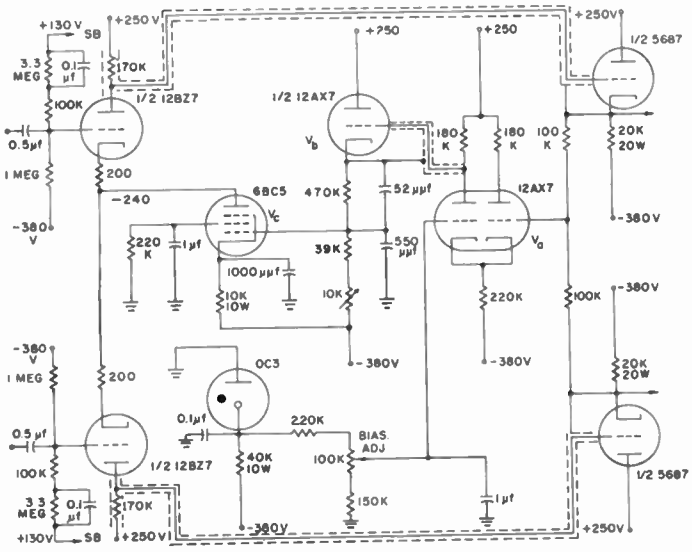

Fig. 3—Driver-amplifier stage circuit.

Part of the modified, direct-coupled, cathode-follower driver circuits are shown in Fig. 3. These special circuits will be discussed in the next section. Their outputs, at the cathodes of the 5687 tube of Fig. 3, go directly to the output tube grids and also, through the matched 100K resistors, to the dynamic balance circuit. The signal at the junction of these resistors is proportional to the average value of the two bias voltages and contains any signal arising from deviations of the driver signals from exact push-pull conditions and any even-order harmonic components of these signals. The average value of the grid bias voltages is stabilized by means of the differential amplifier tube V_a. The voltage on one grid is the desired average bias, adjusted and stabilized by means of the 100K potentiometer and the OC3 regulator tube. The amplified difference between this dc voltage and the actual average bias on the other grid of V_a appears at its plate. This signal, together with other amplified error components, then goes through the frequency-compensated, cathode-follower voltage divider V_b and thence to the constant-current amplifier pentode V_c. The 1,000 $\mu\mu$f cathode bypass capacitor of V_c acts to increase the stage gain at high frequencies. The amplified error signal then passes through the driver amplifier tube halves and the drivers where it re-enters the feedback loop in such phase that it is greatly reduced in magnitude. This direct-coupled feedback loop comprises three gain stages and has a very high gain which is not greatly reduced until the megacycle frequency range is entered. It is, therefore, very effective in eliminating in-phase error components in the driver signals and keeping the average value of the two bias voltages fixed. The shielding shown functions like that of Fig. 2 to improve the high-frequency response of the main amplifier and of the dynamic balance loop. Since the driver amplifier tubes and the series pentode V_c of Fig. 3 operate with their cathodes appreciably below ground potential, they are supplied from a separate, negatively biased heater supply to avoid exceeding their heater-cathode voltage ratings.

The bias adjustment allows the average bias to be adjusted from about -34v to -58v. When reasonably well-matched output tubes are employed, and the static balance circuit used to hold their steady-state cathode currents equal, it is found that their bias voltages differ by less than 0.5v at most over the entire bias and signal voltage ranges.

In an earlier version of the amplifier, the dynamic balance circuit of Fig. 3 was differently arranged so that a signal equal to the sum of a constant voltage and a voltage proportional to the average value of the cathode currents of the output tubes could be used to determine the average value of the output-tube bias voltages. This is a form of automatic bias control so arranged that the magnitude of the average bias is increased as the signal, and so the output cathode currents, increase. This modification was eliminated later after it was found unnecessary from an output distortion viewpoint. Such elimination is desirable, when possible, since the transient reponse of such a circuit is not good. Such automatic bias control should operate as rapidly as possible for good transient response; yet, by definition, its response time must be appreciably slower than the lowest signal frequency of the amplifier. These conditions are somewhat conflicting.

In concluding this section, the desirability of making the signals to the output tube grids accurately push-pull should be emphasized. Accurate push-pull balance at this point can reduce nonlinear distortion in the output tubes appreciably. A number of recent amplifiers[9–11] use balanced push-pull feedback taken from the output tube plates to improve push-pull balance. As Good[12] has pointed out, since the output transformer

[9] B. B. Drisko and R. D. Darrell, "40-db feedback audio amplifier," *Electronics*, vol. 25, pp. 130–132; March, 1952.
[10] J. M. Diamond, "Multiple-feedback audio amplifier," *Electronics*, vol. 26, pp. 148–149; November, 1953.
[11] J. Z. Knapp, "The linear standard amplifier," *Radio and TV News*, vol. 51, pp. 43–46, 113–114; May, 1954.
[12] E. F. Good (Letter), *Electronics*, vol. 25, pp. 420–422; October 1952.

functions as an auto-transformer, the plate voltages will be essentially balanced whether the grid voltages are or not. Thus, such plate feedback is necessarily ineffective in producing output-tube current balance and in reducing unbalance distortion. Although a feedback loop might be arranged to keep the instantaneous output tube plate currents accurately push-pull, the present dynamic balance circuit acting on the grids accomplishes practically the same result (provided the output-tube transconductances are fairly well-matched) and does not reduce amplifier gain as does the ineffective balanced plate feedback.

Augmented Cathode-Follower Driver

In order to obtain maximum power output, it is desirable to drive the grids of the output stage into the grid current region. Such a procedure can increase the output power greatly, but it is eventually limited when the grids are driven positive to the diode line, where they lose control of the plate current. To drive 807 grids to the diode line, peak positive grid currents of the order of 100 to 200 milliamperes are required from the preceding driver stage. In addition, since the input impedance of an output tube grid is a nonlinear function of the grid voltage in the positive grid region, the above large driving currents must be supplied from a source of very low internal impedance to avoid grid-voltage distortion during this part of each cycle.

The output impedance of the driver amplifier of Fig. 3 is quite high; therefore, an impedance converter is required between this stage and the output stage. Since an ordinary direct-coupled cathode-follower driver still has too high an output impedance to be ideal for

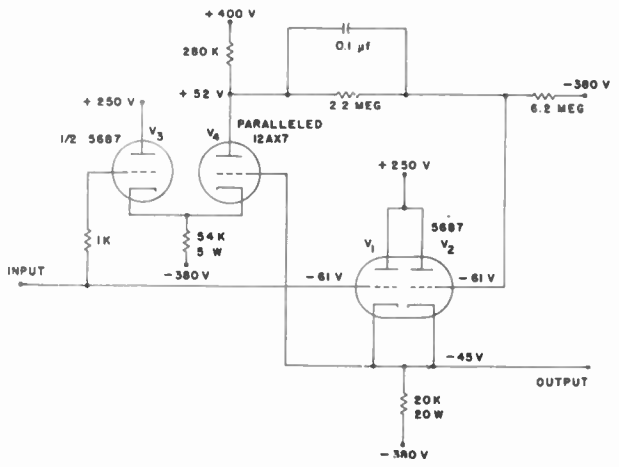

Fig. 4—Direct-coupled driver circuit, one push-pull side only.

such a purpose, the special circuit shown in Fig. 4 has been developed as a virtually distortionless driver for this application. This circuit has been discussed in detail and its operating characteristics compared with other kinds of drivers elsewhere.[7] Therefore, here it need only be mentioned that, like the dynamic balance circuit of Fig. 1, it makes use of active error feedback. The difference between the input to cathode-follower V_1 and its output is amplified in V_4, then injected back into V_2 in such phase as to reduce this difference or error. The circuit is direct-coupled, will operate up into the megacycle range, and has an output impedance of about five ohms. Two such circuits are used in the present amplifier, one for each push-pull side. Since the dynamic balance feedback of Fig. 3 is taken from the outputs of these augmented cathode-follower drivers, this further feedback serves to reduce the actual small-signal output impedances of the drivers to between 2 and 3 ohms. For large positive output currents, the impedance is even further reduced to about one ohm by the increase of the g_m's of the output 5687 tubes. The driver can supply peak positive currents of several hundred milliamperes at 50 to 100v rms per side with little or no distortion.[7]

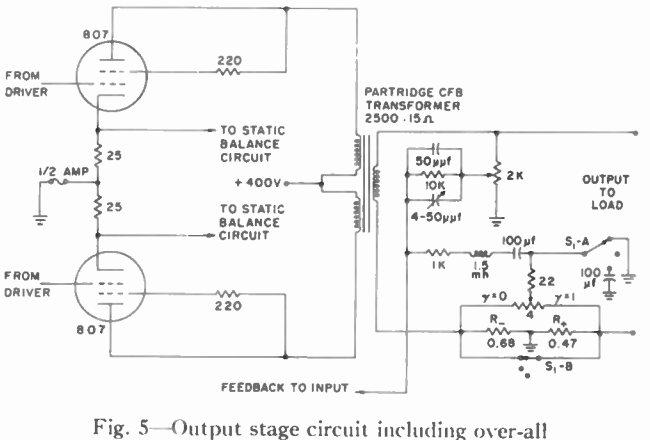

Fig. 5—Output stage circuit including over-all feedback arrangements.

Output Stage

The output stage shown in Fig. 5 uses triode-connected 807 tubes and a high-quality, commercial grain-oriented output transformer rated at 60w between 30 and 30,000 cps with less than 1 per cent total harmonic distortion without feedback. This transformer has eight secondary sections and offers a wide selection of output impedances, but only the 15-ohm output is used in the present design. It has very low leakage inductance between the primary half-sections and hence is suitable for class B operation. Since the variable bias control of Fig. 3 allows the bias on the 807 grids to be adjusted over a wide range, the class of operation of the output tubes may lie anywhere from A_2 to B_2.

For longest tube life and minimum distortion, it is desirable that the quiescent plate currents of the output tubes be equal. Unequal currents tend to saturate the output transformer, with consequent degradation of low-frequency response. The 25-ohm, matched resistors in the cathodes of the 807's produce voltage drops proportional to these currents which are used in an

automatic balancing circuit that ensures current equality to within a few tenths of a milliampere throughout the tube life. This "static" balancing circuit which acts to adjust the bias on the 807 grids will be discussed in the next section.

Feedback to the input of the amplifier from the output transformer secondary is adjustable in magnitude and may consist of a combination of negative voltage feedback and positive or negative current feedback. The sign and magnitude of the latter are determined by the 4-ohm potentiometer. In the upper position, switch S_1 removes all current feedback, while in the lowest position it bypasses the 22-ohm resistor with a large electrolytic capacitor, thus making the current feedback effective only at low frequencies.

The addition of variable current feedback as above allows the output impedance of the amplifier to be varied over a rather wide range of positive and negative values.

Combined feedback for output impedance control seems to have first been suggested by Mayer in 1939[13] and has recently been applied in some commercial high-fidelity amplifiers. One of the recent articles on this technique[14] makes the claim that with the internal impedance of the amplifier made sufficiently negative to cancel out the electrical resistance of a loudspeaker load at low frequencies (damping factor -1), better damping of the speaker is obtained than with a very low, positive amplifier output impedance (damping factor 20 to 40). In addition, it is claimed that better transient response is achieved, the low-frequency response of the speaker is extended, its power handling capacity increased, and its low frequency distortion reduced.

The author has been using another amplifier with combined feedback of the above type for more than four years. It can be set to give a damping factor of -1. It must be admitted, however, that with the author's speaker system no significant improvement in low-frequency speaker response can be detected aurally on varying the amplifier impedance from a small positive value to the negative value which gives a damping factor of almost -1. Since the low-frequency speaker of this horn-loaded system has a fundamental resonance of 23.5 cps and negligible harmonic distortion at 30 cps, it may be that there is little or no room for improvement in its low-frequency response. With speakers that are more poorly loaded acoustically, it is possible that some or all of the above claims of the virtues of a damping factor of -1 may be justified to some degree; for this reason, and because of the simplicity of the addition to the circuit, combined feedback was also incorporated in the present amplifier. It is certainly true that an amplifier with a negative output resistance at low frequencies tapering off to a small positive resistance at higher frequencies will tend to increase the bass response of a speaker used with it. It can thus be used to partly or completely correct for a drooping low-frequency speaker characteristic. Such correction must be applied with moderation, however, to avoid driving the speaker outside its range of linear operation at low frequencies.

It will have been noted that three separate supply voltages have been used in the preceding circuits. For this developmental amplifier, all three voltages were derived from electronically stabilized supplies. Since the bias voltage is separately stabilized within the amplifier with a voltage regulator tube, the $+250$v and -380v supplies do not actually require stabilization. On the other hand, it is very useful to supply the $+400$v for the output stages from a regulated source. Not only is the output voltage of such a supply easily adjusted, but the low output impedance (0.1-ohm in the author's supply) eliminates the possibility of motorboating and helps to improve the linearity of the output stage for large output signals.

Static Balance Loop

The requirements for automatic static balancing need careful consideration. If the balancing action is too slow in response, the output currents may remain unbalanced for appreciable periods. On the other hand, if the response is too rapid, the "static" balancing circuit will tend to destroy the normal low-frequency push-pull response of the amplifier since it will try to balance out the push-pull signal. It is thus evident that the static balancing circuit is not really static, and a happy-medium response time for this circuit must be selected. In this connection, it might be mentioned that Kiebert[15] has given a low-gain static balancing circuit which apparently has very little higher frequency amplitude discrimination. It may, therefore, be expected to degrade appreciably the low-frequency response of amplifiers with which it is used.

The static balancing circuit used in the present amplifier is shown in Fig. 6 (opposite). Unbalance signals from output tube cathodes first pass through a long-constant RC network necessary to roll off frequency response of static-balance loop above a few tenths of a cycle and to reduce the amplitude of signal-frequency components to such a level that they never overload the static balance amplifier of Fig. 6. The static-balance circuit is itself a self-balancing, direct-coupled differential amplifier which responds only to the difference between the dc (or ultra-low frequency) levels of the output-tube cathode voltages. The 12BZ7 tube of Fig. 6 is connected in a dynamic balancing circuit similar to those of Figs. 2 and 3. It ensures that the

[13] H. F. Mayer, "Control of the effective internal impedance of amplifiers by means of feedback," Proc. IRE, vol. 27, pp. 213–217; March, 1939.

[14] C. A. Wilkins, "Variable damping factor control," *Audio*, vol. 38, pp. 31–33, 66; September, 1954.

[15] M. V. Kiebert, Jr., "System design factors for audio amplifiers," 1954 IRE Convention Record, Part 6, "Audio and Ultrasonics," pp. 25–40 (Fig. 11).

output of the differential amplifier will be truly push-pull and, in addition, gives stabilization of the absolute average output level.

The gain of the static-balance differential amplifier is further stabilized by 20 db of balanced negative feedback from the output back to the input cathodes. The differential gain with feedback is 200 from one input to one output. The common-mode response of this amplifier is exceedingly low. Thus, common changes in the absolute levels of the signals at the two cathodes have no appreciable effect on the output level. The outputs are returned through frequency-sensitive networks to the grids of the driver-amplifier tubes of Fig. 3. It thus becomes clear that the driver-amplifier tubes, the drivers, the output tubes, and the static-balance differential amplifier form a direct-coupled, closed feedback loop of very high gain at ultra-low frequencies.

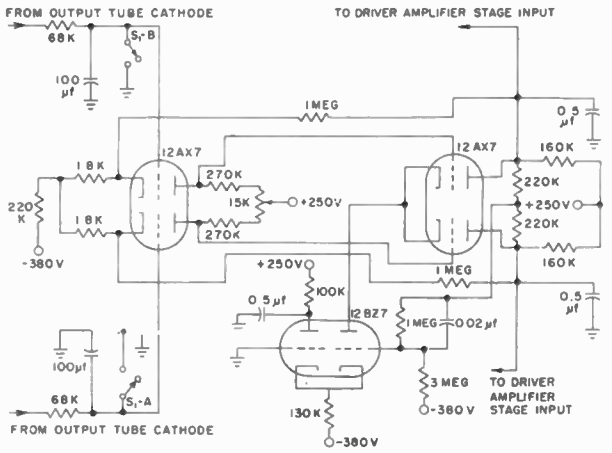

Fig. 6—Static balancing circuit.

With the loop open, measurements show that the limiting low-frequency open-circuit loop gain is 48 db. This is essentially the factor by which differences in the quiescent cathode currents of the output tubes will be reduced by the differential feedback after closing the loop. The switch S_1 of Fig. 6 affords a convenient means of opening the loop without affecting normal operation of the main amplifier. This switch may be used during initial adjustment of the amplifier. After the amplifier has warmed up, the loop is opened and the output tube cathode currents are adjusted to equality by means of the 15K potentiometer in the plate circuit of the first 12AX7 of the static balance circuit. Then after the loop is closed, the feedback has less work to do and can therefore hold the two currents closer to equality. In practice, such an adjustment need never be repeated during the life of the output tubes. It is of interest to note that if one of the output tubes is removed during normal amplifier operation (simulating total failure), the static balance loop entirely cuts off the cathode current of the remaining tube. Unlike an ordinary push-pull circuit which gives a degraded output under such conditions, the present amplifier then produces no output—a much more positive indication of the desirability of tube replacement.

The frequency response of the above feedback loop requires further consideration. The usual Nyquist stability criterion applies to the loop and minimally requires that the upper-frequency open-circuit response of the loop be reduced from 48 db gain to unity gain before a phase-shift of 180 degrees is reached. This condition restricts the rate at which the upper-frequency response can fall with increasing frequency to an absolute maximum of 12 db/octave near unity gain. Unfortunately, this is not yet the whole story. The ordinary amplifier signal is injected into the loop through the 0.5 μf coupling capacitors of Fig. 2. If the present differential-balance feedback loop is temporarily considered to be the main feedback loop, then the signal injected at the 0.5 μf capacitors represents an additional feedback voltage derived from a subsidiary feedback loop which includes the output transformer.[16] At the point of addition of the main and subsidiary feedback voltages, the main feedback voltage (from the balancing loop) decreases with increasing frequency while that from the subsidiary loop increases from zero at zero frequency to a final limiting value at relatively low frequencies. The crossover point of the two voltages essentially determines both the lowest frequency of operation of the amplifier and the response time of the static balancing circuit. In addition, the presence of this subsidiary feedback loop restricts the allowable rate of fall of the main loop response to about 6 db/octave near the crossover region. A faster roll-off causes instability when both loops are closed. This restriction, in turn, requires that the roll-off of the static balance loop begin at ultra-low frequencies so that the crossover point occurs at a low enough frequency that the low-frequency response of the amplifier itself is not appreciably reduced. The 6.8-second RC time constant at the input of the differential amplifier of Fig. 6 yields such a roll-off.

The time constant formed by each 0.5 μf coupling capacitor at the input to the driver-amplifier tubes and the large resistors between each of these grids and the output of the differential balancing amplifier can cause a further roll-off with increasing frequency at a 6 db/octave rate. Since a maximum of only about 6 db/octave in the loop response can be tolerated, this time constant could be used and that at the input of the differential amplifier eliminated were it not for the fact that then the normal amplifier signal appearing at the output-tube cathodes would grossly overdrive the differential amplifier. Because the long input time constant is therefore necessary, the roll-off arising from the 0.5 μf coupling capacitors must be removed. This is accomplished by shunting the 3.3 megohms resistors with the 0.1 μf capacitors shown and isolating the com-

[16] Subsidiary feedback has been discussed by W. T. Duerdoth, "Some considerations in the design of negative-feedback amplifiers," *Proc. IEE*, part III, vol. 97, pp. 138–158; May, 1950.

bination with 100K resistors. The additional 0.5 μf capacitors at the outputs of the differential amplifier become effective in further rolling off the response only at sufficiently high frequencies (greater than 5 cps) that the gain of the balancing loop is less than unity. This fairly complicated tailoring of the asymptotic gain characteristic of the balancing loop results in complete stability, sufficiently fast response time, and excellent low frequency response of the main amplifier itself. The balancing loop has no effect on the transient behavior of the main amplifier so long as signal components below about 1 cps are avoided.

We have now completed discussion of all parts of the main amplifier except feedback. The complete block diagram of Fig. 7 shows all the loops except that for optional positive voltage feedback which will be discussed later. The letters *DB* and *SB* in this diagram stand for dynamic balance and static balance. It will be seen that there are, altogether, ten loops in the amplifier. Only those marked α and β are effective in changing amplifier gain; the others all improve its performance in the various other ways which we have already discussed. Note that the combination of negative voltage and positive or negative current feedback from the output is only symbolically indicated in Fig. 7; the actual circuit employed is given in Fig. 5.

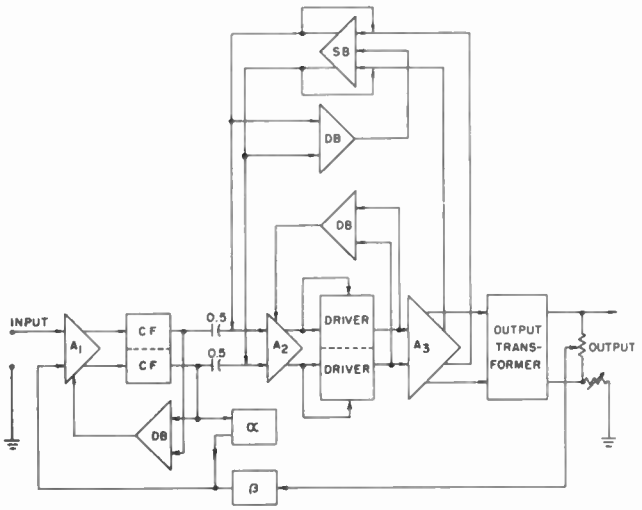

Fig. 7—Complete block diagram of the amplifier.

Feedback Loops to the Input

The main function of feedback in an audio amplifier is to reduce nonlinear distortion. Other desirable results of feedback are a reduction in amplifier output impedance and flattening of the gain-frequency characteristic in the working range. Fig. 8 shows the high frequency gain characteristics of the present amplifier with no over-all feedback at various stages.[17] For easy comparison, all three curves have been normalized to have the same value at low frequencies. The output frequency response is down by 1 db at 38 kc; it is therefore apparent that the response is adequate for audio applications even without feedback. On the other hand, feedback is desirable to reduce the nonlinear distortion of the amplifier, particularly when it is operated in class B.

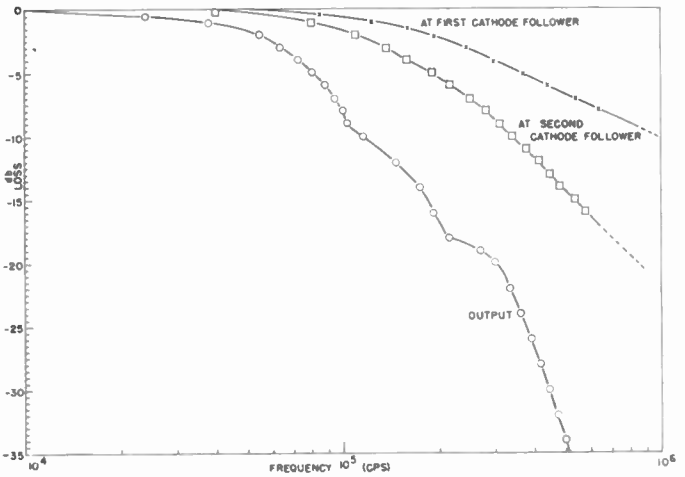

Fig. 8—Gain-frequency characteristics at various points in the amplifier with no over-all feedback.

Feedback is applied in an amplifier in order to make the output signal as close an amplified replica of the input signal as possible. The larger the fraction of the output which is compared with the input, the nearer the desired condition of exact similarity will be approached. It is therefore obvious that any local negative feedback loops within an amplifier which reduce its over-all gain will restrict the amount of output-input negative feedback which may be applied for a given final amplifier gain. For this reason, it is desirable that such local loops be avoided whenever possible so that maximum output-input negative feedback may be employed. Such a system necessarily gives maximum nonlinear distortion reduction. This conclusion has been pointed out before[12,18] but it bears repetition in view of the appearance of recent amplifier articles which stress the advantages of local loops.[10,11] One of these articles,[11] in justification for its point of view, states that, "This approach (the use of output-input feedback) in a multi-stage amplifier, results in a peaked response at both ends of the audio spectrum and a narrow margin of stability." As we shall see, neither of these conclusions is necessarily correct.

For the above reasons, it was decided to use as much over-all negative feedback in the present amplifier as possible, consistent with a final gain of about 30 db. Since the gain of the amplifier with no feedback and with a 15-ohm load was 61 db, some 30 or 31 db of feedback could be applied and still leave sufficient gain. It

[17] Unless otherwise stated, all measurements shown in the figures were taken with an average output tube bias of −45v and with a 15-ohm load resistor. For the frequency response measurements of the present section, the output power level was about 1 watt.

[18] W. B. Bernard (Letters), *Electronics*, vol. 27, pp. 401–404; January, 1954; pp. 372–376; December, 1954.

was first found that using a single feedback resistor shunted with a small capacitor, up to 18 db of over-all negative feedback could be applied before small parasitic oscillations appeared in the output at high power levels. This value is very consistent with the output response curve of Fig. 8.

To ensure stability in a feedback amplifier, it is necessary that the complex feedback factor βG not enclose the point $-1 \not< 0$ on a polar plot. Here G is the complex gain of the amplifier without feedback but loaded with its usual load of 15 ohms. For convenience, we have taken the midfrequency value of βG to be positive real when it represents negative feedback, and shall use the same sign convention for other feedback factors. Further, to eliminate the peaked response at the ends of the audio spectrum mentioned earlier, it is necessary that the absolute value of the gain with feedback G', given by $G/(1+\beta G)$, not exceed its midfrequency value. In addition, it is desirable that even after G' has decreased appreciably from its midfrequency value, there be no secondary rises of G', even though such peaks do not reach the midfrequency value. Exact specification of the form of βG which meets the above requirements is complicated; in practical cases, it is usually only necessary to ensure a wide stability margin such as that produced by restricting the phase angle θ of βG to the range $-90 \text{ degrees} \leqq \theta \leqq +90 \text{ degrees}$, as long as $|\beta G|$ is greater than or equal to unity. This condition requires that the roll-off of βG at either end of the spectrum does not appreciably exceed a rate of 6 db/octave until after $|\beta G|$ is less than unity.

The stability conditions can be met by changing and controlling the frequency response of β, of G, or by a combination of these methods. An additional method is that of subsidiary feedback discussed by Duerdoth.[16] If a negative feedback voltage derived from the output of the first stage is added to βG at the input,[19] the combination can be made to have characteristics yielding excellent stability. If this subsidiary feedback were effective at all frequencies, it would be of the undesirable "local-loop" feedback type already discussed. However, if its magnitude is greatly reduced in the working band of the amplifier and is only greater than unity (referred to the input signal amplitude) beyond either or both ends of the working band, then it will not appreciably affect conditions within the working band. Since the subsidiary feedback voltage is derived after only a single stage of amplification, it will automatically have a high-frequency limiting slope of only 6 db/octave. At very high frequencies, it will decrease less rapidly than βG and will, therefore, eventually dominate the sum of αA_1 and βG. This sum, the over-all feedback voltage, therefore will have the desirable limiting decay rate of 6 db/octave.

[19] We shall use the terms feedback factor (such as βG) and feedback voltage interchangeably for convenience. The actual feedback voltage of an opened loop corresponding, e.g., to βG is βG times the amplifier input voltage.

The combination of over-all and subsidiary feedback gives a final amplifier gain G' of $G'=G/(1+\alpha A_1+\beta G)$. Calculation shows, however, that the factor by which nonlinear distortion arising in the second or third stages is reduced by the combination is not $(1+\alpha A_1+\beta G)$ but $(1+\alpha A_1+\beta G)/(1+\alpha A_1)$ instead. It is therefore particularly desirable to ensure that $|1+\alpha A_1|$ is not appreciably greater than unity within the working band.

The present amplifier makes use of high-frequency subsidiary feedback of the type discussed above to allow 30 db or more of feedback to be used with a wide stability margin. The subsidiary feedback voltage is taken from point a of Fig. 2, passed through the 200 $\mu\mu$f capacitor and 1K resistor shown and added to the over-all feedback. The adding takes place across the series combination of the 1K resistor, 1.5 mh choke, and 100 μf capacitor shown in Fig. 5. The 200 $\mu\mu$f capacitor and 1K resistor in the subsidiary path ensure that the subsidiary feedback factor αA_1 is negligible in the working band.

The main over-all feedback is adjustable by the 2K potentiometer of Fig. 5. It is further reduced about 20 db at low and medium frequencies by the 10K series resistor. The phase angle of the over-all feedback is improved at high frequencies both by the small capacitors in parallel with the 10K resistor and by the 1.5 mh choke. Subsidiary feedback is unnecessary for stabilization of the amplifier at very low frequencies. An adequate stability margin is produced by the 100 μf capacitor of Fig. 5 in series with the 1.5 mh choke. At very low frequencies, it reduces the roll-off rate of βG to an acceptable value near 6 db/octave. It is found that with the present combination of subsidiary and over-all feedback, more than 40 db of over-all negative feedback may be applied in the working band of the amplifier with complete stability.

Results of the above stabilization technique are shown in Figs. 9 and 10 (next page) measured with 30 db of midfrequency negative feedback. Fig. 9 shows G and G' vs frequency plotted on an absolute gain scale. It is seen that the limiting decay rate of G is 24 db/octave. Nevertheless, the amplifier is stable and G' shows no peaks. With feedback, the amplifier is flat to within 1 db from below 5 cps to 72 kcps. Fig. 10 shows how the various feedback voltages add at high frequencies. It also is plotted to show both absolute and relative amplitudes. Measurements were not extended to sufficiently high frequencies to show that the combined characteristic $(\beta G+\alpha A_1)$ has a final limiting slope of 6 db/octave, but such behavior must be finally reached. The curve including the factor $-\rho A_1$ will be discussed later.

The magnitude of the feedback effective in reducing distortion is of interest. Since it is given by the quotient of two complex terms, it cannot be inferred directly from measurements which do not include phase angles. However, up to 50 kc or so, the phase angle of $(1+\alpha A_1$

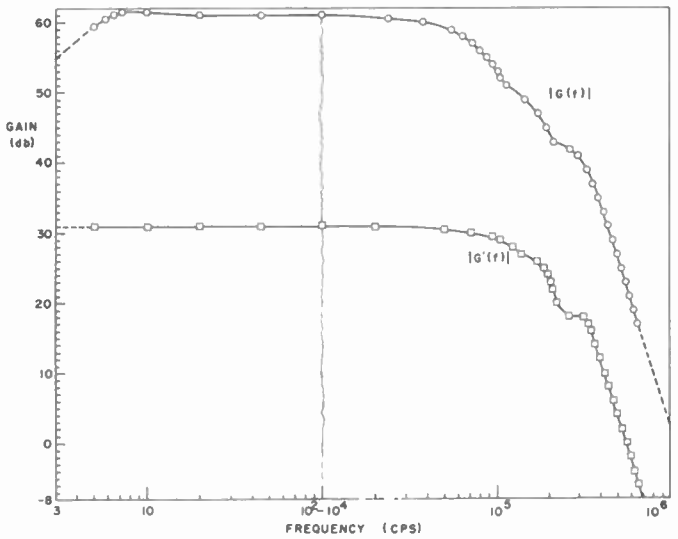

Fig. 9—Loaded amplifier gains $|G|$ (without feedback), and $|G'|$ (with 30 db of over-all feedback) *vs* frequency.

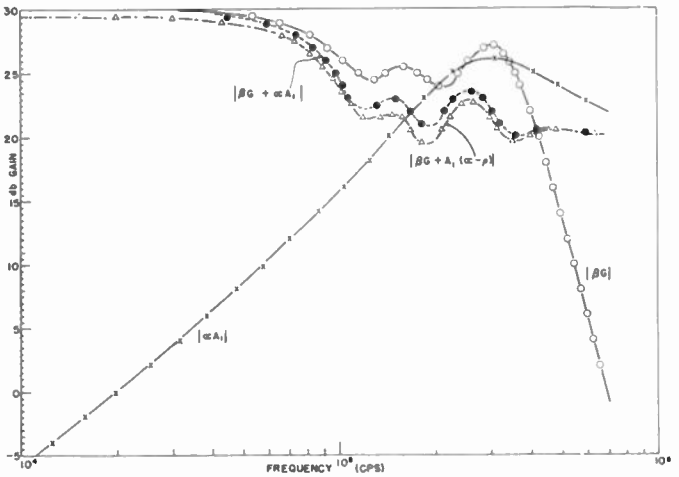

Fig. 10—High-frequency variation of the amplitudes of various feedback factors.

$+\beta G$) is very close to zero. Hence, we need be concerned only with the magnitude of $|1+\alpha A_1|$. Again up to 50kc or more, it is obvious from the curve of $|\alpha A_1|$ of Fig. 9 that the phase angle of αA_1 must be close to 90 degrees. Its magnitude at 20kc is zero db, or unity. Hence $|1+\alpha A_1|$ must be $\sqrt{2}$ at 20kc, or 3 db. Similarly, it is found that this quantity is 1 db at 10.8kc and about 6 db at 35kc. When these factors are subtracted from the midfrequency feedback of 30 db, one obtains the resultant feedback effective in reducing distortion at the given frequency. For example, this so-called harmonic feedback is 27 db at 20kc.

The above results show that the addition of subsidiary feedback has reduced the effective feedback by only an unimportant factor within the working band of the amplifier to 20kc. In order to keep the harmonic feedback nearer 30 db out to frequencies of the order of 70 to 100kc, the low-frequency roll-off of the subsidiary feedback can be made more rapid than the present 6 db/octave. Using a constant-k filter in the subsidiary loop, such a result was indeed obtained. It was found that although it did result in the maintenance of increased negative feedback to much higher frequencies, it also produced an initial peak in the high-frequency square-wave response. More careful control of the characteristics of the two feedback voltages in the neighborhood of their crossover undoubtedly could eliminate this effect, but the extra effort necessary was felt unwarranted for the present amplifier.

The addition of the over-all and subsidiary feedback voltages has been carried out so as to minimize $|1+\alpha A_1|$ in the working band and to produce the best possible high-frequency square-wave response. The small, variable 50 $\mu\mu$f capacitor across the feedback resistor of Fig. 5 is used to adjust for best response. With the best adjustment, 10kc square waves show almost square corners and flat tops and bottoms with at most only a trace of greatly damped high-frequency parasitic oscillation on the tops. The rise time of the amplifier with 30 db over-all feedback and subsidiary feedback is 3 μs between 10 and 90 per cent amplitude points. The recovery of the amplifier from overloads also occurs in approximately this interval. As the output square-wave amplitude is increased, the only change in square-wave shape is a slight sharpening of the upper left corner. More than 0.01 μf of external capacitance can be connected in parallel with the load without any appreciable effect on the shape of square waves. Further, square-wave shape and amplitude are virtually independent of load from open circuit to a very heavy load. It was also found, using a direct-coupled oscilloscope, that the tilt of low-frequency square waves of any amplitude within the amplifier capabilities was 7, 9, and 10 per cent respectively, at 30, 20, and 17 cps. These results are consistent with a measured phase angle of -8 degrees at 5 cps.

Although the above over-all harmonic feedback of almost 30 db over the entire working band of the amplifier results in exceptionally low output distortion, it was of interest to see if this distortion could not be reduced even further by the addition of a positive voltage feedback loop around the first stage in the manner of Miller.[20] If the positive feedback factor is denoted by $-\rho A_1$, then the combination of over-all, subsidiary and positive feedback results in an output gain reduction factor of $N=(1+\beta G+\alpha A_1-\rho A_1)$. Nonlinear distortion in the first stage is also reduced by this factor. Distortion produced in the rest of the amplifier is reduced by the factor $M=N/[1+A_1(\alpha-\rho)]$, however. In the working band, the factor αA_1, may be neglected. We see that if we make ρA_1 equal to unity in the working band, the factor $[1+A_1(\alpha-\rho)]$ approaches zero and M becomes very large. Thus, a small amount of positive feedback

[20] J. M. Miller, Jr., "Combining positive and negative feedback," *Electronics*, vol. 23, pp. 106–109; March, 1950.

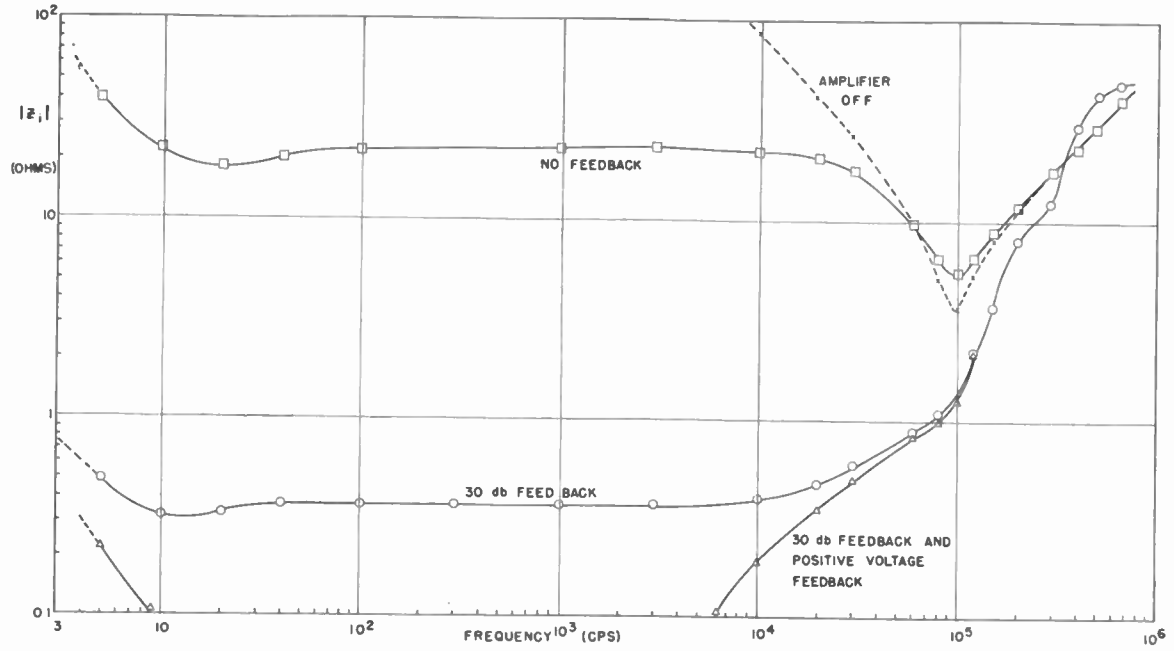

Fig. 11—Frequency dependence of the magnitude of amplifier internal impedance for various feedback conditions.

can reduce the output distortion of the amplifier by a large factor. Although the distortion of the first stage is increased slightly by the addition of positive feedback, it can be made so low initially that a small increase is immaterial. Since the maximum distortion of usual amplifiers occurs in the last stages, it is particularly helpful that the distortion reduction of positive feedback is most effective for these stages.

Positive feedback is taken from the point *b* of Fig. 2. It passes through a 1 μf capacitor, an on-off switch S_1, and the 25K potentiometer and 43K fixed resistor. It is then added to the other feedback voltages and is applied to the lower input grid of Fig. 2. The 470K resistor connected to the off position of S_1 is used to keep the coupling capacitor charged so that switching transients are eliminated on turning the positive feedback on and off. The combination of positive and negative feedback will be stable so long as the composite feedback factor $[\beta G+A_1(\alpha-\rho)]$ does not enclose the $-1\not<0$ point on a polar plot. It is therefore necessary that the positive feedback decrease more rapidly outside the working band (or change over to negative feedback) than does the negative feedback. In the present amplifier, stability is ensured at the low-frequency end by the 1 μf capacitor which reduces ρA_1 to zero at zero frequency and shifts its phase by 90 degrees. At the same time, this capacitor is still sufficiently large that positive feedback is fully effective down to the lowest signal frequencies to be passed by the amplifier. At the high-frequency end, the progressive increase in αA_1, a negative feedback factor, soon cancels out the positive feedback beyond the working band. The 25K potentiometer shown is used to adjust ρA_1 to exactly unity for midfrequencies. Fig. 10 shows the effect of $-\rho A_1$ on the composite feedback factor

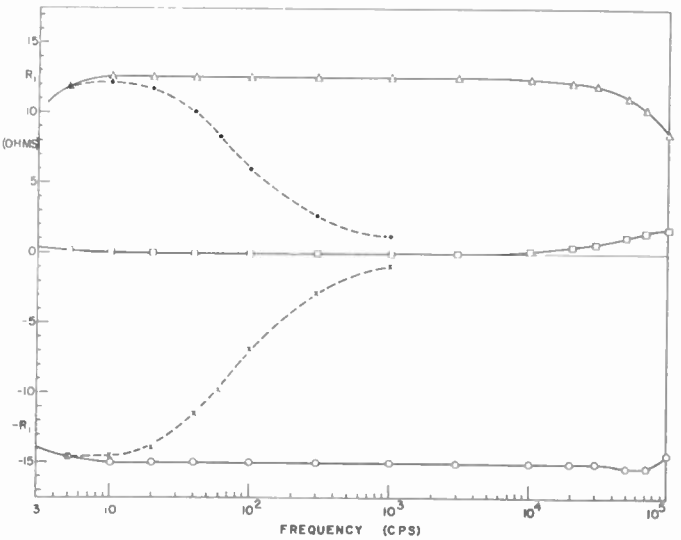

Fig. 12—Frequency dependence of amplifier internal resistance with 30 db over-all negative voltage feedback and positive or negative output current feedback.

at high frequencies. For this measurement, ρA_1 was adjusted to unity in the working band.

An excellent indirect measure of the effectiveness of feedback in reducing nonlinear distortion is afforded by its reduction of amplifier output impedance. We shall discuss distortion results later; meanwhile, Figs. 11 and 12 present measurements of amplifier internal impedance $|Z_i|$ for various feedback conditions. These measurements were made with a bias of -41 volts. With no feedback, the magnitude of this impedance is about 22 ohms over the working band, slightly larger than the nominal value of 15 ohms. The internal impedance of the amplifier without feedback increases with the magnitude of the bias value used. The above

internal impedance value indicates that an output-transformer primary winding impedance somewhat greater than the 2,500 ohms employed might be desirable for best operation. However, the present transformer impedance ratio, 2,500 to 15, is close to the ideal in terms of low distortion and maximum output power, as we shall see in the next section. The application of 30 db of over-all feedback reduces the impedance to about 0.36 ohms over most of the working band. Finally, the application of positive voltage feedback reduces $|Z_i|$ to a value no greater than 0.01 ohms over much of the working band. Phase measurements indicated that Z_i was essentially resistive over this band.

Fig. 12 shows the output impedance with no positive voltage feedback but with negative or positive current feedback from the output, in addition to the usual 30 db over-all negative voltage feedback. The top and bottom curves are the results for the two extreme settings of the 4-ohm potentiometer of Fig. 5. They are actually presented as positive and negative resistances since phase measurements indicated that the output impedance was almost entirely resistive over the greater part of the band shown. The two dotted curves are similar to the outer curves, but the 100 μf bypass capacitor of Fig. 5 is used to limit the output current feedback to low frequencies. The dotted curves are not extended beyond 10^3 cps since the output impedance has appreciable phase shift, arising from the bypass capacitor, above 10^2 cps for either positive or negative current feedback. The output impedance for either condition eventually reaches the small positive value shown in Fig. 11 for negative voltage feedback alone. The center curve is the output impedance or resistance measured with the 4-ohm potentiometer adjusted for zero impedance in the midfrequency range. We see that it remains essentially zero over a wide frequency band.

It is of interest to give the expression for Z_i when negative voltage feedback βG, negative subsidiary feedback αA_1, positive voltage feedback $-\rho A_1$, and positive or negative output current feedback may all be present simultaneously. Neglecting loading of the various feedback paths by each other (a good approximation in the working band), we find for the present amplifier

$$Z_i = \frac{[1 + A_1(\alpha - \rho)][Z_0 + R_+ + R_-] + [1 + (Z_0 + R_+ + R_-)/Z_L][(\gamma + \beta)R_+ + (\gamma - 1)R_-]G}{1 + A_1(\alpha - \rho) + [1 + (Z_0 + R_+ + R_-)/Z_L]\beta G}.$$

where Z_0 is the amplifier internal impedance without feedback. The current feedback resistors R_+ and R_- are indicated in Fig. 5; the quantity γ specifies the setting of the 4-ohm potentiometer of this figure. We see from the above formula that Z_i may be made zero by adjustment of either the positive voltage feedback factor $-\rho A_1$ alone, by positive current feedback alone, or with both types simultaneously. The foregoing measurements are in general agreement with the above formula, and the amplifier is completely stable with any combination of the above types of feedback.

When output current feedback in addition to over-all negative voltage feedback is employed, the effective gain with feedback, G', is given by

$$G' = \frac{G}{1 + A_1(\alpha - \rho) + [\beta + (\gamma + \beta)R_+/Z_L + (\gamma - 1)R_-/Z_L]G}.$$

Thus, negative current feedback decreases G' and positive current feedback increases it. We have dealt throughout thus far with the loaded gains G and G' since it is these gains which are important in practice. For some purposes, it may be desirable to express the above formulas in terms of the unloaded gain K of the amplifier. The relation between G and K is $G = K/[1 + (Z_0 + R_+ + R_-)/Z_L]$. If usual amount of feedback employed in present amplifier were expressed as the difference between, unloaded gain with and without feedback, rather than between loaded gains, instead of 30 db it would amount to between 36 and 38 db.

Power and Distortion Measurements

Fig. 13 (opposite) shows maximum "undistorted" power output of amplifier vs frequency. This measurement was made using a Ballantine type 310A ac voltmeter to indicate rms load voltage and an oscilloscope to indicate distortion. Power output of amplifier was increased at a given frequency until distortion could be observed on the oscilloscope then reduced to the point where distortion was no longer detectable. From comparison with intermodulation measurements it is estimated that the actual distortion level of the "undistorted" power output shown in this graph probably does not exceed 2 per cent intermodulation and is less over much of the range.

It may be calculated from Fig. 13 that the maximum output power is flat within minus 0.5 db from 19.8 cps to 22.4 kcps. The roll-off on the low-frequency end has a slope of about 6 db/octave and is due to the inability of the output tubes to supply sufficient magnetizing current to the transformer at very low frequencies. On the other hand, the high-frequency roll-off has an initial slope of 3 db/octave which probably arises from the inability of the output tubes to supply the necessary charging currents for the transformer primary winding capacitance. In the midfrequency region, the maximum power is limited by the diode line of the output tubes, the point where the grids lose control of the plate currents of the output tubes. The drivers of the amplifier can drive the grids considerably more positive than the diode line with negligible dis-

tortion, but as soon as the diode line is reached and exceeded, the output signal begins to show symmetrical peak clipping.

The point where the diode line is intersected by the load line of the output tubes is determined (for fixed load resistance) by the plate supply voltage available. Increasing this voltage increases the maximum power available before diode-line clipping becomes apparent; it was found that with an E_{bb} voltage of the order of 500v, more than 80w of output power could be obtained before such clipping occurred. Such supply voltages of course exceed the rating of the 807 output tubes.

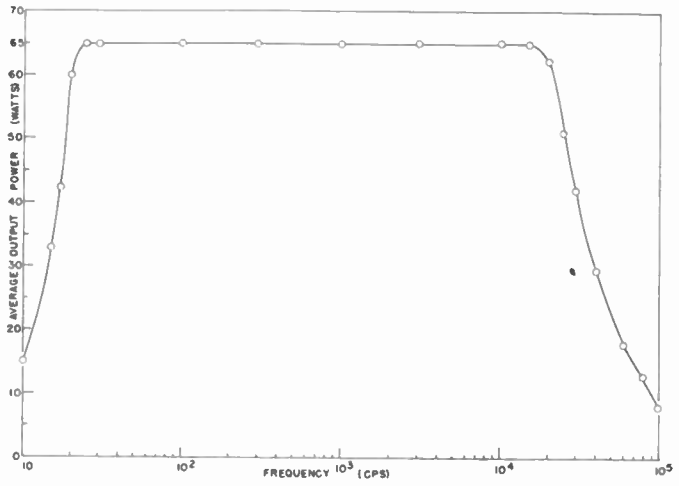

Fig. 13—Maximum "undistorted" average power output *vs* frequency.

In audio applications, very high power peaks occur quite seldom; yet when they do, it is desirable for the amplifier to handle them without clipping if possible. It occurred to the author that since an electronically stabilized power supply for E_{bb} was used with the present amplifier, it might be possible to drive the power supply with the driver signal from the amplifier in such a way that above 60w or 65w output, the value of E_{bb} increased automatically with the signal level from its usual value of +400v to whatever higher value was required to eliminate diode-line clipping at the given signal level. Such an increase in E_{bb} is eventually limited by the quiescent voltage drop initially available across the series current tube of the electronically stabilized supply; an increase of more than 100v above +400v could be obtained in the author's supply. The above idea was investigated in a preliminary fashion using biased diode rectifiers to derive a power-supply driving signal from the amplifier drivers only when the driver signal exceeded the value which resulted in an output power of about 65w. Quite an appreciable increase in unclipped output power could be obtained in this fashion. The circuit is not described in detail here since output powers exceeding 65w were not really necessary for the author's application. It should be noted that although the maximum rated value of dc plate voltage is exceeded in the above scheme, this may be expected to occur only rarely in most applications. This operation of the output tubes, therefore, should be satisfactory in terms of tube life. Should greater output power than 65w be required without the use of the above scheme, tubes with higher ratings such as the new type 6550 could be used in place of the 807's. It may be mentioned that this idea of driving a regulated power supply may be used with a driving signal from the amplifier output arranged to reduce the supply voltage after a given delay in order to allow the amplifier to produce full power for short periods but only reduced power for longer periods, thus avoiding loudspeaker damage. A similar idea is presently employed in a high-power commercial amplifier. The use of a fast-acting fuse in the speaker line will achieve the same result in a much simpler fashion, however.

Triode-connected, push-pull 807 tubes operated in class AB_1 are rated at only 15w output power. Operating them in class AB_2, B_2, or A_2 as in the present amplifier results in more than a fourfold increase in output power. We see that the following quoted statements are therefore unjustified: "Obtaining 15 to 20 watts output without using four output tubes and a large power supply, and without operating the power tubes beyond ratings, rules out a triode output stage;"[10]—"push-pull class *A* 6L6's will give 18.5 watts output with two-percent harmonic distortion. There are no receiving-type triodes which will match this performance . . . there is no longer any reason to use triodes in amplifiers up to 100 watts."[18] Although the 807 is not strictly a receiving-type triode, comparable results to those of the present amplifier could be obtained using 6L6's, 5881's, or 6AR6's triode-connected, operated within their ratings up to 30 to 50w output. For the same or greater power output, the advantages of triodes over beam-power tetrodes and pentodes in terms of lower output impedance and less higher-order harmonic distortion scarcely have to be mentioned.[21]

The noise level of the present amplifier with no input signal and the usual 30 db of over-all feedback was found with the Ballantine 310A meter to be about 95 db below 60w output. In spite of the use of ac-operated tube heaters with one side grounded and the use of a number of cathode-followers, no hum signal could be distinguished in the output. This output consisted largely of unavoidable radio signals picked up on the measurement leads. When these signals were filtered out at the voltmeter, the residual noise voltage was about 106 db below 60w and was equivalent to an input signal of about 5 μv rms. A single ground buss connected to chassis at input is used in this amplifier.

The power efficiency of the amplifier is of some interest. This efficiency is greatest for class B operation and since, as we shall see later, distortion is acceptably low even for this mode of operation, we shall consider its

[21] F. Langford-Smith, "Radiotron Designer's Handbook," Amalgamated Wireless Valve Co., Ltd., Sydney, Australia, 4th ed., pp. 546 *et seq.*; 1952.

efficiency only. At full-power output of 65w, the total plate input is about 125w, slightly exceeding the rated value of 100w. The plate efficiency is, therefore, about 52 per cent and the plate dissipation per tube 30w, the maximum ICAS rating. The total efficiency should include the grid power input, but this is difficult to estimate because of the peaked shape of the grid current waveform. Measurement indicates that it certainly does not exceed 8w at maximum power output; thus, it does not change the efficiency very much. Of the order of 2w of power are dissipated in the winding resistances of the transformer (about 90 ohms total referred to full primary) at full-power output. About another half-watt is dissipated in the 2K feedback potentiometer across the output.

The above results were obtained with average grid bias of about −55v; the quiescent plate currents under these conditions were 6 milliamperes each, giving a quiescent plate dissipation of 2.4w for each tube. This low value is a good indicator of long tube life; very seldom will the full 65w of power be required from the amplifier under ordinary conditions. About 60w of power can be obtained continuously from the amplifier, however, without even exceeding the CCS ratings of the 807's. By increasing the load resistance seen by the output tubes, the plate efficiency can be appreciably increased if desirable and the distortion reduced; at the same time, however, the maximum available power is reduced.

A considerable amount of nonlinear distortion measurements on the present amplifier has been carried out by various methods. We shall first discuss the results of intermodulation (IM) measurements with the usual SMPE rms sum method.[22] Because of the very low distortion of the amplifier under certain conditions, a commercial intermodulation tester was modified to reduce its own nonlinearity and to improve its filtering and was then accurately calibrated from 30 per cent to 0.04 per cent IM.[23] Intermodulation readings were made on the Ballantine 310A rather than the meter of the test set. In spite of these precautions, the readings obtained in the neighborhood of 0.05 per cent may be slightly high. For the following measurements, output power was found using the General Radio Type 783-A output power meter set to 15 ohms load.

The intermodulation distortion of the amplifier with a bias of −45v and no subsidiary or over-all feedback is presented in Fig. 14 as a function of equivalent single-frequency average output power, This bias value corresponds to class AB operation. Greater distortion over most of the range was observed with class B, less with class A. In all the SMPE IM distortion measurements, essentially equivalent results were obtained using either 60 and 5,600 cps or 60 and 2,500 cps signals mixed so

[22] *Ibid.*, pp. 612–613.
[23] J. R. Macdonald, "The calibration of amplitude modulation meters with a heterodyne signal," PROC. IRE, vol. 42, pp. 1515–1518; October, 1954.

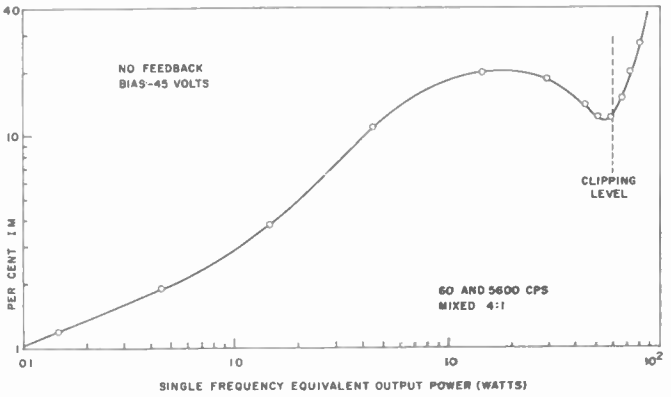

Fig. 14—Percentage intermodulation distortion *vs* output power; no feedback, class AB.

that the 60-cps signal was four times greater than the higher frequency signal.

Figs. 15, 16, and 17 show the IM results for class B, AB, and A with 30 db of over-all feedback and without and with the local positive voltage feedback already discussed. Even without the positive feedback, the amplifier shows an extremely low distortion for all three biases right up to the peak clipping point (about 65w). With positive feedback, the distortion is even smaller. We see that, in general, the larger the distortion obtained without positive feedback, the more effect the positive feedback has. The positive feedback adjustment was unchanged during measurements for a given bias but was adjusted slightly differently for the different biases in order to give minimum distortion over the whole power range for each curve. Positive feedback can do little to reduce distortion once peak clipping commences and the final steep rise of distortion begins.

Some of the pertinent results shown in Figs. 15 through 17 are summarized in Table I which gives the output power at 0.1 and 1 per cent IM distortion for the various bias and feedback conditions. We see that, as expected, class A operation is superior at the lower power levels. At the maximum power levels just before and after peak limiting begins, it is very interesting to note, however, that the −45v bias gives the best result at a given power or distortion level. It was expected that class B operation, with its greater bias, would be superior in this region. Although the differ-

TABLE I

OUTPUT POWER (WATTS) AT TWO INTERMODULATION DISTORTION LEVELS FOR VARIOUS BIAS AND FEEDBACK CONDITIONS

Per cent IM	Bias = −57 v Class B		Bias = −45 v Class AB		Bias = −35 v Class A	
	No Positive Feedback	Positive Feedback	No Positive Feedback	Positive Feedback	No Positive Feedback	Positive Feedback
0.1	—	6	1.5	45	20	33
1.0	0.8, 37 63	65	66	67	62	63

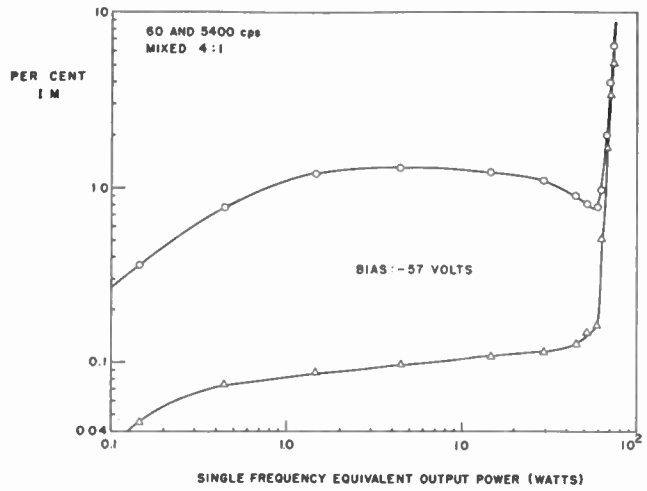

Fig. 15—Percentage intermodulation distortion *vs* output power; 30 db over-all feedback, class B. Lower curve taken with positive voltage feedback.

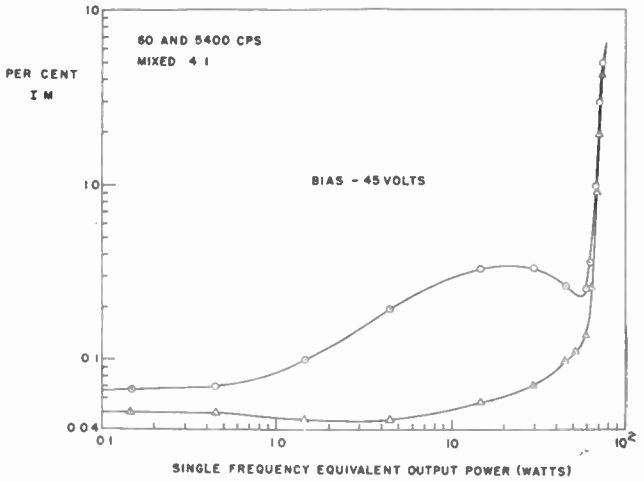

Fig. 16—Percentage intermodulation distortion *vs* output power; 30 db over-all feedback, class AB. Lower curve taken with positive voltage feedback.

ence between the results with −45v and −57v bias is slight in this region, it is still large enough to be significant. Therefore, automatic bias control, which would increase the bias at high signal levels, is undesirable here, and a fixed bias of about −45v gives the maximum power-over-distortion quotient at high levels.

For most practical purposes, the differences between the curves obtained with class B and Class AB operation are only of academic interest, and the amplifier can be operated in class B for minimum quiescent power, maximum plate efficiency, and longest tube life. Even the largest value of IM distortion obtained with class B operation without positive feedback (1.3 per cent) is much too small to be audible. Measurements of the amplifier linearity characteristic (output vs input) with or without positive voltage feedback show no measurable deviations from linearity over the useful dynamic range of the amplifier limited at the low end by its intrinsic noise output of about 2 millimicrowatts and at the high end by diode-line peak clipping.

Several other intermodulation measurements of the above type have been made on the amplifier. In particular, it is found that IM distortion at the driver outputs with output tube loads is less than 1 per cent at a signal level giving maximum power output, when no over-all feedback is employed. Most of the output distortion at all levels thus occurs in the output stage. Measurements of the output distortion as a function of load resistance R_L with 30 db of over-all but no positive feedback, show that it decreases proportional to R_L^{-n} over the range from 5 to 50 ohms with the exponent n slightly greater than unity. An increase in load resistance also increases the plate efficiency of the output stage, but the maximum output power is reduced. A measurement of output power vs load at the 2 per cent IM level showed that maximum power was available with a load of about 10 ohms but the increased power was only slightly greater than that available with the usual 15-ohm load.

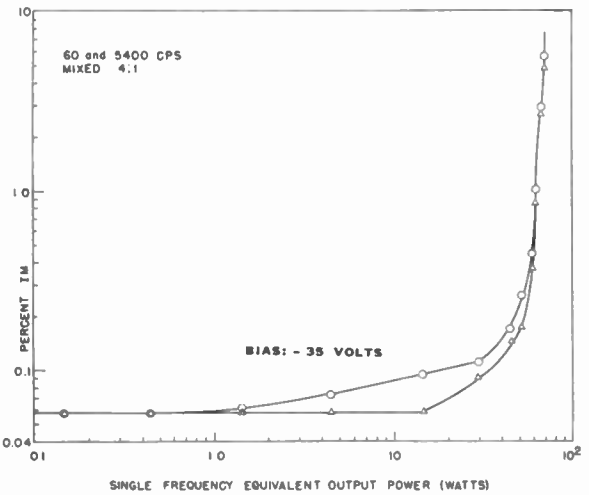

Fig. 17—Percentage intermodulation distortion *vs* output power; 30 db over-all feedback, class A. Lower curve taken with positive voltage feedback.

In addition to the above SMPE intermodulation measurements, it was desirable to check the nonlinear distortion over a wide-frequency band to make sure that it did not rise greatly at the ends of the working band. All the succeeding measurements were made with a bias of −45v. First, a General Radio Type 736-A wave analyzer was used to measure harmonic distortion directly. Because of unavoidable oscillator distortion, it could only be verified that the total harmonic distortion, D_h, was less than 0.2 per cent from 20 to 5,000 cps (the limits of measurement) when 30 db over-all feedback was employed, and positive voltage feedback used or not. The distortion did not exceed the above value at any frequency in this range until clipping began, and a value of only 0.85 per cent was obtained with visible clipping at slightly greater than 65w output power.

Next, harmonic distortion was measured at the 30w level on the amplifier without any feedback. A value of 4.65 per cent was found for D_h from 5,000 to 300 cps. Below 300 cps, the distortion rose slowly to 5.3 per cent

at 32 cps and to 5.9 per cent at 20 cps. The distortion was almost entirely made up of third and fifth harmonics with the fifth three times smaller than the third. Since we have shown already that feedback is fully effective down considerably below 20 cps, we can have confidence that with feedback applied D_h is exceedingly low even at the lowest frequencies to be passed by the amplifier.

The CCIF difference-frequency intermodulation method[24] was then used to investigate amplifier behavior at medium and high frequencies. Here two signals of equal amplitude and frequencies f_1 and f_2 are applied to the input, and f_1 and f_2 are varied in such a manner that their difference Δf remains constant. Using a wave analyzer, the distortion component D_d at the difference frequency Δf is measured and expressed as a percentage of either applied voltage. With the usual 30 db of over-all feedback, this measurement showed that D_d was less than 0.2 per cent from 500 to 15,000 cps using a value of Δf of 100. The value 0.2 per cent represented the residual intermodulation in the amplifier input signal arising from oscillator pulling. Without feedback, and using signals of 1,000 and 1,100 cps, D_d was found to be about 0.26 per cent at a 15w level.[25] This result may be compared with the value of D_h of 4.65 per cent and of rms-sum intermodulation of 18.5 per cent at the 30w power level. The ratio of the last two figures is 3.97, satisfactorily close to the value of 3.84 to be expected for third harmonic distortion alone.[26]

Although the residual value of D_d in the input signal applied to the amplifier was too large to allow accurate measurements of D_d to be made when feedback was used, this was not the case with distortion components occurring at frequencies of $(2f_1-f_2)$ and $(2f_2-f_1)$. These two components had approximately equal amplitudes under all conditions, and the ratio of their average value to the rms value of either input signal will be denoted by D_n. Its value for the amplifier without feedback at a 15w average power level was 2.94 per cent. With 30 db of over-all feedback, the value dropped to 0.06 per cent, and with positive voltage feedback applied the value dropped at least another factor of ten to below 0.006 per cent. Note that the peak rms power under these conditions was 60w.[25]

The intermodulation components at $(2f_1 - f_2)$ and $(2f_2-f_1)$ are considerably larger than that at (f_2-f_1) and seem to be the largest intermodulation distortion components under most conditions. They arise entirely from third-harmonic type distortion. The fact that they are far below the level of audibility may be graphically illustrated by considering the above results where the rms value of either of the applied voltages was 15v and that of either of the above largest intermodulation components was 9 mv with 30 db of over-all feedback. The average output power with both signals applied is 15w; the output power in either of the above distortion components is about 5 microwatts. With positive voltage feedback in addition, this power drops to less than 50 millimicrowatts. No wonder such distortion products are masked by the undistorted components of the output signal.

Finally, the quantity D_n was measured for values of f_1 between 1 and 15 kcps keeping Δf equal to 100 cps. Measurements were made with 30 db over-all feedback and with and without positive voltage feedback. Without the latter feedback, D_n had increased by only 2 per cent at 15 kcps over its 1,000 cps value. The effectiveness of the positive feedback decreased appreciably with frequency however, and at 15 kcps it only reduced D_n by an additional factor of two. This decrease in effectiveness arises from the increase in the subsidiary feedback factor αA_1 with frequency. By keeping the latter quantity smaller out to higher frequencies, positive voltage feedback could be made even more effective in the high frequency range. The above results all combine to indicate that the distortion of the amplifier with feedback is held to an exceedingly low value over the entire working band of the amplifier.

In conclusion, a word of justification is desirable for building an amplifier with 65w of output power (or 130w peak, as the advertisements say!). The peak rms sound intensity level attained near an orchestra or chorus, a large organ, cymbals, or bass drum, is of the order of 110 db.[27] If this intensity level is to be reproduced in a 3,000-cubic-foot room, about 4.5 acoustic watts are required.[28] On assuming a speaker efficiency of 5 per cent, we see that the maximum rms peak power input to the speaker must be some 90w. Horn-loaded loudspeakers, which can be more efficient than 5 per cent would require less input power to produce the above level. Finally, it is rarely desirable to reproduce exactly the maximum original level unless the room is very large or its walls reinforced. These considerations indicate that an average output power of 20w to 30w would be quite sufficient for the vast majority of applications. Since the bass drum has its maximum acoustical output power below 60 cps and the cymbals theirs above 8kc, it is particularly important, however, for true reproduction that the power-handling capacity of the amplifier not fall off appreciably near the ends of the working band. Flat power response between 30 and 15,000 cps would certainly be adequate.

For the exceptional applications such as filling large auditoria or driving magnetic disk cutters, the present amplifier, with its vanishingly small distortion, is a

[24] Langford-Smith, *op. cit.*, p. 613.

[25] Since the peak rms power in the output is four times the average rms power (equal to that for either of the input signals alone), an average power much greater than 15w cannot be used with the present amplifier when the CCIF method is employed.

[26] Langford-Smith, *op cit.*, p. 612.

[27] H. Fletcher, "Hearing, the determining factor for high-fidelity transmission," PROC. IRE, vol. 30, pp. 266–277; June, 1942.

[28] Langford-Smith, *op. cit.*, p. 864.

possible solution either in its present form or in a modification which eliminated some of the frills, such as dynamic and static automatic balancing. Such elimination would increase the distortion, but since it is initially so low, the final value should still be quite acceptably low.

Some of the salient amplifier features are summarized below, and we see that they more than meet the original design goals.

Amplifier Specifications

Frequency and Power Response

1w output: −1 db down at considerably below 5 cps and at 72 kcps.

65w output: −0.5 db down at 19.8 cps and at 22.4 kcps.

Nonlinear Distortion

Less than 0.2 per cent intermodulation distortion up to 60w; 0.1 per cent at 45 w; 1 per cent at 67w.

Noise Level

−106 db referred to 60w output.

Voltage Gain

31 db.

Rise Time

3 μs.

Square-Wave Response

9 per cent tilt at 20 cps. No parasitic oscillations.

Special Features

Automatic circuits ensure continuous push-pull signal balance and static balance of output tube cathode currents. The incorporation of 30 db of negative feedback over three stages and the output transformer is accomplished without peaks in the response curve. Provision is made for adjustable positive or negative output current feedback and for local positive voltage feedback.

Properties of Junction Transistors

R. J. Kircher†

This is the first of a group of three tutorial papers on transistors, with special emphasis on use at audio frequencies, prepared by the Bell Telephone Laboratories Staff at the request of the editorial committee of the Transactions on Audio. The other two articles, "Design Principles of Junction Transistor Audio Amplifiers," by R. L. Trent, and "Design Principles for Junction Transistor Audio Power Amplifiers," by D. R. Fewer, will appear in succeeding issues of this publication.—*The Editor.*

***Summary*—The motion of electrons and holes is considered in relation to the PN junction and it in turn is considered in relation to the junction transistor. Electrical properties, equivalent circuit diagrams, and limiting conditions of operation of junction transistors are discussed. Special equations and features of the common base, common emitter, and common collector configurations are developed and tabulated.**

Introduction

THE TRANSISTOR is the result of intensified research in the domain of solid state physics following World War II. From this work Shockley, Bardeen and Brattain conceived the idea that amplifying properties should be obtainable from semiconductors. This concept became a reality with the announcement of the point contact transistor in 1948.[1] The certainty that an amplifier could be made from a semiconductor element gave a tremendous impetus toward the development of an amplifying structure which would not require point contacts. By 1951 this objective was realized with the announcement of the junction transistor.[2] With the development of the junction transistor communications engineers, and particularly audio engineers, have received a new and versatile electronic device. The stature of the junction transistor grows on reviewing its unique features. Most striking is the property that electronic amplification occurs within a solid substance. This action is realized without the equivalent of heater or cathode power, so that it is instantaneous. Amplification comparable to that of a pentode electron tube is obtained for electrode

† Bell Telephone Labs., Murray Hill, N. J.

[1] J. Bardeen and W. H. Brattain, "The transistor, a semiconductor triode," *Phys. Rev.*, vol. 74, pp. 230–231; July 15, 1948.

[2] W. Shockley, M. Sparks, and G. K. Teal, "*P-N* junction transistors," *Phys. Rev.*, vol. 83, pp. 151–162; July 1, 1951.

voltages of the order of one volt, with current drains of a fraction of a milliampere. Although efficient low-power operation is a salient feature, it is not restricted to such operation, as late designs provide for power output of the order of several watts. The frequency of operation has been steadily pushed upward so that units are now available in the 30mc band, and it appears to be only a matter of time until transistors become available which will operate at hundreds of megacycles.

In view of the rapid growth and highly diversified nature of its applications, there is a growing interest and an expanding need for a working knowledge about the junction transistor which it is hoped this paper and the two associated papers will help to supply.

Because the transistor has its full share of intricacies both in theory and in practice, the level of this paper has been restricted to that of a practical tutorial viewpoint in which the objectives are (1) to give a working knowledge of the important properties of the device, and (2) to review the principles governing its application in audio frequency circuits.

Although similar to the electron tube, in that it provides amplification, the transistor differs from the electron tube in important respects. In considering the electrical characteristics of the transistor, comparisons will be made with the well-known properties of the electron tube in order to associate the properties of the new device with those of the tube.

Review of Physical and Electrical Properties of Semiconductors[3]

Transistors are made from two elements, germanium and silicon. These elements are called semiconductors because their electrical conduction properties are much poorer than those of good conductors, the metals, yet much better than those of nonconductors, the insulators. Germanium is a hard, dense, element with a metallic lustre which melts at about 937 degrees C. Silicon is a hard light element, graphitic in appearance which melts at about 1,415 degrees C. Germanium is recovered as a by-product of zinc refining in the United States. In Europe it is recovered from flue dust. Recent surveys indicate it is widely but diffusely distributed. Silicon, in its various compounds, is one of the most common elements in the earth's surface. To be used in transistors these elements must be concentrated and then purified to a degree never before attained. Thereafter, by special processing, a substantial amount of each element is produced in a single crystal, assuring a homogeneous material for fabricating transistors. Although these elements differ greatly in physical properties, they have an important feature in common; both crystallize in the same structure as diamond, the crystal form of carbon. Carbon, silicon and germanium are found in group IV of the periodic table of elements.

An understanding of electrical conductivity in semiconductors is as basic for solid-state devices as an understanding of thermionic emission is for electron tubes. A review of the fundamentals of this property will be useful for later discussion on the properties of the transistor.

The conductivity, σ, of a sample of material is by definition the ratio of the current density (current per unit area) to the voltage applied per unit length. This is expressed by

$$\sigma = \frac{\dfrac{I}{\text{Area}}}{\dfrac{V}{\text{length}}} = \frac{I}{V}\left(\frac{\text{length}}{\text{Area}}\right). \tag{1}$$

I is the total current, V is the impressed voltage. If the unit of length is the centimeter, the conductivity is expressed in ohm^{-1} cm^{-1}. Resistivity is the reciprocal of conductivity, and is therefore written as,

$$\rho = \frac{1}{\sigma} = \text{(ohm cm)}. \tag{2}$$

It is interesting to compare the relative resistivities of pure samples of copper, germanium, silicon and quartz at room temperature as listed below.

Copper	Germanium	Silicon	Quartz	
10^{-6}	60	1.5×10^{5}	10^{14}	ohm cm.

The resistivity of pure germanium is about ten million times greater than copper, and pure silicon has a thousand times greater resistivity than germanium. A good insulator, like quartz, has a resistivity 10^{9} greater than pure silicon.

In a metal, the flow of current is made up entirely of electrons moving through the conductor in response to an applied voltage. Likewise the space current in an electron tube is exclusively a flow of electrons. A distinguishing feature of semiconductors is that current can consist of electrons and entities which act like positive charges called "holes." Semiconductor physics identifies a hole as an electron deficit in the valence structure of the crystal lattice. Both kinds of carriers of electric charge are relatively scarce in semiconductors compared to the great abundance of free electrons which determine the conductivity of metals. The relative contribution of holes and electrons to current in the semiconductor will be discussed later. The concept of a "hole" as a discrete and real quantity with approximately the same mass as the electron, but of opposite charge, is basic to an understanding of conduction in semiconductors.

From these concepts (1) can be expressed by,

$$\sigma = \frac{q(nv_n + tv_p)}{E}. \tag{3}$$

[3] W. Shockley, "Electrons and Holes," D. Van Nostrand Co., Inc., New York, N. Y., chs. 1 and 3; 1950.
E. M. Conwell, "Properties of silicon and germanium," Proc. IRE, vol. 40, pp. 1327–1337; November, 1952.

where:

q = electron charge
n = density of electrons
p = density of holes
v_n = drift velocity of electrons, cm/sec
v_p = drift velocity of holes, cm/sec
E = electric field, volts per cm.

This expression for conductivity is more significant when written in terms of the mobility of the charge carriers. Mobility is the drift velocity of a carrier in a unit electric field. This gives,

$$\sigma = q(n\mu_n + p\mu_p), \tag{4}$$

where, μ_n and μ_p are respectively the electron and hole mobilities. Since the mobilities are relatively constant quantities under normal conditions, and q is a constant, it is seen that a change in the density of either or both types of charge carriers will change the conductivity of the semiconductor. Holes and electrons do not have the same mobility. Typical values for mobility in germanium and in silicon at room temperature are listed below.

Germanium	*Silicon*
cm/sec / v/cm	cm/sec / v/cm
$\mu_n \cong 3600$	$\mu_n \cong 1200$
$\mu_p \cong 1700$	$\mu_p \cong 400.$

It is characteristic of semiconductors that light and heat produce marked changes in the conductivity of the material. The mechanisms which cause these changes may be qualitatively explained by consideration of energy absorption effects. The atoms in a crystal are held together by the valence electrons in the outermost shells of adjacent atoms. Germanium and silicon atoms have four valence electrons in the outermost shell, each of which pairs with an electron of an adjacent atom to form a covalent bond between the atoms. Thus each atom is electrically tied to four adjacent neighbors. In a single crystal the result is a very orderly arrangement of the atoms in a geometrical pattern. Germanium and silicon crystalize in the tetrahedron configuration. The electronic covalent bond of the semiconductor can be broken by absorption of energy, the source of which can be light or heat. Light supplies energy packets (quanta) the energy being inversely proportional to the wavelength. Absorption of a quantum of energy greater than 0.72 electron volt (ev) in germanium, or 1.12 ev in silicon, will separate an electron from its covalent bond. The freed electron can move about in the crystal with little constraint. The rupture of the electronic bond simultaneously produces a "hole" at the place vacated by the electron. This hole is also free to move about in the crystal. Hence the density of charge carriers is increased by the production of equal numbers of holes and electrons. Consequently, when a voltage is applied to the semiconductor, and the material is illuminated, a marked increase in current will occur. This is the photo-electric conductivity effect.[4]

In a similar way, thermal energy absorbed from any source, even from ambient temperature as low as 100 degrees C., can cause some energy absorptions of 0.72 ev or 1.12 ev to take place in germanium or silicon respectively. The energy absorbed releases an electron from its covalent bond, and this simultaneously generates its complement, a "hole." When the material is heated with a voltage applied, a marked increase in the current occurs. This is the thermoelectric conductivity effect. Minimizing the extraneous effects of heat is a major problem in semiconductor devices.

The conductivity of germanium and silicon can be altered in a controlled manner by chemically adding minute amounts of certain other elements. The effects of such doping agents will be discussed in the following section.

The parallelism between germanium and silicon has been carried this far to familiarize the reader with their similarities. In subsequent discussions where germanium is specifically mentioned, silicon can usually be assumed to have similar properties.

The Meaning of the *PN* Junction[5]

Chemically pure germanium is referred to as an intrinsic semiconductor. At room temperature it has a resistivity of about 60 ohm cm. The resistivity of intrinsic germanium can be greatly altered by the addition of minute quantities of elements from group III or V of the periodic table. The addition of group V elements (phosphorus, arsenic, antimony) produces *N*-type conductivity. On the other hand, the addition of group III elements (boron, aluminum, gallium, indium) produces *P*-type conductivity. The expression "*N*-type conductivity," designates an excess of free negative carriers (electrons) in the semiconductor. The expression "*P*-type conductivity," denotes a deficit of electrons (holes). When both classes of impurity are simultaneously present, the dominant impurity determines the resulting conductivity type. Addition of no more than one impurity atom in ten million or a hundred million germanium atoms has a marked effect on the resistivity of intrinsic germanium. There are approximately 5×10^{22} atoms of germanium or silicon in a cubic centimeter.

It has been noted that the conductivity of the semiconductor depends on the density and mobility of each type of carrier (4). For one type to control, the density mobility product for that carrier must dominate the corresponding factor for the other type of carrier. By using first one kind of impurity doping, then the other, regions of alternating conductivity types (*NP* or *PN*) can be produced in the same crystal. Where two opposite conductivity regions come together in the same

[4] The effect of light can be eliminated by using an opaque case for the semiconductor device.
[5] Shockley, *op. cit.*, ch. 4.

crystal a *PN* (or *NP*) junction is produced. This junction has the electrical properties of a diode. A diode is characterized by its unilateral transmission property. This rectifying action permits an easy flow of current for one direction of electrical potential, but permits little current to flow on reversal of the applied voltage. In order to account for this property, several important concepts about the internal nature of the *PN* diode will be reviewed.

A *PN* diode is represented in Fig. 1(a) with no external applied voltage. The *P* region is shown as thickly populated by positive charges (holes), and the *N* region by negative charges (electrons). These charges are free to move about in their respective regions but no interchange can take place from one region to the other because of an internal electric field which opposes such migrations. It is noted that in each region there are a few charges of opposite sign to the majority type. These are called minority carriers. They are produced by the thermal agitation of the atoms which results in the thermoelectric conductivity property. A qualitative explanation for the occurrence of an internal electric field at the *PN* junction will be helpful in understanding the diode.

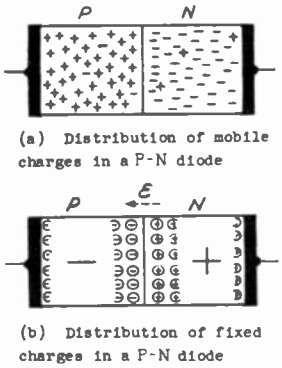

Fig. 1—Representation of *PN* diode, no externally applied voltage.

As a specific illustration, let the *N* region of Fig. 1(a) be produced by adding one antimony atom for each ten million atoms of germanium. The antimony atom normally has five electrons in its outermost shell. When it substitutes for a germanium atom in the crystal lattice, only four of these electrons can be used. The fifth electron is therefore free to move about in the *N* region of the crystal. Even though there are very few antimony atoms compared to germanium atoms, the actual number is of the order of 10^{15} per cubic cm, and therefore there are this number of free electrons per cubic cm. The antimony atom by losing an electron becomes a positively charged ion. Because it is bound in the crystal lattice it cannot move about, and therefore cannot contribute to the electrical conductivity. This impurity ion can be thought of as being embedded with millions of others in a vast uniform array of neutral germanium atoms which has a dielectric constant of about 16. The dielectric constant for silicon is about 12.

Similarly, let the *P* region result from the addition of one gallium atom for each ten million germanium atoms. Gallium normally has three electrons in its outermost shell. In substituting for a germanium atom, it lacks one electron. The missing electron is supplied by an adjacent germanium atom which thereby acquires an electron deficit. The movement of the electron deficit from one germanium atom to another is the movement of a hole, which contributes to the electrical conductivity of the *P* region. Adding the fourth electron to the gallium atom results in a negatively charged ion which is firmly bound in the crystal lattice. Millions of this type of impurity ion are embedded in the matrix of germanium atoms to constitute the *P* region.

Note that in the *N* and *P* regions the fixed ionic charges are opposite in sign to the mobile charges which characterize the region as indicated in Fig. 1(b). At the interface between *P* and *N* regions (the junction) a surface with negatively charged atoms faces a surface of positively charged atoms. This produces an internal potential difference across the junction which has the value:

$$\left(\frac{kT}{q}\right) \ln \left(\frac{N_n P_p}{N_i^2}\right).$$

where

k = Boltzmann's constant
T = Absolute temperature
q = Electronic charge
N_n = Density of electrons in the *N* region
P_p = Density of holes in the *P* region
N_i = Density of electrons or holes in the intrinsic semiconductor.

At room temperature the value of kT/q is approximately 0.026v. Since the internal field is from *N* to *P*, holes in the *P* region cannot move across the junction into the *N* region, and vice versa. For this condition of equilibrium, each region retains its own type of mobile charge. Since the sum of all fixed and mobile negative charges equals the sum of all fixed and mobile positive charges, the crystal as a whole remains electrically neutral. Under these conditions, no current can flow in an external circuit connecting the *PN* regions.

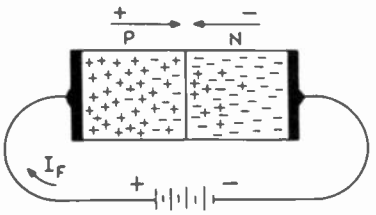

Fig. 2—*PN* diode forward-biased.

In order for current to readily flow from the *P* region to the *N* region, an external battery voltage must be applied, as shown in Fig. 2. This external voltage must make the *P* region positive relative to the *N* region so

that the majority carriers of each region will move across the junction. In this condition the diode is biased in the "easy flow" direction and a substantial current can flow in the external circuit. The amount of current will depend on (1) the density of the two kinds of charge carriers, (2) the area of the junction, and (3) the value of the external potential.

From (4) it is seen that the current can be made up chiefly of one kind of charge carrier by having its density greatly exceed that of the other type of carrier. This depends on the relative amount of the impurities added to produce the P and N regions. In a qualitative way the relative amount of impurities is given by the ratio of the resistivities of the two regions. The lower the resistivity the greater the density of the mobile carrier of electric charge. For example, if the resistivity of the P region were one-tenth that of the N region, this would not mean that the hole density was ten times that of the electrons but rather that,

$$\frac{\rho_p}{\rho_n} = \frac{n\mu_n}{p\mu_p} = \frac{1}{10}.$$

Since the ratio of electron to hole mobility is about 2.1, for this case, the hole density in the P region would be actually twenty-one times the electron density in the N region.

From this example it appears that if the P region is much lower in resistivity than the N region, and the diode is forward biased, that the current will be predominantly due to holes flowing from the P region into the N region. The reverse flow of electrons from N to P will be small, contributing little to the forward current across the junction. These holes ultimately disappear by combining with electrons. By itself this would represent a "disappearance" of charge which would violate the conservation law. Therefore an electron must be supplied by the external battery for each hole neutralized in the body of the crystal. This means that conventional current flows out of the N region and into the P region.

In an analogous way, when the N region is much lower in resistivity than the P region, the current across the junction will be predominantly due to electrons flowing from N to P. The result is that conventional current flows into the P region and out of the N region. Note that for either the PN or NP forward-biased diode, current flows into the P region and out of the N region.

On reversing the polarity of the voltage across the diode, the condition is as represented in Fig. 3. In this case, the majority carriers move away from the junction so that only the thermally-generated minority carriers in each region move across the junction to produce a very small current. In this case, the diode presents a very high impedance. The presence of a dipole of fixed opposite charges in the neighborhood of the junction results in a capacity (depletion layer capacity) which corresponds to the collector capacity of the junction transistor. Fortunately, the effect of this capacity can usually be neglected at audio frequencies.

Over a wide range of operating conditions, the current voltage expression for a junction diode is given by

$$I = I_s(\epsilon^{qV/kT} - 1), \tag{5}$$

where

I = diode current[6]
I_s = saturation current
V = voltage applied to the diode (effective at the junction); positive voltage produces forward current
k, q, T as previously defined.

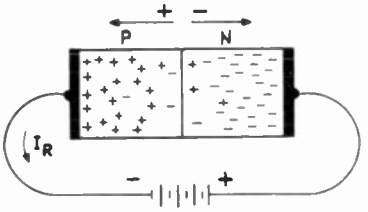

Fig. 3—PN diode reverse-biased.

A number of methods have been developed for producing PN junctions. The commercial process used is identified by a significant feature such as,

(1) Double-doped grown junctions[7]
(2) Rate grown junctions[8]
(3) Fused alloy junctions.[9]

Other methods such as vapor diffusion techniques, and electrolytic etching and plating, show great promise for the future. It is the feature of control in producing PN (or NP) junctions which has made possible most of the striking advances in semiconductor device development. With these techniques alternating conductivity type zones can be produced such as PNP or NPN in which the central zone is made quite thin. After suitable mechanical and chemical treatments, these structures are fabricated into junction transistors. It is more than a superficial observation that the latter configurations have the relationship of two PN diodes back to back in the same crystal.

Geometry of Junction Transistors

In the first two methods listed for the production of crystals with alternating conductivity types, a rod of single crystal material about an inch in diameter is produced. In the first method, a single NPN section

[6] The diode current is ideally independent of the applied voltage, for a negative voltage greater than several times kT/q.
[7] G. K. Teal, M. Sparks, and E. Buehler, "Single-crystal germanium," Proc. IRE, vol. 40, pp. 906–909; August, 1952.
[8] R. N. Hall, "Segregation of impurities during the growth of germanium and silicon crystals," *Jour. Phys. Chem.*, vol. 57, pp. 836–839; March, 1953.
[9] R. N. Hall and W. C. Dunlap, "P-N junctions prepared by impurity diffusion," *Phys. Rev.*, vol. 80, pp. 467–468; September, 1950.

(produced by two successive "dopings" of the melt as the material is withdrawn from a crucible of molten germanium) is cut from the rod and divided into bars retaining the *NPN* configuration. The rate grown method produces in succession a number of *NPN* sections in the same rod each of which is subdivided into a quantity of small *NPN* bars. These bars are roughly about 3/16 inch long and 1/16 inch on a side. The thickness of the central zone is about 1/1,000 inch or less.

After mechanical and chemical treatments, low resistance ohmic contacts are made to the two ends and to the central zone. One end is collector terminal *C*, the other end emitter terminal *E*, and the central terminal is base electrode *B*. This type of structure is shown in Fig. 4. For future reference the electrical symbol and the corresponding vacuum tube analog is given.

The third method (fused alloy) is extensively used in making junction transistors. The principle is to alter the conductivity of a thin wafer of germanium in localized zones on opposite faces. (The wafer dimensions are about 0.10×0.10×0.0025 inch.) This alteration is done by fusing into the zones a doping agent of the opposite conductivity type to that of the wafer. The depth of penetration of the change in conductivity type is controlled by time and temperature so that a thin unaltered web (0.001 inch) of the wafer remains between the altered regions to yield the *NPN* or *PNP* structure.

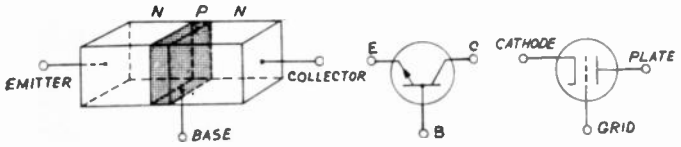

Fig. 4—Representation of grown junction transistor.

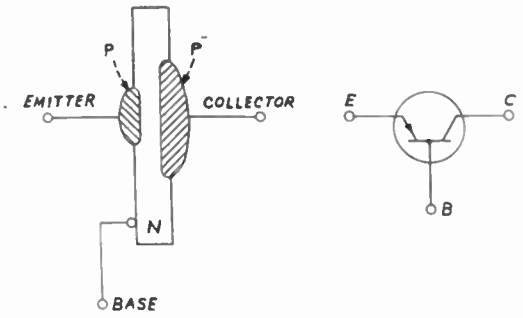

Fig. 5—Representation of fused alloy junction transistor.

After chemical etching, ohmic connections are made to the altered zones and to the body of the wafer. In some designs the diameter of the collector zone is made larger (0.030 inch) than that of the emitter zone (0.015 inch) in order to improve the collector efficiency. The base connection is made on the emitter side well outside the altered area. Fig. 5 is a diagram of this type of junction transistor. The electrical symbol indicates a *PNP* unit which it will be noted has the head of the arrow on the emitter opposite to that shown in Fig. 4 for the *NPN* unit. The arrow points in the direction for easy flow of current. These structures are preferably mounted in small hermetically-sealed cases with the terminals brought out through a header.

Electrical Properties of the Junction Transistor

The first step in describing the electrical properties of the transistor will be to consider the properties of two separate diodes connected to form a two-terminal pair network, as shown in Fig. 6. Before doing this, however, it is desirable to introduce four parameters which are useful in the characterization of transistors.

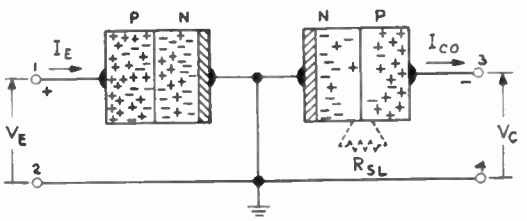

Fig. 6—Two *PN* junction diodes back-to-back.

These parameters, called hybrid parameters, are borrowed from classical linear network theory,[10] and will be considered in greater detail in the following section. Their definitions are as follows:

$$h_{11} = \left.\frac{\partial v_1}{\partial i_1}\right|_{v_2=0}$$ Input *IMPEDANCE* with ac short-circuited output

$$h_{12} = \left.\frac{\partial v_1}{\partial v_2}\right|_{i_1=0}$$ Reverse transfer *VOLTAGE RATIO* with ac open-circuited input

$$h_{21} = \left.\frac{\partial i_2}{\partial i_1}\right|_{v_2=0}$$ Forward transfer *CURRENT RATIO* with ac short-circuited output

$$h_{22} = \left.\frac{\partial i_2}{\partial v_2}\right|_{i_1=0}$$ Output *ADMITTANCE* with ac open-circuited input.

It is understood that in general these parameters are the slopes of functions describing the characteristics of the transistor at an appropriate dc operating point. This requirement is imposed for small-signal analysis.

The *PN* diode shown on the left side of Fig. 6 is biased in the forward direction. A constant current, I_E is assumed to flow across the junction. The diode on the right is reverse biased by the voltage V_C.

Since no interaction can take place between the two diodes, the input impedance of the combination (terminals 1, 2) is that of the forward-biased diode alone, and the output admittance (terminals 3, 4) is that of the reverse-biased diode alone. By definition, the forward resistance of the first diode is

$$h_{11} = \left.\frac{\partial V_E}{\partial I_E}\right|_{V_C=0}.$$

[10] E. A. Guillemin, "Communication Networks," John Wiley & Sons, New York, N. Y., vol. II, ch. 4; 1935.

From (5)

$$I_E = I_S\epsilon^{qV_E/kT}; \qquad (\epsilon^{qV_E/kT} \gg 1).$$

Differentiating this equation and solving for $dV_E/dI_E = r_e$,

$$h_{11} = \frac{kT}{qI_E} = r_e. \tag{6}$$

Previously the reverse current of the diode was attributed to the presence of minority carriers near the junction. Ideally this is the case, but in practical units there is usually a leakage current across the junction which may be larger than that of the back diffusion or saturation current, I_S. The surface leakage current, I_{SL}, varies directly with the applied voltage, V_C. Including the leakage current, the reverse current of the diode is given by

$$\begin{aligned} I_{C0} &= -I_S + I_{SL}; && (\epsilon^{qV_C/kT} \ll 1) \\ I_{C0} &= -I_S + g_{SL}V_C, && (V_C \text{ is negative}) \end{aligned} \tag{7}$$

where g_{SL} is the conductance due to surface leakage. In the following derivations let,

$$\frac{dI_{C0}}{dV_C} = g_{C0} = g_{SL}.$$

The output admittance defined by,

$$h_{22} = \frac{\partial I_C}{\partial V_C}\bigg|_{I_E=0} = \frac{\partial I_{C0}}{\partial V_C},$$

has the value,

$$h_{22} = g_{C0} = \frac{1}{r_{C0}}, \tag{8}$$

where r_{C0} is the ac leakage resistance of the junction. With no interaction between the diodes, the forward and backward transfer parameters are zero.

$$h_{12} = \frac{\partial V_E}{\partial V_C}\bigg|_{I_E=0} = 0 \tag{9}$$

$$h_{21} = \frac{\partial I_C}{\partial I_E}\bigg|_{V_C=0} = 0. \tag{10}$$

The next step in the synthesis of the transistor is to bring the two diodes together so that they are in the same crystal but with a single N region between two P regions as shown in Fig. 7(a). Assume the emitter diode junction (on the left) is so far from the collector diode junction (on the right) that all of the injected carriers recombine in the base region between junctions.[11] Consequently none of the input current will appear in the output. The input impedance in this case is larger than in the preceding arrangement, because the injected current must pass through more of the semiconductor to reach the base terminal, which, for practical reasons, is smaller and farther away from the junction than in the separate diode structure. This additional resistance is the series base spreading resistance, r_b'. For this case the input impedance is given by,

$$h_{11} = \frac{kT}{qI_E} + r_b'. \tag{11}$$

By symmetry, the output admittance is slightly modified because the I_{C0} current must flow through a corresponding spreading resistance of value, r_b', to reach the base terminal. Since r_b' is common to the input and output current paths it is convenient to consider it as removed from the structure and placed in the external connection to the base as shown in Fig. 7(b). An effect which moderately alters the value of r_b' can be considered as a perturbation of the value of r_b' and can be introduced in series with r_b'. The result of this artifice is two-fold.

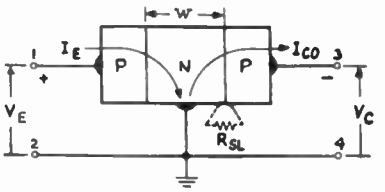

(a) Base spreading resistance within the crystal

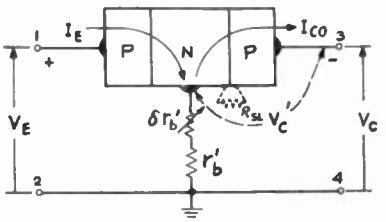

(b) Base spreading resistance treated as an external element

Fig. 7—Two PN junctions back-to-back in the same crystal, but widely separated.

1. The base region can be assumed to be the same potential throughout its length.
2. The effective potential across the collector junction, V_C', is to a good approximation, V_C, at low frequencies.

The output admittance for this case is to a very good approximation,

$$h_{22} = \frac{\partial I_C}{\partial V_C}\bigg|_{I_E=0} \cong \frac{\partial I_{C0}}{\partial V_C} \cong g_{C0}, \ (r_{C0} \gg r_b'). \tag{12}$$

The I_{C0} current flowing through r_b' produces a voltage at the open-circuited input. The ratio of this voltage to

[11] A minority carrier disappears by recombining with its opposite entity. The interval of time for which an electron or a hole retains its identity as a minority carrier is the lifetime of the carrier. Representative lifetimes are 1 to 10 microseconds.

the voltage at the output is the feedback voltage ratio given by,

$$h_{12} = \frac{r_b'}{r_{C0} + r_b'} \cong g_{C0} r_b'. \tag{13}$$

Since there is no transfer of current from input to output, the forward current transfer ratio is nil, and

$$h_{21} = 0. \tag{14}$$

The concluding step is to consider the case in which the emitter and collector junctions are close together as in the normal transistor, as indicated in Fig. 8. Fig. 8(a) applies to the derivation of parameters h_{21} and h_{11}; Fig. 8(b) to the derivation of parameters h_{22} and h_{12}.

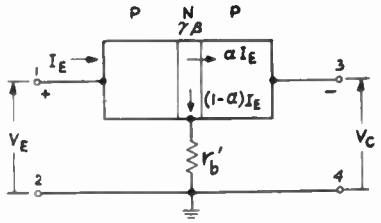

(a) Determination of input impedance and forward current transfer properties

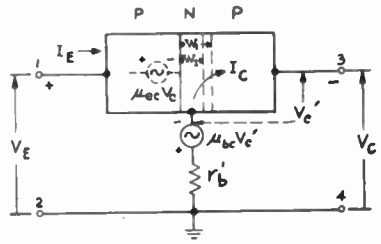

(b) Determination of output admittance and backward voltage transfer properties

Fig. 8—The *PNP* junction transistor.

Two factors which affect the output current must be considered now.

1. The primary function of the emitter is to inject minority carriers (holes) into the base region most of which will contribute to the collector current. Since a few of the majority carriers of the base (electrons) diffuse back into the emitter, emitter current will have two components. The ratio of injected carriers (holes) to total emitter current (holes and electrons) is emitter injection efficiency factor, gamma (γ). This factor, the fraction of emitter current which can contribute to collector current, is usually slightly less than unity.
2. The injected carriers (holes) must diffuse across the base region in order to reach the collector. In doing so a small fraction recombine with electrons and therefore do not reach the collector. The ratio of holes collected to those injected is the transport factor, beta (β). Both a magnitude and a delay (phase shift) are associated with beta. At audio frequencies the magnitude is usually a few per cent less than unity, and the phase can usually be neglected.

The product of these two factors is an important parameter of the junction transistor. It is expressed by,[12]

$$a = \gamma\beta. \tag{15}$$

For frequencies up to at least 20,000 cycles per second this factor is usually indistinguishable from the short-circuit current gain, alpha (α). With this reservation, the forward current transfer parameter for this connection is,

$$-h_{21} = \alpha \cong a. \tag{16}$$

The closeness of the collector to the emitter alters the input impedance. Refer to Fig. 8(a). Most of the emitter current goes to the collector (αI_E), so that only the fraction $(1-\alpha)I_E$ will pass through the base spreading resistance to the base terminal. As a result the previous expression for the input impedance is modified to,

$$h_{11} = \frac{kT}{qI_E} + (1-\alpha)r_b'. \tag{17}$$

The output admittance h_{22} and the backward transfer property of the junction transistor h_{12} differ from the values of the previous example because of space-charge layer widening due to collector voltage, as described by Early.[13] [See Fig. 8(b).] In fused alloy junction transistors (and to a lesser degree in grown units) an increase in collector voltage causes the collector region to move closer to the emitter, thereby reducing the effective width of the base region. Narrowing the base width, w, increases the probability that an injected carrier will cross to the collector. As a result, alpha is increased by an increase in collector voltage. This phenomenon affects the output admittance so that it becomes,

$$h_{22} = \left.\frac{\partial I_C}{\partial V_C}\right|_{I_E=0} \cong \frac{\partial(I_{C0} + \alpha I_E)}{\partial V_C}$$

$$\cong g_{C0} + I_E \frac{\partial \alpha}{\partial V_C} = g_c. \tag{18}$$

The dependence of g_c on emitter current and collector voltage is shown in Fig. 16. It is noted that the collector admittance increases linearly with emitter current, and inversely with the collector voltage. The effect of g_{C0} is to establish a conductance intercept for zero emitter current.

Space-charge layer widening also affects the backward transfer voltage ratio h_{12} in several ways. One effect occurs because a base region change appears as a change

[12] The intrinsic current multiplication property of the collector junction is designated a_i. For a conventional junction transistor and for normal conditions, a_i is taken as unity. The general expression for (15) is $a = \gamma\beta a_i$.

[13] J. M. Early, "Effects of space-charge layer widening in junction transistors," PROC. IRE, vol. 40, pp. 1401–1406; November, 1952.

in the open circuit input potential. This can be attributed to an incremental change in the spreading resistance, $\partial r_b'$, such that a small voltage, due to the current through it, is introduced in series with r_b'. This small voltage is expressed as a fraction, μ_{bc}, of the collector junction voltage. A second effect is due to the relationship between emitter and collector voltages given in terms of the base width change by;

$$\frac{\partial V_E}{\partial V_C} = \frac{\partial V_E}{\partial w} \frac{\partial w}{\partial V_C}.$$

Early has expressed this in the form,

$$\frac{\partial V_E}{\partial V_C} = \frac{kT}{qw} \frac{\partial w}{\partial V_C} = \mu_{ec}.$$

In addition to the above two terms, the output voltage division contribution due to the current through r_b' must be included. The sum of these three terms gives the backward transfer voltage ratio,

$$h_{12} = g_c r_b' - \mu_{bc} + \mu_{ec}. \tag{19}$$

Thus by successive steps, using the analogy of the transistor as two back-to-back diodes, the terminal properties of the transistor have been obtained in terms of the hybrid (h) parameters. Other parametric representations can be used to specify the transistor. The relationships between several of the generally used representations will be developed in the next section.

Transistor Equivalent Circuits

The input and output terminal properties, and the transfer characteristics of the device have been obtained from a consideration of the physics of the transistor. These properties are measurable quantities which can be used in various electrical configurations in terms of impedances or admittances or a combination of both, to simulate the transistor. Any network which adequately represents the electrical behavior of the device is its equivalent circuit.

The point of view adopted in this paper is that while measurements on the transistor are most effectively made in terms of the hybrid parameters, in circuit analysis it is often more convenient to use the open-circuit impedance or the short-circuit admittance parameters. Since there are a number of technical articles dealing with the development of the latter two equivalent circuits,[14] it will be the purpose of this section to show the interrelationships between the hybrid parameters and the impedance and admittance parameters.

Considering the transistor as a three-terminal device (since two terminals coalesce), it can be represented as shown in Fig. 9. The conventions for terminal currents and voltages are as shown. It should be kept in mind that any one of three ways of connecting to the transistor may be included in this representation. The transistor terminal which is common to the input and output designates the connection; viz., common base, common emitter, common collector. When a specific circuitry is discussed, the common base connection will be used. Equivalent circuitry for the other two connections can be derived by parallel methods.

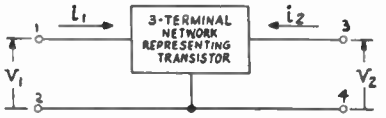

Fig. 9—Generalized representation for the transistor.

Using hybrid parameters, the terminal conditions are given by the following two equations.

$$\begin{aligned} v_1 &= h_{11} i_1 + h_{12} v_2 \\ i_2 &= h_{21} i_1 + h_{22} v_2, \end{aligned} \tag{20}$$

where the h coefficients are as defined in the previous section.

The merit of the hybrid parameters is due to their compatibility with the low input and high output impedance properties of the transistor. These measurements are made using the common base or common emitter connection where the input impedance is very low, and the output impedance is very high. The input impedance and the output admittance (instead of impedance) can be obtained with conventional measuring equipment for the conditions imposed at the terminals for the hybrid parameters.

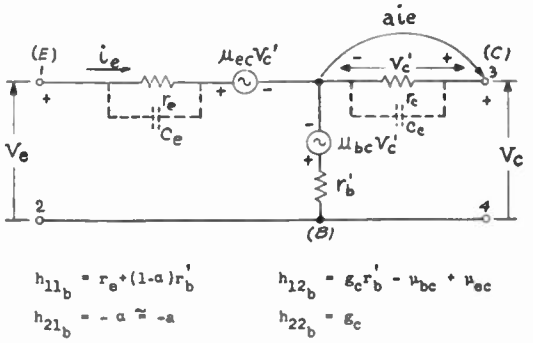

Fig. 10—Hybrid parameter equivalent-T circuit representation for the common base connection.

When hybrid parameters are used in analysis they are generally introduced into an equivalent T or an equivalent π network. The configuration used in the previous section leads to a common base equivalent T network as represented in Fig. 10 for small signal ac conditions. The collector capacity, C_c, which does not affect the low-frequency (audio) performance is shown in phantom. At higher frequencies this capacity, and a capacity at the input (also shown in phantom), must be considered.

[14] L. C. Peterson, "Equivalent circuits of linear active four-terminal networks," *Bell. Sys. Tech. Jour.*, vol. 27, pp. 593–622; October, 1948.
R. M. Ryder and R. J. Kircher, "Some circuit aspects of the transistor," *Bell Sys. Tech. Jour.*, vol. 28, pp. 367–400; July, 1949.
L. J. Giacoletto, "Junction transistor equivalent circuits and vacuum-tube analogy," Proc. IRE, vol. 40, pp. 1490–1493; November, 1952.

The synopsis on this figure shows the equivalence between the expressions for the hybrid parameters given heretofore and those for the corresponding equivalent circuit elements. The elements, r_e and r_c are respectively the ac forward and reverse resistances of the emitter and collector junctions. The latter includes the leakage resistance. The base spreading resistance is as before, r_b'. The two generators, $\mu_{ec}V_C'$ and $\mu_{bc}V_C'$ are introduced by the space-layer widening effect previously discussed.

In the discussion of this effect it was noted that an incremental increase in collector junction voltage caused an incremental decrease in the effective width of the base region.[15] This has two effects:

1. The base spreading resistance r_b' shows an incremental increase. This incremental resistance change multiplied by the current through it is equivalent to a small emf $(\mu_{bc}V_C')$ in series with r_b'. The polarity of the emf shows the nature of the incremental change.
2. Narrowing the base width has the effect of producing more collector current for the same emitter current. This effect is as though a small emf $(\mu_{ec}V_C')$ were inserted in the emitter branch so poled that a lower net emitter potential is required to maintain the same emitter current. The polarity shown in Fig. 10 is appropriate for a *PNP* unit.

The magnitudes of the terms $V_C'\mu_{bc}$ and $V_C'\mu_{ec}$ are very small.[16] It will be noted that as V_C' is reduced the values of these terms diminish. At audio frequencies the voltage drop across the collector junction, V_C', is slightly less than V_C, the external potential. At higher frequencies the shunting effect of the collector capacity reduces the value of V_C' so that the above emf's become negligible. For this equivalent circuit, the infinite impedance current generator, ai_e, provides the short-circuit current when terminals 3, 4 are shorted. Operating on the terminals of this circuit as required for hybrid parameter measurements, the values of h_{11}, h_{12}, h_{21}, h_{22} are obtained as shown.

Probably the best known equivalent circuit representation for the transistor is by the "open-circuit" impedance parameters. This also leads to an equivalent T network for the transistor. Within the scope of this paper, all impedance parameters are considered to be resistive. The equations for the "open-circuit" resistance parameters are,

$$\begin{aligned} v_1 &= r_{11}i_1 + r_{12}i_2 \\ v_2 &= r_{21}i_1 + r_{22}i_2, \end{aligned} \tag{21}$$

where

$r_{11} = \left.\dfrac{\partial v_1}{\partial i_1}\right|_{i_2=0}$ Input *IMPEDANCE* with ac open-circuited output

$r_{12} = \left.\dfrac{\partial v_1}{\partial i_2}\right|_{i_1=0}$ Reverse transfer *IMPEDANCE* with ac open-circuited input

$r_{21} = \left.\dfrac{\partial v_2}{\partial i_1}\right|_{i_2=0}$ Forward transfer *IMPEDANCE* with ac open-circuited output

$r_{22} = \left.\dfrac{\partial v_2}{\partial i_2}\right|_{i_1=0}$ Output *IMPEDANCE* with ac open-circuited input.

The circuit determinant given by

$$\Delta = r_{11}r_{22} - r_{12}r_{21} \tag{22}$$

is often used to simplify lengthy expressions.

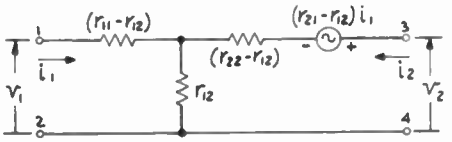

Fig. 11—Generalized equivalent-T circuit, resistance parameters.

From these equations, the generalized equivalent T network of Fig. 11 is obtained. The values of the resistance parameters in terms of the hybrid parameters are found by writing (20) in the form of (21) and comparing the coefficients. This gives,

$$\begin{aligned} r_{11} &= h_{11} - \frac{h_{12}h_{21}}{h_{22}} \\ r_{12} &= \frac{h_{12}}{h_{22}} \\ r_{21} &= -\frac{h_{21}}{h_{22}} \\ r_{22} &= \frac{1}{h_{22}}. \end{aligned} \tag{23}$$

With these values for the r's, the corresponding equivalent T circuit for the common-base connection is obtained as shown in Fig. 12. Because of its impor-

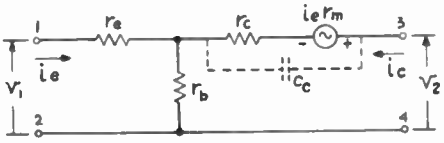

Fig. 12—Common base equivalent-T circuit.

tance, the collector capacity is shown in phantom, although it is neglected at audio frequencies. The effect of $\mu_{bc}V_C'$ can be neglected in obtaining the equivalent circuit elements of this figure. However, $\mu_{ec}V_C'$ cannot be neglected because it can significantly increase the value of the base resistance at low frequencies, as indicated by the following equation relating the backward transfer properties of Figs. 10 and 12,

$$\begin{aligned} i_2r_b &= i_2r_b' + \mu_{ec}V_C' \\ r_b &= r_b' + \mu_{ec}r_c. \end{aligned} \tag{24}$$

The second term on the right is appreciable at audio frequencies because of the high value of r_c. As the fre-

[15] This discussion is particularly applicable to the fused alloy junction transistor.

[16] The value of μ_{ec} is of the order of 10^{-4}, that of μ_{bc}, 10^{-5}. The effect of $\mu_{bc}V_C'$ can usually be neglected, even at very low frequencies. It is chiefly of academic interest.

quency of measurement is increased, the value of V_C' is reduced because of the shunting effect of the collector capacity.[17] At frequencies well above the audio range (z_c substituted for r_c) r_b approaches r_b'. The value of the equivalent circuit element, r_m, is obtained by the substitution, $r_m = r_{21} - r_{12} \cong a r_c$.

Following the same procedure, the four short-circuit conductance parameters can be derived from the hybrid parameters. The defining equations are:

$$\begin{aligned} i_1 &= g_{11}v_1 + g_{12}v_2 \\ i_2 &= g_{21}v_1 + g_{22}v_2. \end{aligned} \tag{25}$$

By the same algebraic method outlined for obtaining resistance parameters, the conductance parameters are obtained in terms of hybrid parameters as,

$$\begin{aligned} g_{11} &= \left.\frac{\partial i_1}{\partial v_1}\right|_{v_2=0} = \frac{1}{h_{11}} \\ g_{12} &= \left.\frac{\partial i_1}{\partial v_2}\right|_{v_1=0} = -\frac{h_{12}}{h_{11}} \\ g_{21} &= \left.\frac{\partial i_2}{\partial v_1}\right|_{v_2=0} = \frac{h_{21}}{h_{11}} \\ g_{22} &= \left.\frac{\partial i_2}{\partial v_2}\right|_{v_1=0} = h_{22} - \frac{h_{12}h_{21}}{h_{11}}. \end{aligned} \tag{26}$$

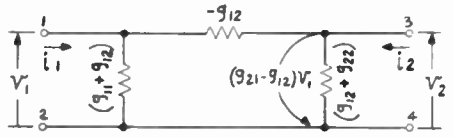

Fig. 13—Generalized equivalent π circuit. Conductance parameters.

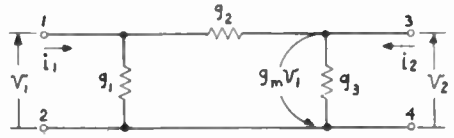

$$g_{21} + g_{12} = g_1 = \frac{r_{22} - r_{12}}{\Delta}$$

$$-g_{12} = g_2 = \frac{r_{12}}{\Delta}$$

$$g_{22} + g_{12} = g_3 = \frac{r_{11} - r_{12}}{\Delta}$$

$$g_{21} - g_{12} = g_m = \frac{-r_{21} + r_{12}}{\Delta},$$

where

$$\Delta = r_{11}r_{22} - r_{12}r_{21}$$

Fig. 14—Equivalent π circuit; conductance parameters in terms of open-circuit resistance parameters.

The resulting equivalent short-circuit π network is shown in Fig. 13. This can be given by simple conductance elements as represented in Fig. 14.

In summary, it is noted that the transistor is characterized by its terminal behavior as obtained by direct measurements. These measurements are for terminal conditions defined by a set of parametric coefficients. For accurate measurements the hybrid parameters are preferred. Given a particular set of parametric coefficients, those of the other two widely-used sets of parameters can be derived.

Operating Point and Temperature Effects[18]

The elements in the transistor equivalent circuit are dependent on the dc operating point, the operating temperature and the frequency. The latter dependence has been taken as negligible in this paper. In this section the nature of the variation of the equivalent circuit elements with operating point and with temperature will be outlined. By taking into account these relationships, the equivalent circuit can be adopted over a wide range of operating conditions.

Variation of Parameters with Dc Operating Point

The physical significance of the equivalent circuit elements, α, g_c, r_e, r_b has been discussed. In the discussion it was assumed that the value of each element was measured at a particular dc operating point. (Transistor specifications are frequently given at room temperature for an emitter current of 1 ma and a collector voltage of 4.5v.) The way an equivalent circuit element depends on either current or voltage can be plotted as shown in Figs. 15, 16, and 17 on the next page. With such information the effect of changing the operation point can readily be evaluated.

There are several points of interest regarding alpha. It is noted that the current amplification factor, α, increases rapidly (from a very low value) for the first few microamperes of emitter current, and then approaches a relatively constant value less than unity at high currents. The value of alpha is usually specified at a particular operating point for emitter current and collector voltage. This is the low frequency value of alpha, designated α_0. The frequency and phase properties of alpha, unlike the g_m property of the electron tube, must be considered for relatively low frequencies (above the audio band).[19] In commercial units the values of α_0 range from 0.900 to 0.990. In some special types of units α_0 may have values lower than 0.900. The way alpha varies with emitter current is representative of the various types of junction transistors. Not illustrated is the fact that alpha tends to increase slightly with an

[17] The general expression for collector impedance is: $z_c = r_c/1 + pr_cC_c$; $p = j2\pi f$; C_c is the collector capacity shunting r_c.

[18] R. F. Shea, Ed., "Principles of Transistor Circuits," John Wiley & Sons, Inc., New York, N. Y., ch. 3; 1953.

[19] The expression for alpha as a function of frequency is given by:

$$\alpha = \frac{\alpha_0}{1 + j\dfrac{f}{f_a}}$$

α_0 = zero frequency value of alpha
f_a = the frequency of operation
f_a = the cutoff frequency of alpha (response of α, -3 db relative to α_0).

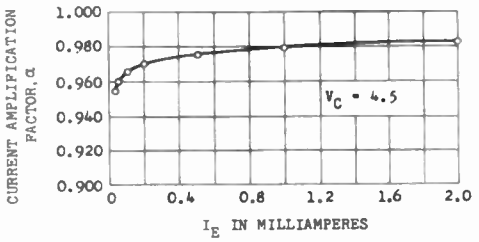

Fig. 15—Variation of α with emitter current.

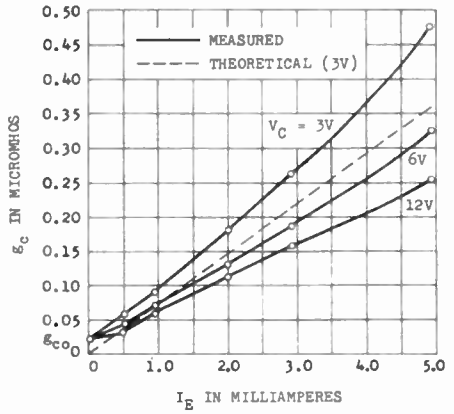

Fig. 16—Variation of collector conductance with emitter current and collector voltage.

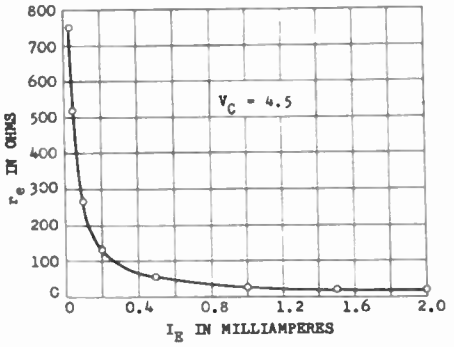

Fig. 17—Variation of r_e with emitter current.

increase in collector voltage (space-layer widening effect). This may be slightly more pronounced in fused alloy junction units than in grown junction transistors.

The dependence of collector conductance on emitter current and collector voltage has been referred to before. Note that the conductance increases linearly with emitter current. It should be kept in mind that there is an internal capacitive effect in shunt with this conductance which has been assumed to be negligible in this instance, but which can become the dominant factor at sufficiently high frequencies.

From the relationship previously obtained for the emitter junction resistance, $r_e = kT/qI_E$, it is expected that r_e would vary inversely with the value of emitter current. For an emitter current of 1 ma, the value of r_e at toom temperature is approximately 26 ohms. The value of r_e is relatively insensitive to collector voltage. As pointed out earlier, the equivalent circuit element, r_b, is influenced by internal feedback. As a result widely different values can be expected for the several types of junction transistors. In general r_b has values between 100 and 400 ohms for the usual operating conditions. It is relatively insensitive to moderate changes in emitter current and collector voltage.

For specific circuit design, detailed knowledge is required concerning the values of the equivalent circuit elements for the particular type of transistor selected.

Variation of Parameters with Temperature

The performance of germanium transistors degrades for temperatures exceeding 50 degrees C. The upper limit of useful operation is in the vicinity of 100 degrees C. Silicon is appreciably better temperature wise, the high temperature limit being over 200 degrees C. The operation of the transistor at higher temperatures is affected chiefly by the change in the saturation current and in alpha, both of which increase with temperature.

The saturation current of the collector, I_s, follows an exponential law with temperature given by,

$$(I_s)_{T_2} = (I_s)_{T_1}\epsilon^{\xi(T_2-T_1)}, \qquad (27)$$

where

T_1 = lower temperature in absolute degrees
T_2 = higher temperature in absolute degrees
ξ = temperature coefficient (about 0.08 per degree absolute for germanium).

This law predicts that I_s should double for each increment of 8.5 degrees C. (15 degrees F.) as the temperature increases. This is a remarkably consistent phenomena for germanium independent of the design of the transistor. This law of variation is modified in considering the variation of I_{c0} with temperature by the effect of leakage current which is very little affected by temperature. Typical data for the variation of I_{c0} with temperature is given in Fig. 18 for a unit with relatively low-leakage current. For this unit I_{c0} doubled with each increase of 11 degrees C. (20 degrees F.). This change with temperature is important especially in the common emitter connection when I_{c0} changes are multiplied by a large factor to produce a correspondingly large change in the collector current. As a result the operating point can be altered appreciably by a marked change in temperature. Various ways have been developed to provide temperature compensation for I_{c0}. Since the saturation current of silicon is of the order of 1/1,000 that of germanium at 25 degrees C., it offers a marked advantage in this respect even though the temperature coefficient is somewhat larger than that of germanium.

The effect of temperature on alpha is important because, as will appear in the next section, alpha enters into determining the input and output impedances and the gain of the transistor. Increasing temperature moderately increases alpha, but this increase is magnified in the expression for the short-circuit current gain of the

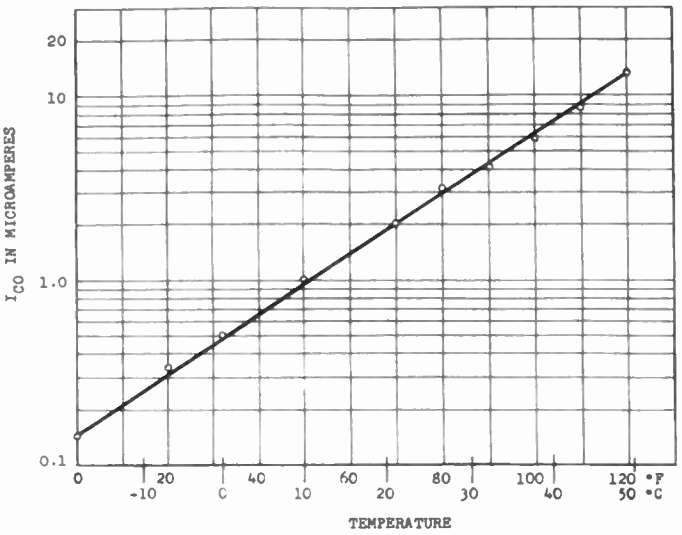

Fig. 18—Temperature dependence of I_{c0}.

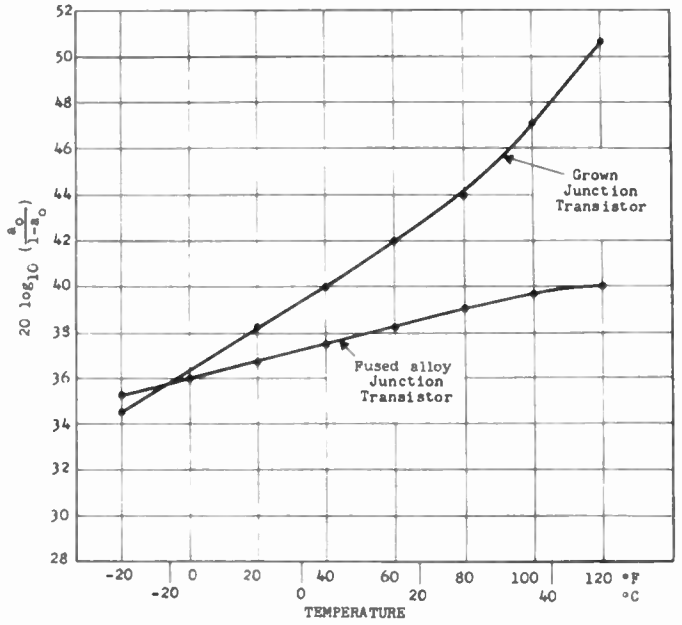

Fig. 19—Temperature dependence of $(a_0)/(1-a_0)$.

common emitter connection, $\alpha/(1-\alpha)$.[20] The effect of temperature on this factor is shown in Fig. 19 for grown junction and fused alloy junction transistors. In some double-doped grown transistors alpha can exceed unity at high temperatures in which case instability may occur. The input and output impedances can also be appreciably altered by a large increase in temperature. Fig. 20, indicates on relative scales, the way the equivalent circuit elements r_c, r_b, r_e tend to change with temperature.

A limiting factor in operation which cannot be represented by the equivalent circuit elements is that there is a maximum voltage which can be applied to the collector. For voltages in excess of the maximum, the collector back resistance rapidly decreases as though the

[20] This expression, and the corresponding expression for the common collector connection, is developed in the following section.

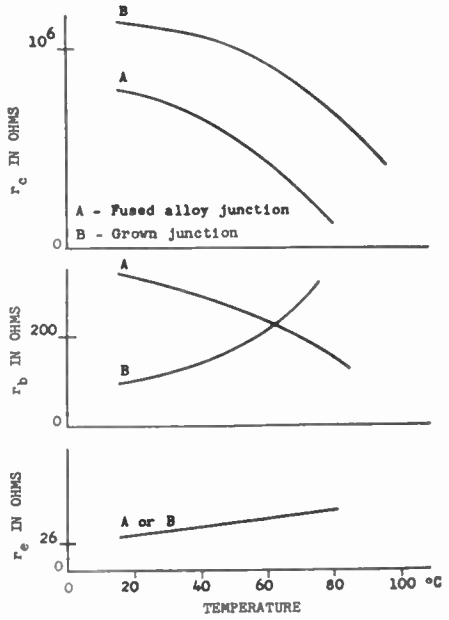

Fig. 20—Temperature dependence of r_c, r_b, r_e.

junction had been broken through. Permanent damage to the transistor may result if this occurs.

Another factor which can be limiting in the application of transistors is transistor noise. This property can be described in terms of equivalent circuit element values at the operating point. It is felt that this topic can be considered better in the light of circuit performance, and so it is included in the following section.

Circuit Aspects and Operating Properties[21]

The behavior of a transistor differs most strikingly from a pentode vacuum tube in that changes in the terminal conditions interact on each other. As a result more complicated analytical expressions are required to describe the transistor properties than those used for the electron tube. Approximations can be made in many cases which aid in obtaining simplified relationships which are adequate for most designs. Because there are a number of comprehensive articles available in this field, the material of this section will be essentially a synopsis of the important analytical relationships commonly used in single-stage transistor circuitry. The three ways of connecting the transistor in a circuit are examined and their significant features highlighted. Fig. 21 (next page) gives a synopsis for the general case of transistor for any one of the three connections in the open-circuit impedance equivalent-T network.

The Common Base Connection

A typical audio amplifier stage is shown in Fig. 22(a) which indicates a method for setting the dc operating currents and voltages. This circuit can be represented

[21] R. L. Wallace, Jr. and W. J. Pietenpol, "Some circuit properties and applications of *n-p-n* transistors," *Bell Sys. Tech. Jour.*, vol. 30, pp. 530–563; July, 1951.
"Principles of Transistor Circuits," *op. cit.*, ch. 4.

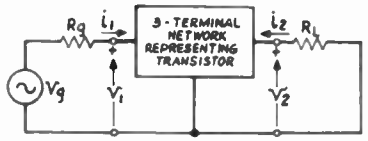

$$v_g = (r_{11} + R_g)i_1 + r_{12}i_2$$
$$0 = r_{21}i_1 + (r_{22} + R_L)i_2$$

Voltage Amplification

$$\frac{v_2}{v_g} = \frac{r_{21}R_L}{(r_{11} + R_g)(r_{22} + R_L) - r_{12}r_{21}}$$

Current Amplification

$$\frac{i_2}{i_1} = -\frac{r_{21}}{r_{22} + R_L}$$

Operating Gain

$$(\text{O.G}) = \frac{4R_gR_Lr_{21}^2}{[(r_{11} + R_g)(r_{22} + R_L) - r_{12}r_{21}]^2}$$

Input Impedance

$$R_i = r_{11} - \frac{r_{12}r_{21}}{r_{22} + R_L}$$

Output Impedance

$$R_0 = r_{22} - \frac{r_{12}r_{21}}{r_{11} + R_g}$$

Matched Input Impedance

$$R_{im} = r_{11}\left(1 - \frac{r_{12}r_{21}}{r_{11}r_{22}}\right)^{1/2}$$

Matched Output Impedance

$$R_{0m} = r_{22}\left(1 - \frac{r_{12}r_{21}}{r_{11}r_{22}}\right)^{1/2}$$

Maximum Available Gain

$$\text{MAG} = \frac{4R_{im}R_{0m}r_{21}^2}{[(r_{11} + R_{im})(r_{22} + R_{0m}) - r_{12}r_{21}]^2}$$

Fig. 21—Synopsis of generalized open-circuit impedance T network.

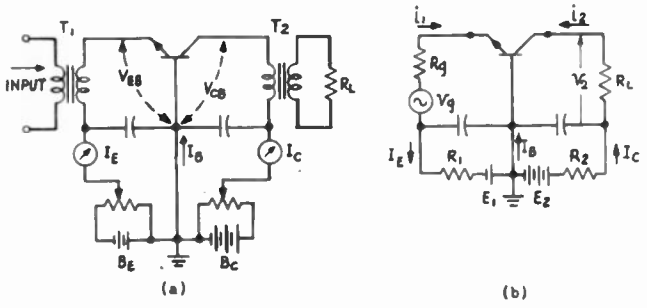

Fig. 22—Single stage common base amplifier.

as in Fig. 22(b). Direct currents are designated by I_B, I_C, I_E, and ac mesh currents by i_1, i_2; ac currents at the terminals are sometimes designated i_b, i_c, i_e. The equivalent-T networks are as shown in Figs. 23(a) and 23(b), for the open-circuit voltage generator, i_er_m, and for the infinite impedance current generator, ai_e, respectively. These generators are related by the open-circuit equality:

$$r_mi_e = ar_ci_e$$

$$a = \frac{r_m}{r_c}.$$

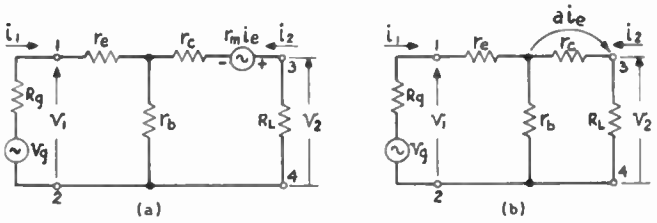

$$r_{11_b} = r_c + r_b \qquad r_{12_b} = r_b$$
$$r_{21_b} = r_m + r_b \qquad r_{22_b} = r_e + r_b$$
$$\alpha = \frac{r_b + r_m}{r_b + r_c}$$
$$v_g = (r_e + r_b + R_g)i_1 + r_bi_2$$
$$0 = (r_m + r_b)i_1 + (r_c + r_b + R_L)i_2$$

Voltage Amplification

$$\frac{v_2}{v_g} = \frac{\alpha R_L}{(r_e + r_b + R_g)\left(1 + \frac{R_L}{r_c}\right) - \alpha r_b}$$

Current Amplification

$$\frac{i_2}{i_1} = -\frac{r_m + r_b}{r_c + r_b + R_L}$$

Operating Gain

$$\text{O.G.} = \frac{4R_gR_L(r_m + r_b)^2}{[(r_e + r_b + R_g)(r_c + r_b + R_L) - r_b(r_m + r_b)]^2}$$

Input Impedance

$$R_i = r_e + r_b - \frac{r_b(r_b + r_m)}{r_b + r_c + R_L}$$

Output Impedance

$$R_0 = r_c + r_b - \frac{r_b(r_b + r_m)}{r_e + r_b + R_g}$$

Fig. 23—Synopsis of common base circuit.

The short-circuit current gain, which is designated as alpha (α) in this connection, is obtained from current amplification equation (Fig. 23).

$$\left.\frac{i_2}{i_1}\right|_{R_L=0} = -\alpha = -\frac{r_b + r_m}{r_b + r_c} \cong -a. \qquad (28)$$

Alpha (α) and, a, should not be confused. Within the scope of this paper they are indistinguishable, but at higher frequencies this may not be true. Very useful approximations can be obtained from the exact expressions under the following conditions. In general the base resistance, r_b, can be neglected in comparison with the collector resistance, r_c. The emitter resistance, r_e, can be neglected compared to $(r_c - r_m)$, r_c, or r_m. Often the load resistance, R_L, can be neglected compared to $(r_c - r_m)$, r_c, or r_m. The relationships of (28) are frequently used. Limiting values for the exact expressions are obtained with these assumptions, and by allowing either R_g or R_L to go to zero or infinity. The limiting voltage gain results when $R_g = 0$ and $R_L = \infty$.

The dc emitter current, I_E, is set by the effective bias voltage in the emitter base circuit, divided by the total dc resistance of that mesh. By making the external resistance much greater than the internal resistance of the emitter to base path, the external resistance determines the value of the dc emitter current. The dc collector current I_C is set when I_E has been determined. The value of I_{C0} is either specified or found by measuring

the collector current at the operating bias, with the emitter open-circuited.

Data is given in the following Table I to illustrate typical numerical values for an *NPN* transistor in the common base connection at a frequency of 1,000 cycles

TABLE I

Measured h Parameters	Calculated r Parameters (23)	Calculated g Parameters (26)
$h_{11b}=$ 35 ohms	$r_{11b}=233$ ohms	$g_{11b}=$ 28,000 μmhos
$h_{12b}=$ 1.3×10^{-4} (ratio)	$r_{12b}=217$ ohms	$g_{12b}=-3.7$ μmhos
$h_{21b}=-0.91$ (ratio)	$r_{21b}=1.5$ megohms	$g_{21b}=-26{,}000$ μmhos
$h_{22b}=$ 0.60 (μmho)	$r_{22b}=1.7$ megohms	$g_{22b}=$ 4.0 μmhos

per second, and for $I_E=-1.0$ ma, $V_{cb}=4.5$v. The subscript, b, on the parameters designates the common circuit element (b = base) as the abbreviation for the common base connection. The features of the common base connection are:

1. It is suitable for working between a low impedance source and a high impedance load. (Unlike the vacuum tube the input impedance is very low.)
2. In this connection the current amplification is less than unity.
3. Power gains of the order of 40 db can be obtained between matched impedances, and appreciable power gain can be realized for load resistances of only a few thousand ohms.
4. The output voltage is in phase with the input voltage. (This resembles the grounded grid connection for a vacuum tube.)
5. The widest operating frequency range is obtained with this connection. (The top frequency is at present very much less than that of conventional electron tubes).
6. It is necessary to use interstage transformers in cascading common base stages in order to obtain gain.

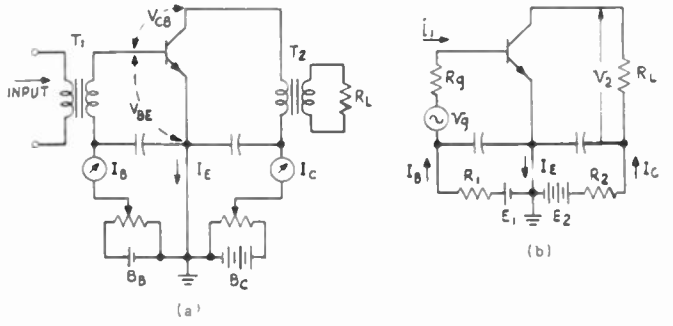

Fig. 24—Single stage common emitter amplifier.

The Common Emitter Connection

A typical circuit for this connection is shown in Fig. 24(a) and (b). The equivalent-T networks and a synopsis of properties are given in Fig. 25. It is often more useful to use a current generator instead of a voltage generator as the active element in the equivalent circuit. The way this is done is indicated in Fig. 26. The first two diagrams (a) and (b) relate the current and voltage generators as functions of the emitter current.

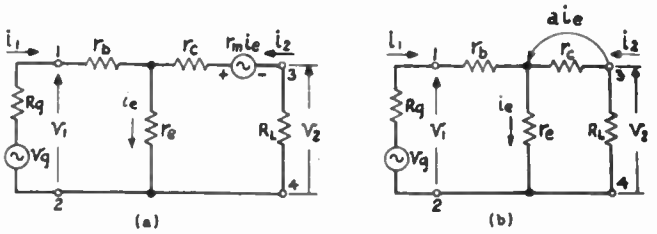

$$r_{11_e}=r_b+r_e \qquad r_{12_e}=r_e$$

$$r_{21_e}=r_e-r_m \qquad r_{22_e}=r_e+r_c-r_m$$

$$v_g=(r_b+r_e+R_g)i_1+r_e i_2$$

$$0=(r_e-r_m)i_1+(r_e+r_c-r_m+R_L)i_2$$

Voltage Amplification

$$\frac{v_2}{v_g}=\frac{(r_e-r_m)R_L}{(r_b+r_e+R_g)(r_e+r_c-r_m+R_L)-r_e(r_e-r_m)}$$

Current Amplification

$$\frac{i_2}{i_1}=-\frac{r_e-r_m}{r_e+r_c-r_m+R_L}$$

Operating Gain

$$\text{O.G.}=\frac{4R_gR_L(r_e-r_m)^2}{[(r_b+r_e+R_g)(r_e+r_c-r_m+R_L)-r_e(r_e-r_m)]^2}$$

Input Impedance

$$R_i=r_b+r_e-\frac{r_e(r_e-r_m)}{r_e+r_c-r_m+R_L}$$

Output Impedance

$$R_0=r_e+r_c-r_m-\frac{r_e(r_e-r_m)}{r_b+r_e+R_g}$$

Fig. 25—Synopsis of common emitter circuit.

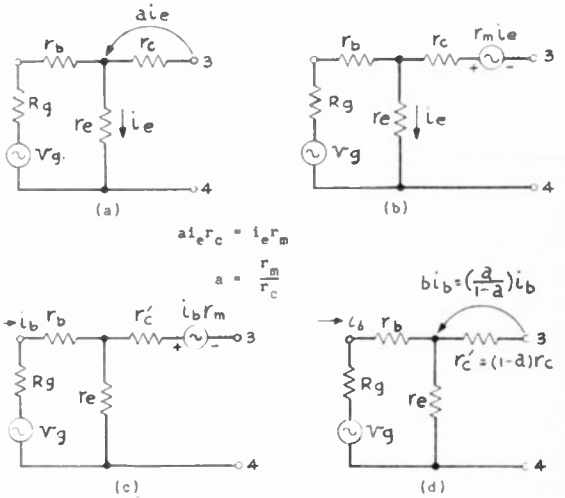

$$ai_e r_c = i_e r_m$$

$$a=\frac{r_m}{r_c}$$

$$i_b r_m = b i_b r_c'$$

$$\therefore\quad r_c'=\frac{a}{b}r_c$$

$$bi_b=ai_e$$

$$i_b=(1-a)i_e$$

$$\therefore\quad b=\left(\frac{a}{1-a}\right)$$

and

$$r_e'=(1-a)r_e$$

Fig. 26—Current generator transformations, common emitter circuit.

Diagrams (c) and (d) relate current and voltage generators as functions of the input (base) current. From the relationship between the current generators of (a) and

(d) and the value of the base current in terms of emitter current, the current gain factor, b, is obtained. Note the following features of this circuit connection.

1. A large current gain can be realized which has a short circuit value of

$$b = \frac{a}{1 - a}. \tag{29}$$

2. The output impedance is reduced by the factor (1−a). It follows from (2) that the capacity shunting r_c will be multiplied by the factor $[1/(1-a)]$ as r_c is reduced to $(1-a)r_c$. This effect reduces the frequency response inversely as the gain factor as compared to the response of the common base connection. If the frequency at which the response of a is reduced 3 db in the common base connection is designated f_1, and the frequency at which the response of b is down 3 db in the common emitter connection is designated f_b, the relationship between these two cut off frequencies is

$$f_b = (1 - a)f_a. \tag{30}$$

For example: if $a = 0.980$ and $f_a = 1$ mc.

$$f_b = 20 \text{ kc}.$$

This points up a limitation in the use of this connection in which bandwidth is exchanged for gain.

The effect of the gain parameters is clearly brought out by the relationships between the currents of the transistor. These are given for both ac and dc conditions in Table II and are independent of the transistor connections.

TABLE II

Ac Conditions	Dc Conditions
$i_c = ai_e$	$I_C = aI_E + I_{c0}$
$i_b = i_e - i_c$	$I_B = I_E - I_C$
$= (1 - a)i_e$	$= (1 - a)I_E - I_{c0}$
$i_c = \left(\frac{a}{1-a}\right)i_b$	$I_C = \left(\frac{a}{1-a}\right)I_B + \frac{I_{c0}}{(1-a)}$
$i_e = \left(\frac{1}{1-a}\right)i_b$	$I_E = \frac{I_B}{(1-a)} + \frac{I_{c0}}{(1-a)}$

In this connection the dc emitter current, I_E, depends on the value of the base current and on the value of a. It is noted that I_{c0} also contributes to the value of I_E because of the large multiplication factor $[1/(1-a)]$. When I_B is much larger than I_{c0}, I_B determines I_E. The base current is given by the base to emitter voltage divided by the mesh resistance. Again, if the external resistance is much larger than the internal resistance, the external resistance establishes the value of the base current. The significance of temperature effects on a, and I_{c0}, as discussed in the previous section can now be fully appreciated in the light of the changes produced by these effects in the ac and dc currents.

Typical numerical values for this connection for the transistor of the previous example are given in Table III at 1,000 cycles per second and for $I_B = 80$ μamp., $V_c = 4.5$v.

TABLE III

Measured h Parameters	Calculated r Parameters (23)	Calculated g Parameters (26)
$h_{11e} = 500$ ohms	$r_{11e} = 380$ ohms	$g_{11e} = 2{,}000$ μmhos
$h_{12e} = 0.72 \times 10^{-4}$ (ratio)	$r_{12e} = 16$ ohms	$g_{12e} = -0.14$ μmhos
$h_{21e} = 7.8$ (ratio)	$r_{21e} = -1.7$ megohms	$g_{21e} = 16{,}000$ μmhos
$h_{22e} = 4.5$ μmhos	$r_{22e} = 0.22$ megohms	$g_{22e} = 3.4$ μmhos

Important features of the common emitter connection are:

1. The input impedance is relatively low (of the order of 1,000 ohms).
2. Power and voltage gains can be realized with a relatively low load impedance (of the order of 1,000 ohms).
3. Large current gain is realized.
4. The frequency range is reduced inversely as the gain factor.
5. There is a phase reversal between the input and output voltages.
6. The input and output impedances are very dependent on the factor α.
7. Several stages can be effectively cascaded without interstage transformers.

The Common Collector Connection

A representative circuit for the common collector connection and its equivalent diagram is shown in Fig. 27(a) and (b). The corresponding equivalent-T net-

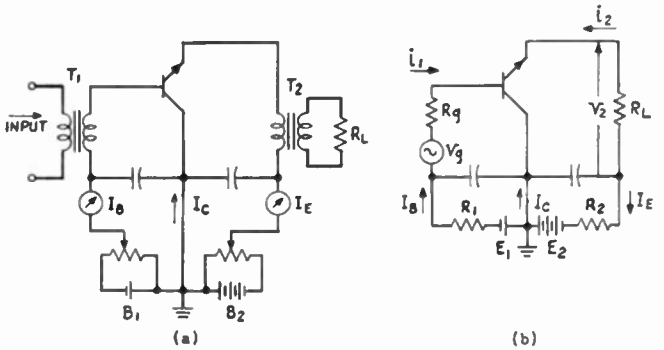

Fig. 27—Single-stage common collector amplifier.

works and the synopsis of its properties are given in Fig. 28. The equivalent circuit in terms of the base current is obtained from Fig. 26(d), as shown in Fig. 29. From this circuit, as well as from current amplification equation, Fig. 28, it is noted that the short-circuit current gain, $(R_L = 0)$ is

$$\frac{i_2}{i_1} = \frac{i_2}{i_b} = -\frac{1}{1 - a}. \tag{31}$$

and that the output impedance is reduced by the same factor $(1-a)$, as in the common emitter case. The same limitation with respect to frequency results. An important property of this circuit is the relatively high input impedance which can be developed by using a high load resistance (input impedance equation, Fig. 28). Since no voltage gain is possible (voltage amplification equation, Fig. 28) and the phase is unchanged, this connection resembles the cathode follower connection for the electron tube.

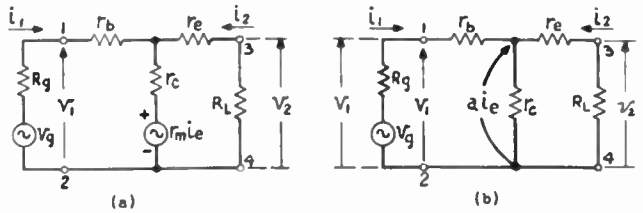

$$r_{11_c} = r_b + r_c \qquad r_{12_c} = r_c - r_m$$
$$r_{21_c} = r_c \qquad r_{22_c} = r_e + r_c - r_m$$
$$v_g = (r_b + r_c + R_g)i_1 + (r_c - r_m)i_2$$
$$0 = r_c i_1 + (r_e + r_c - r_m + R_L)i_2$$

Voltage Amplification

$$\frac{v_2}{v_g} = \frac{r_c R_L}{(r_b + r_c + R_g)(r_e + r_c - r_m + R_L) - r_c(r_c - r_m)};$$

Current Amplification

$$\frac{i_2}{i_1} = -\frac{r_c}{r_e + r_c - r_m + R_L}$$

Operating Gain

$$\text{O.G.} = \frac{4R_g R_L r_c^2}{[(r_b + r_c + R_g)(r_e + r_c - r_m + R_L) - r_c(r_c - r_m)]^2}$$

Input Impedance

$$R_i = r_b + r_c - \frac{r_c(r_c - r_m)}{r_e + r_c - r_m + R_L}$$

Output Impedance

$$R_0 = r_e + r_c - r_m - \frac{r_c(r_c - r_m)}{r_b + r_c + R_g}$$

Fig. 28—Synopsis of common collector circuit.

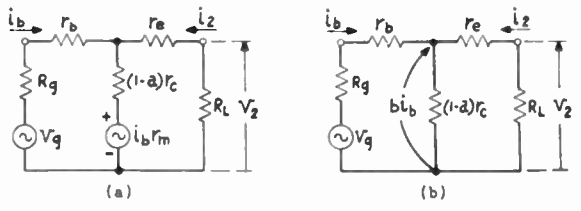

Fig. 29—Equivalent circuit generators for input current, common collector circuit.

The significant properties of the common collector connection are:

1. Moderate power gain realized by high current gain.
2. No voltage gain.
3. Output voltage in phase with input voltage.
4. Much higher input impedance realizable for this connection than for either of other connections.
5. Operating frequency bandwidth reduced by the increased current gain factor relative to that of the common base connection.
6. Only current gain can be realized by directly coupling these stages in cascade, the voltage gain approaching unity.

Properties Affecting Frequency Response

Physical phenomena, discussed in the introductory part of this paper, lead to the expectation that the frequency response of the junction transistor will fall off at much lower frequencies than is noted in well-designed electron tubes. The controlling properties involve the geometry of the transistor and the physical constants of the germanium, modified by processing techniques.

One of the basic mechanisms limiting the frequency response is qualitatively described as follows. The carriers of charge injected from the emitter into the base region move by a process of diffusion which requires a small but appreciable time for a carrier to complete the journey to the collector. Because there is a dispersion in the transit time for a group of carriers which started at the same instant, they do not arrive at the same instant. When this difference in the time of arrival becomes an appreciable part of a cycle of the input excitation, the dispersion causes some of the carriers to cancel the effect of others at the collector, and frequency response falls off. At higher frequencies the effect becomes more pronounced, and the response continues to decrease as the frequency increases.

Identifying this property with the equivalent circuit, this means that above a certain frequency, r_m, and therefore, a, starts to decrease for increasing frequency. The frequency for which, a, has decreased to 0.707 of its dc value is the cutoff frequency of the transistor, f_a. This frequency is inversely proportional to the square of the base layer thickness. It can be measured in common base connection from which corresponding cutoff frequencies for the other two connections can be derived.

The frequency response of the transistor (as a voltage amplifier) is also limited by shunt capacity effects at both the emitter junction and the collector junction. In terms of the equivalent circuit elements, this means that r_e and r_c are each shunted by a capacitor. With respect to the emitter junction, this effect can be reduced by lowering the impedance of the driving source. Since r_b remains in series with the source impedance, the value of r_b ultimately determines the emitter cutoff frequency.

Collector capacitance can result in a cutoff frequency appreciably lower than that expected from emitter cutoff, or even the cutoff due to dispersion in transit times. The effect of collector capacity is to shunt the series combination of r_c and the generator $i_e r_m$ in the equivalent-T common base circuit. The equivalent circuits of the common emitter and common collector connections are correspondingly affected. The effect of higher frequencies on the performance of the transistor will be discussed in the next paper in this series.

Noise Properties

Noise in junction transistors appears to be generated by physical properties which are being improved as the transistor is improved. Much study has been given to methods for evaluating the noise produced by the transistor.[22] In this respect, the noise figure is the most satisfactory. This figure is the ratio of the signal-to-noise for the ideal noiseless amplifier, to the signal-to-noise for the actual amplifier having the same gain and bandwidth and terminations. The noise figure of a transistor amplifier depends on the input generator resistance, the gain, the bandwidth and the dc operating point of the transistor. For transistors the noise figure is usually given in db per cycle of bandwidth at 1,000 cycles per second. Noise figures still show an undesirably large spread in values, but there are indications that a noise figure near 10 db can be consistently attained. A noise figure of 20 db appears to be representative at the present time. These values are for an emitter current of 1.0 ma and a collector voltage of 4.5v. The noise figure varies slightly with the source impedance in the vicinity of a match with the input impedance, where it is minimized. It is frequently improved by operating the transistor at as low a collector voltage and current as practical. Below 1,000 cycles per second, the noise figure generally increases, and may be appreciably greater at 100 cycles per second. The noise figure increases again at higher frequencies when the gain of the device falls off faster than the generated noise.

Special Features

It is appropriate to close this review of the basic properties of junction transistors by pointing out several features in which it is markedly superior to electron tubes.

The first of these is that it is free from microphonic effects, thus eliminating the need for shock mounting or vibration isolation, so often required in vacuum tube applications. The transistor is a "cold emitter" device, and therefore no power corresponding to that for the vacuum tube filament or cathode is required.

Other features can be brought out by a consideration of the static characteristics of the junction transistor. These are of great utility paralleling in this respect, the use of vacuum tube static characteristics which they resemble. A representative set of junction transistor characteristics is given in Fig. 30(a) for the common base connection. This shows the collector current, collector voltage characteristics, with emitter current as the parameter. The almost ideal nature of the family of output characteristics is a feature not found in electron tube characteristics. By amplifying the co-ordinate scales near the origin, as shown in Fig. 30(b) the low-power performance capability is clearly illustrated. This highlights an important feature of the junction transistor which is that it can operate at maximum gain with only a few microwatts of input power. The broken lines across the characteristics are for constant power dissipation in the unit of 10, 50 and 100 microwatts. For these powers, a collector voltage of the order of a half a volt can be effectively used. Class A operating efficiencies of 48.5 per cent have been obtained with junction transistors where the theoretical limit is 50 per cent. This brief résumé does not give a complete picture of the static characteristics of the device as there is a set of input characteristics which must also be considered in large signal operation where input distortion is important.

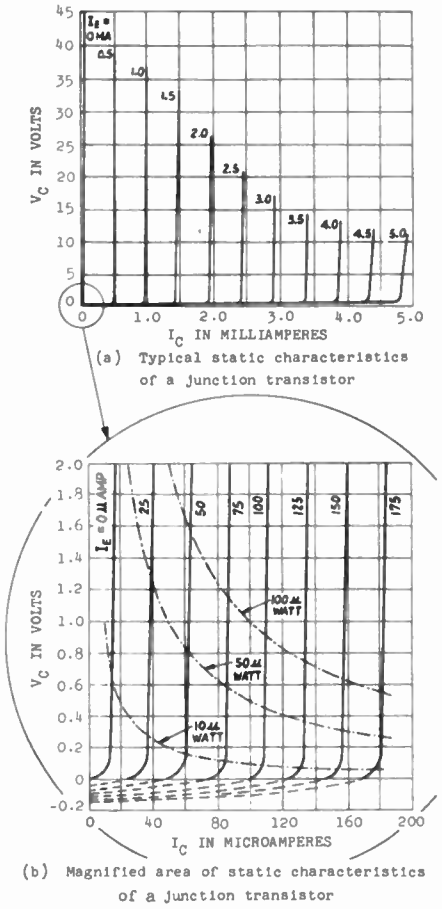

Fig. 30—Output static characteristics, common base connection.

Similar sets of static characteristics are obtained for the common emitter and the common collector connection with base current as the parameter. These are generally less ideal than those of the common base circuit. More comprehensive discussions of the static characteristics of the junction transistor and their uses will be found in the next two papers of this series.[23,24]

[22] E. Keonjian and J. S. Schaffner, "An experimental investigation of transistor noise," PROC. IRE, vol. 40, pp. 1456-1460; November, 1952.
H. C. Montgomery, "Transistor noise in circuit applications," PROC. IRE, vol. 40, pp. 1461-1471; November, 1952.

[23] R. L. Trent, "Design principles of junction transistor audio amplifiers," *Trans.-PGA* (to be published).

[24] D. R. Fewer, "Design principles for junction transistor audio power amplifiers," *Trans.-PGA* (to be published).

Low Distortion Operation of Some Miniature Dual Triodes*

J. Z. KNAPP†

Summary—**The variation of distortion with available parameters for low level rc-coupled triode stages is investigated and, the possibility of minimizing second harmonic distortion utilizing signal-source impedance and the nonlinear, noninfinite dynamic grid resistance as an amplitude-correcting device, is explored and found to warrant further consideration. Some data on distortion-level reproducibility for randomly-selected tubes is presented and the limitation of local feedback as a distortion reduction scheme is pointed out. Variation of distortion with signal level is discussed and demonstrated.**

INTRODUCTION

IN DISTORTION, as in any other measurable quantity, the engineering questions are: What is attainable? What is reproducible? What is the effect of a tolerance margin on reproducibility? For low-level audio-frequency work, the rc-coupled stage is the accepted building block. I will center this discussion around four of the more widely used miniature dual triodes in this type of service; since this discussion is inherently a laboratory report, mention of the test setup and measuring equipment is germane.

In Fig. 1, the GR oscillator is terminated in a 600-ohm T pad to permit operations of the oscillator at constant level and distortion. The UTC 1kc bandpass filter is fed from the specified 10K source and terminated in a 10K potentiometer. The lower end of the "pot" is used as an output vernier in conjunction with the stepped T pad. The measured signal distortion was 0.035 per cent and was constant with level.

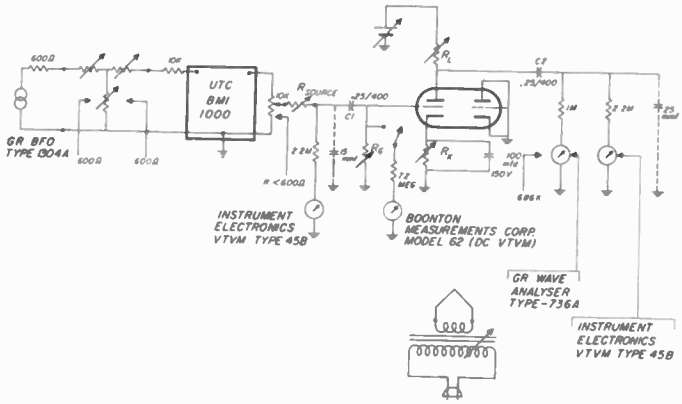

Fig. 1—Test setup schematic.

Since the rc stage as used is almost never fed from a source within looking distance of being zero impedance, we have included a series source resistor and will shortly find that it can play an important role in the net distortion measured in the output signal.

The rc stage has been set up so that all available variables can be controlled. To eliminate any possibility of interaction, the elements of the second triode have been strapped together and tied to ground. The ac load presented to the stage by the parallel combination of the wave analyzer and VTVM is 686K in parallel with 25 mmfd, a fairly typical value for a stage at this level. The values of input and output coupling capacitors are large enough and the values of input and output shunt capacity are small enough to justify the neglect of their effect at the 1,000 cycle frequency used throughout this paper. The cathode bypass capacitor voltage rating was selected to minimize the effect of capacitor leakage current on the tube operating point. All curves will be recorded at a constant 2v output unless otherwise specified.

Using the 12AT7 and selecting a fairly typical set of operating conditions ($E_{bb}=250$v, $R_g=500$K, $R_L=100$K).

Fig. 2 (next page) shows variation of second harmonic distortion as source impedance is varied, R_K being the independent variable. It can be seen for a sufficiently large R_K, i.e., sufficiently negative grid, all curves coalesce to a single value. Curve 2 is typical of the measurements usually shown, a rc stage with its dc operating conditions isolated by the coupling capacitors and fed from low impedance source. At $R_K=0$, stage bias is determined by the intersection of the grid circuit load line with the e_c-i_c characteristic; this bias point was at 0.78v for the tube used. With a low impedance source, we can see a rather broad shallow second harmonic null (D_2 min = 0.40 per cent) centered around a mean R_K of 1.4K ohms. In curve 3, the source impedance has been raised to 5K ohms, and the distortion null is 6 db better than the best obtainable with a low impedance source. For curve 4, source impedance has been raised to 50K ohms; since this is typical of many interstage values, it will be used as a comparison standard. We can see a rather sharp null at 600 ohms whose best value is 0.135 per cent, 9.5 db better than the low impedance source value. Curves 5 and 6 are for respectively 100K and 500K source impedances. Distortion minima are respectively 6.8 and 4.6 db better than that obtained from low impedance source.

Curve 1 represents a 12AT7 fed from a 600-ohm source with a total grid circuit DCR 600 ohms, conditions equivalent to transformer coupling. The second harmonic null is now 18 db better than that obtainable from a low impedance source. Final determination of

* Manuscript received March 8, 1955.
† United Transformer Co., 150 Varick St., New York, N. Y.

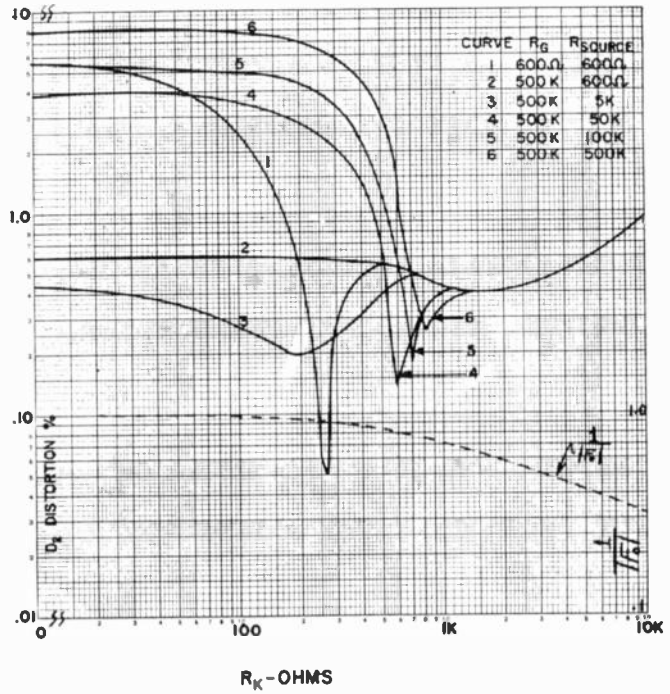

Fig. 2—Second harmonic distortion with variation of source impedance. Schematic per Fig. 1 with 12AT7. $R_L = 100K$, $E_{bb} = 250$.

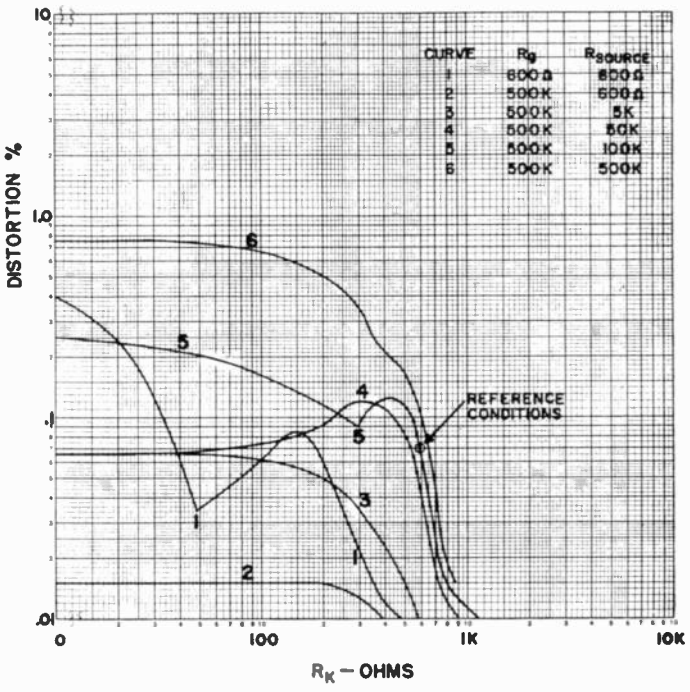

Fig. 3—Third harmonic distortion with variation of source impedance, schematic per Fig. 1 with 12AT7. $R_L = 100K$, $E_{bb} = 250$.

operating point will, of course, await an inspection of third harmonic distortion and reproducibility.

At the bottom of Fig. 2 is a curve of $1/|F_0|$, the available local feedback. We can see that the net second harmonic distortion using local feedback will be approximately constant as R_K increases. However, if we adopt a criterion of maximizing the $(A_O)(1-D_T)$ product, which is the raw material of any feedback amplifier, we shall see that this is a losing battle indeed; since the net second harmonic is roughly constant with increase of local feedback (unbypassed R_K) any additional reduction of distortion must be accomplished in some overall loop.

Fig. 3 shows the variation in third harmonic distortion corresponding to the preceding second harmonic distortion. Minimum total distortion for curve 1, the transformer equivalent condition is 0.056 per cent; for the case of the 50K ohm source with the usual capacitor isolation of the dc grid circuit the minimum for this tube is 0.14 per cent (the best attained was 0.07 per cent total harmonic at this value of source impedance as will be seen later), while conventional biasing will produce 0.40 per cent total harmonic for this tube. An inspection of Figs. 2 and 3 will show that the worst possible condition was obtained with grid leak bias and high source impedance.

In the distortion curves of Figs. 2 and 3, the plate load impedance has been held constant; we can assume that gain and plate current (Fig. 4) variations should be small for all curves. The cross-hatched area in the gain curve of Fig. 4 represents the total variation in measured gain, due in large part to waveform distortion in the region of low cathode bias.

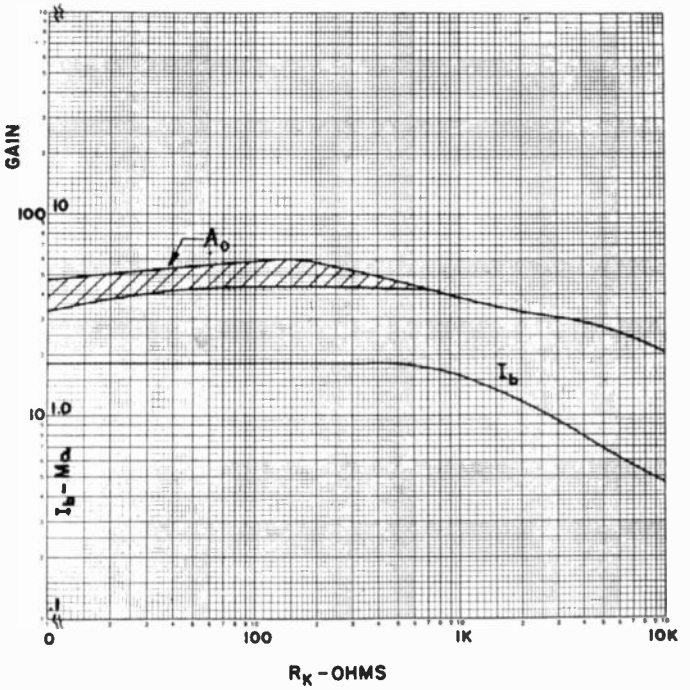

Fig. 4—Gain and plate current variation of conditions of Figs. 2 and 3.

From the fact that the plate current is constant from the region of grid leak bias practically up to the point where grid current cuts off, we can conclude that

$$e_c = {}_{ic}R_g + {}_{ib}R_k \doteq \text{constant}$$

in this region.

In Fig. 5, source impedance and load impedance ($R_L = 100K$, $R_S = 50K$) have been kept constant and second harmonic distortion has been determined for variation of R_G, R_K is again the independent variable.

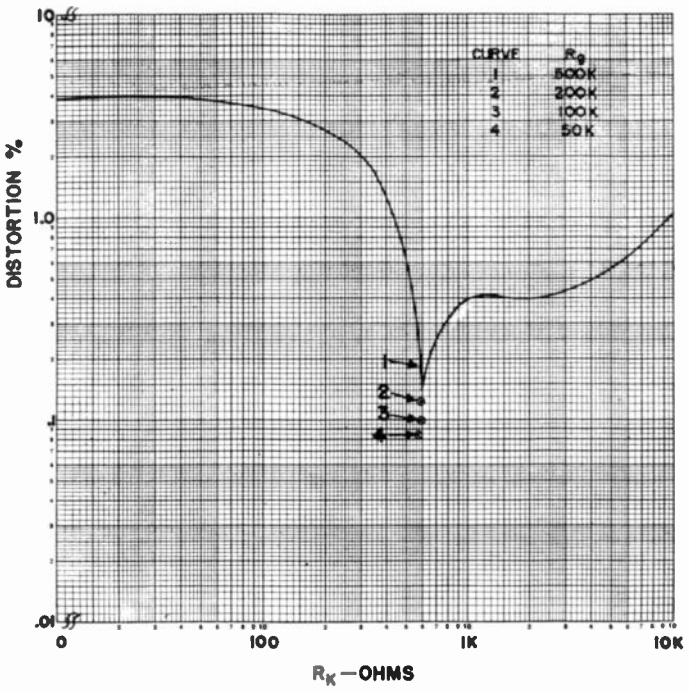

Fig. 5—Variation of second harmonic distortion. Schematic per Fig. 1 with 12AT7. $R_{source}=50K$, $R_L=100K$, $E_{bb}=250$.

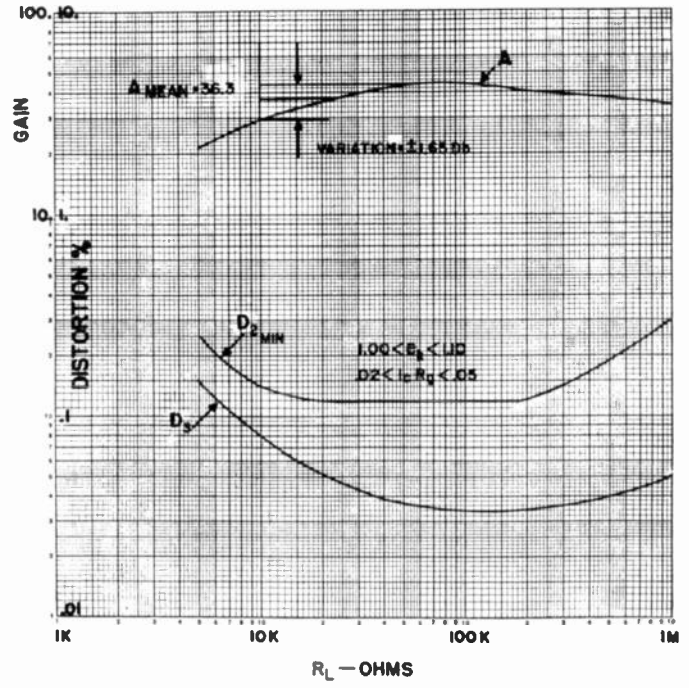

Fig. 6—Gain and distortion variation with variation of R_L schematic per Fig. 1 with 12AT7. $R_{source}=50K$, $E_{bb}=250$.

Data was taken for an R_g variation of 500K, 200K, 100K and 50K. Since the curves separate only in the vicinity of the minimum point, the $R_g=500K$ curve has been drawn and the minimum points of the other curves indicated. It will be seen that the second harmonic null increases as R_g decreases, an indication that we are selecting a more favorable operating point on the e_c-i_c characteristic. Within the limits of experimental error, no variation in third harmonic distortion was recorded.

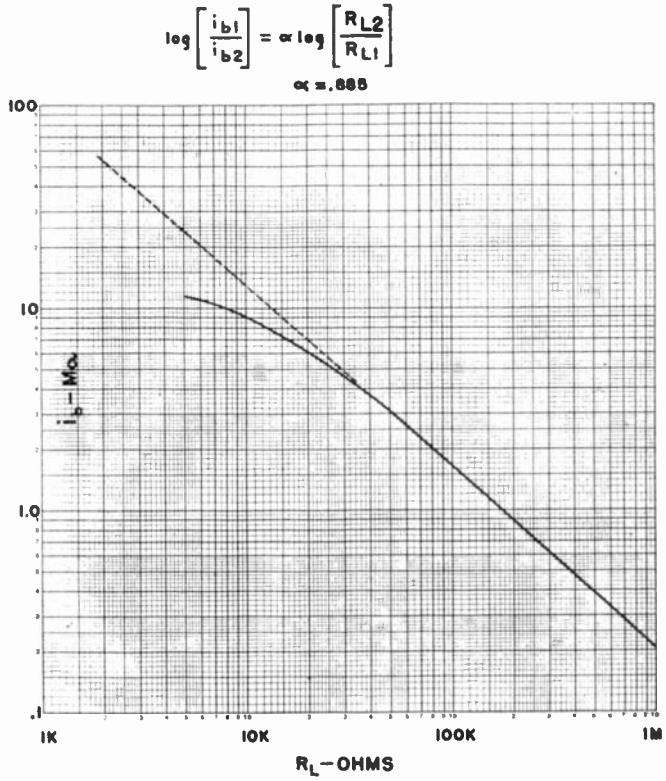

Fig. 7—Plate current variation for minimum second harmonic distortion. Schematic per Fig. 1 with 12AT7. $R_{source}=50K$, $E_{bb}=250$.

The data for Fig. 6 was taken using a 50K ohm source impedance, a 500K R_g, and an R_K selected to give minimum second harmonic distortion at each data point. For an R_L variation from 10K to 1 megohm the total gain variation, with constant E_{bb}, was ± 1.65 db. On the basis of a total distortion minimum, it can be seen that the preferred operating range is somewhat smaller ranging from approximately 60K to 200K ohm plate loads. The rather small variations of e_K and e_{CG} for minimum distortion operation are indicated in Fig. 6.

In Fig. 7, a plot of *ib* vs R_L for the minimum distortion condition shows good log-log linearity (5 per cent error at $R_L=27K$) from the straight line graph. The straight line equation is found at the head of the graph.

So far we have seen an effect, to examine the cause we must refer to Fig. 8 (next page). Fig. 8 is typical of the simplified grid current component graphs available in the literature (grid current and plate current are drawn to different scales here). Considering the grid load line indicated, the intersection of the grid load line and the e_c-i_c characteristic (in the absence of any other bias) will determine the grid operating point. With cathode bias at the operating point the dynamic grid resistance

$$r_g = \left.\frac{de_c}{d_{ic}}\right|_{eb=K}$$

in parallel with the grid leak and this combination in series with the source impedance will, with fair accuracy,

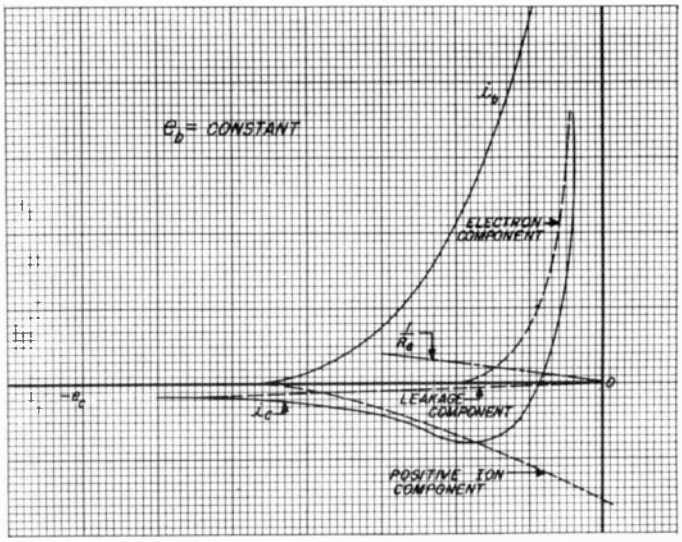

Fig. 8—Simplified e_c-i_c and e_c-i_b characteristic.

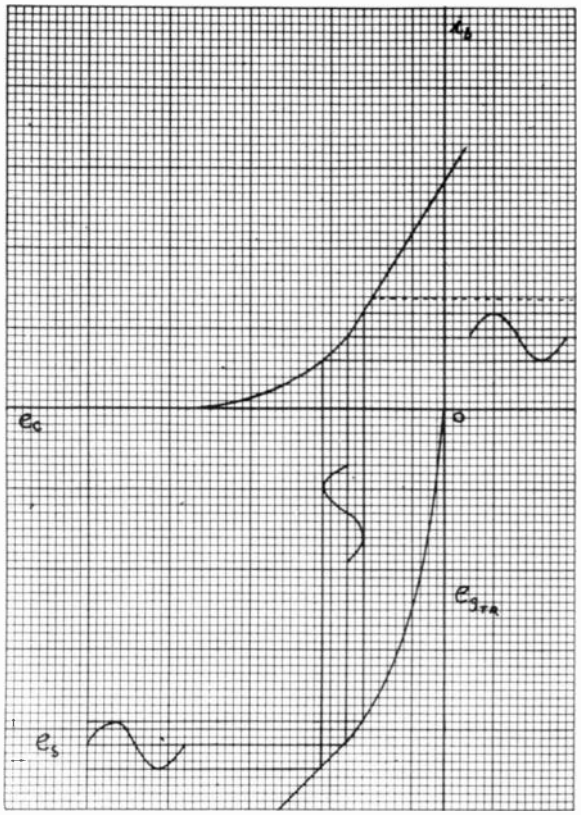

Fig. 9—Grid circuit cancellation of plate circuit distortion.

determine the actual signal grid voltage. As can be seen from the e_c-i_c characteristic, r_g decreases as e_c goes positive. The positive ion component of grid current, in the miniature dual triodes considered, was of negligible importance; there was, therefore, no point of zero slope (r_g maximum) other than that encountered at $i_c=0$.

In Fig. 9, the mechanism of distortion reduction through the use of source impedance has been indicated. On the positive signal swing, r_g decreases, decreasing the net signal voltage at the control grid, the predistorted signal is then amplified and undergoes compression on the negative half-cycle. If the operating point has been judiciously chosen, the distortion reduction previously noted is encountered.

In Fig. 10 (opposite), the sensitivity to R_L tolerance of this distortion reduction (comparison standard schematic values) has been investigated. To retain a 6 db reduction of distortion total over plateau operation, a variation of slightly more than ± 5 per cent in R_L can be tolerated. It is interesting to note that the gain variations are miniscule for the -30 per cent R_L variation from normal. The circled points are circuit response with comparison standard valued components and voltages.

In Fig. 11 (opposite), sensitivity to E_{bb} and in Fig. 12 sensitivity to E_F have been investigated. In each case, a variation of approximately 5 per cent in nominal still resulted in 6 db distortion reduction. In Fig. 12, a second harmonic minimum 6 db greater than that previously encountered was found at a 6.8 filament voltage. We might expect, therefore, that some higher Gm specimen might give us this greater reduction at normal filament operating voltage. Further specimens of this tube will be examined to determine reproducibility of this phenomena from tube to tube.

At this point it might be desirable to stop and ask: We have considered the effects of E_F and E_{bb} separately. Consider an amplifier with unregulated plate and filament voltage where both are at the mercy of line variation. Can we predict the results that appear in Fig. 13 from a consideration of Figs. 11 and 12 (on the next page)?

Fig. 13 shows circuit sensitivity to E line and underscores the fact that we are dealing with a path of operation on a three-dimensional envelope complicated further by the effect of the nonlinear dynamic grid impedance.

Figs. 14 through 21 on the following pages 130, 131, and 132, show distortion reproducibility for five randomly selected tubes of each of the types considered—12AT7, 12AU7, 12AX7, 12AY7. Each type exhibits the same distortion cancellation effect. The variation of second harmonic distortion in the region of recommended operation is as follows in Table I below.

TABLE I

Tube	D_{Min}/D_{Max}
12AT7	1:1.38
12AU7	1:1.23
12AX7	1:1.5
12AY7	1:1.27

A tabulation of conditions at the point of minimum distortion is listed in Table II (next page) ($R_L=100$K, $R_G=500$K, $E_{bb}=250$v, $R_{source}=50$K).

All previous measurements were made at a constant output level of 2v; it is also of interest to see what variation of distortion will occur with change of level. Figs. 22 and 23 (page 132) show variation of second and

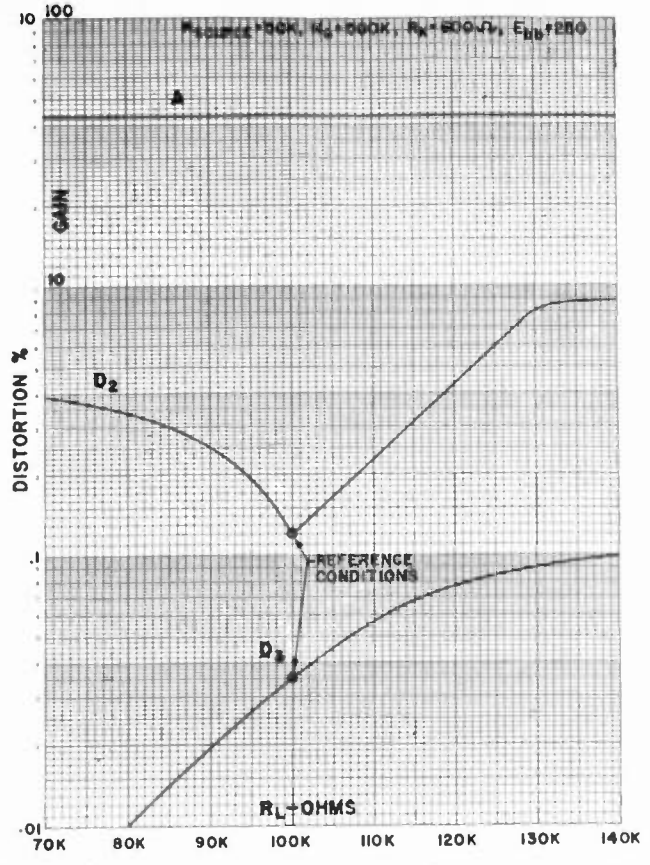

Fig. 10—Gain and distortion variation for ΔR_L schematic per Fig. 1 with 12AT7. $R_{source}=50K$, $R_G=500K$, $R_K=600\Omega$, $E_{bb}=250$.

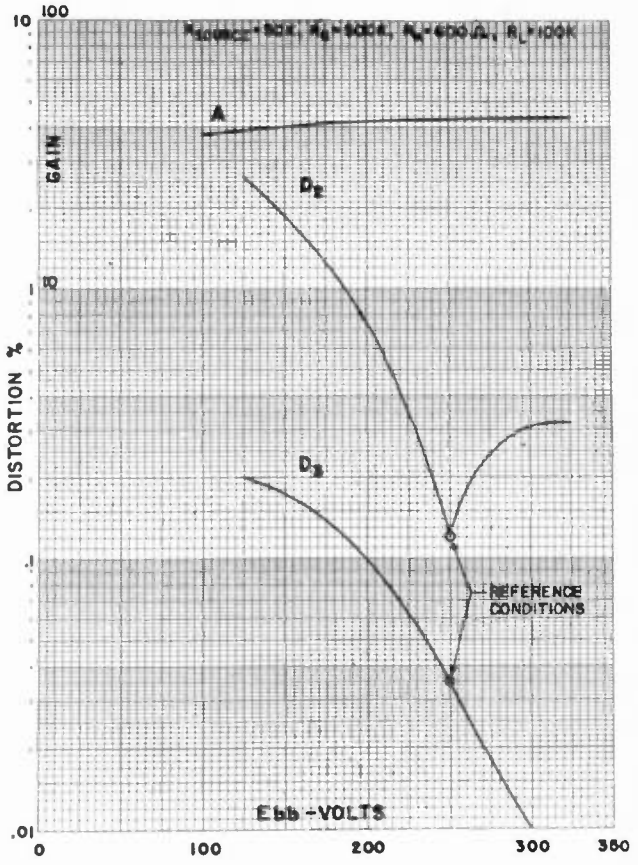

Fig. 11—Gain and distortion variation for ΔE_{bb} schematic per Fig. 1 with 12AT7. $R_{source}=50K$, $R_G=500K$, $R_K=600\Omega$, $R_L=100K$.

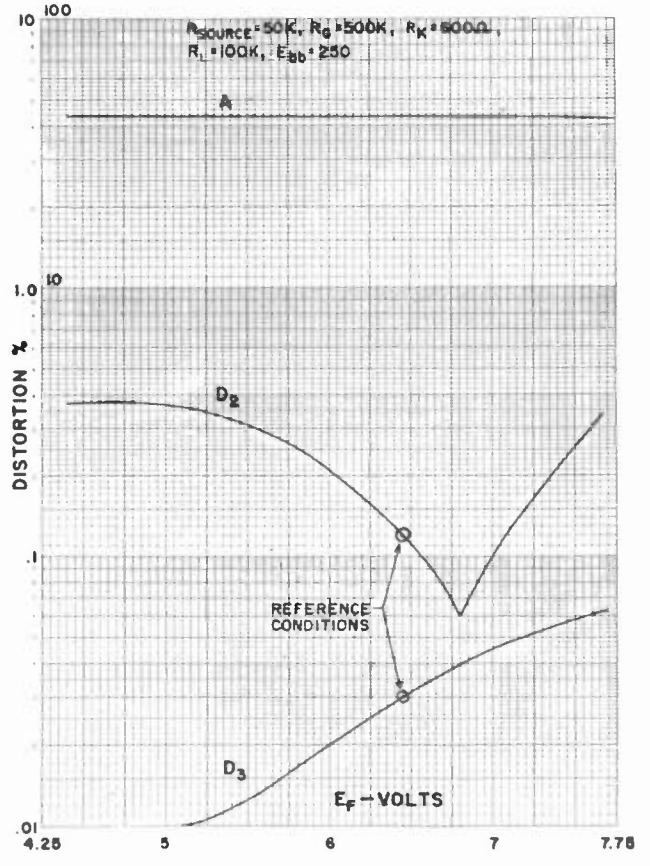

Fig. 12—Gain and distortion variation for ΔE_{FIL} schematic per Fig. 1 with 12AT7. $R_{source}=50K$, $R_G=500K$, $R_K=600\Omega$, $R_L=100K$, $E_{bb}=250$.

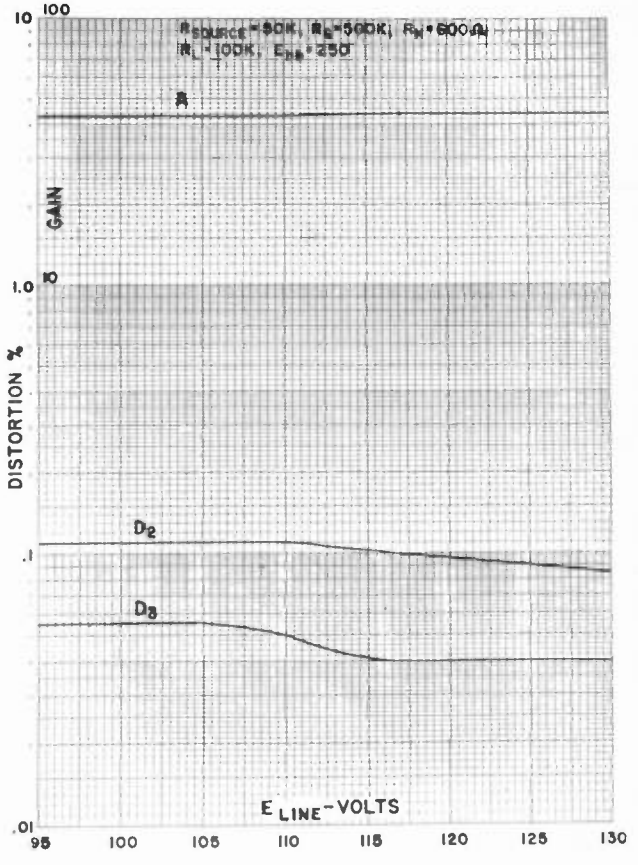

Fig. 13—Gain and distortion variation for ΔE_{line} schematic per Fig. 1 with 12AT7. $R_{source}=50K$, $R_G=500K$, $R_K=600\Omega$, $R_L=100K$, $E_{bb}=250$.

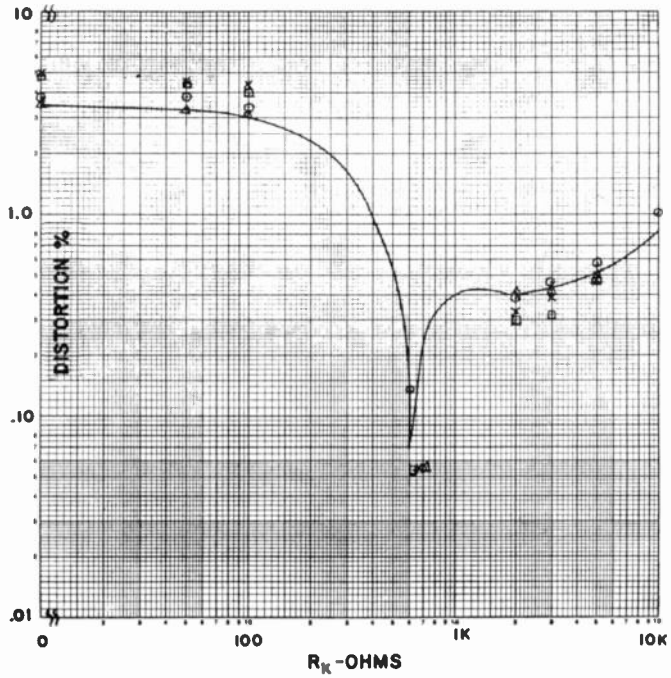

Fig. 14—Second harmonic distortion variation for five randomly-selected 12AT7 in schematic per Fig. 1. $R_{source}=50K$, $R_G=500K$, $R_L=50K$, $E_{bb}=250$.

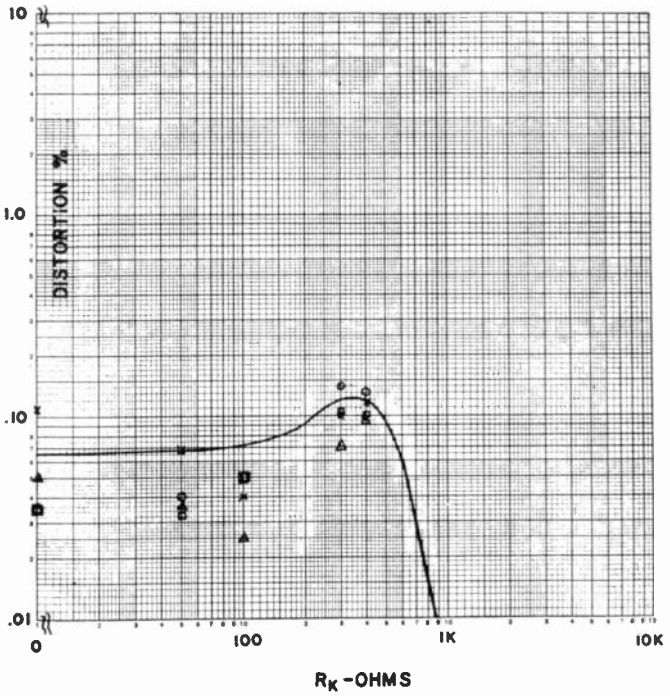

Fig. 15—Third harmonic distortion variation for five randomly-selected 12AT7 in schematic per Fig. 1. $R_{source}=50K$, $R_G=500K$, $R_L=50K$, $E_{bb}=250$.

TABLE II

Tube	e_K	e_G	R_K	D_2	D_3	Gain	Available Local FB-db
12AT7							
#1	1.00	0.04	600	0.135	0.045	43.4	2.55
#2	1.02	0.04	600	0.07	0.045	38.5	2.15
#3	1.18	0.03	720	0.055	0.04	40.9	3.00
#4	1.10	0.02	670	0.055	0.04	42.5	3.20
#4	1.05	0.02	640	0.05	0.04	39.1	2.67
12AU7							
#1	0.94	0.04	460	0.065	0.23	17.0	0.68
#2	0.69	0.03	330	0.065	0.13	17.8	0.58
#3	0.85	0.03	420	0.060	0.20	16.9	0.68
#4	0.98	0.04	490	0.065	0.19	17.6	0.91
#5	0.83	0.04	404	0.065	0.19	16.6	0.68
12AX7							
#1	1.20	0.008	1000	0.06	0.02	53.5	5.00
#2	1.10	0.03	740	0.05	0.022	53.5	3.41
#3	1.12	0.03	1000	0.055	0.035	54.0	5.00
#4	0.86	0.02	1000	0.05	0.02	52.9	4.15
#5	1.12	0.02	1100	0.05	0.015	57.0	5.32
12AY7							
#1	0.93	0.01	590	0.035	0.025	34.4	1.72
#2	1.05	0.01	635	0.05	0.025	32.2	1.86
#3	1.00	0.015	650	0.045	0.030	35.1	1.86
#4	0.95	0.015	400	0.030	0.035	34.4	1.66
#5	0.98	0.005	550	0.030	0.030	34.4	1.66

third harmonic distortion for output levels of 1v, 2v, and 3v, with R_K again as independent variable. Prediction of distortion change with level can very conveniently be made from the Taylor series expansion of plate current evaluated at operating point. For single-ended operation well below clipping level we may have:

$$i = I_{c0} + ae_g + be_g^2\, ce_g^3 + \cdots$$

assuming $e_g = E_{gm} \sin wt$

$$\begin{aligned} i &= I_{c0} + AE_{gm} \sin wt + bE_{gm}^2 \sin^2 wt \\ &\quad + CE_{gm}^3 \sin^3 wt + \cdots \\ &= I_{c0} + AE_{gm} \sin wt + \frac{bE_{gm}}{2}(1 - \cos 2wt) \\ &\quad + C\frac{E_{gm}^3}{4}(3 \sin wt - \sin 3wt) + \cdots \\ &= \left(I_{c0} + \frac{bE_{gm}^2}{2}\right) + \left(aE_{gm} + \frac{3cE_{gm}^3}{4}\right) \sin wt \\ &\quad - \left(\frac{bE_{gm}}{2}\right) \cos 2wt - \left(\frac{cE_{gm}^3}{4}\right) \sin 3wt + \cdots . \end{aligned}$$

With small signals this is in general a rapidly convergent series; to a first approximation, since $a \gg c$

$$D_2 = \frac{\frac{b}{2}E_{gm}^2}{aE_{gm}} = \left(\frac{b}{2a}\right) E_{gm}$$

$$D_3 = \frac{\frac{c}{4}E_{gm}^3}{AE_{gm}} = \left(\frac{c}{4a}\right) E_{gm}^2$$

i.e.,

$$D_2 \alpha E_{gm} \alpha E_{pm}$$

$$D_3 \alpha E_{gm}^2 \alpha E_{pm}^2$$

and except in the immediate vicinity of the distortion null, there is rather good agreement with the measured values of Figs. 22 and 23.

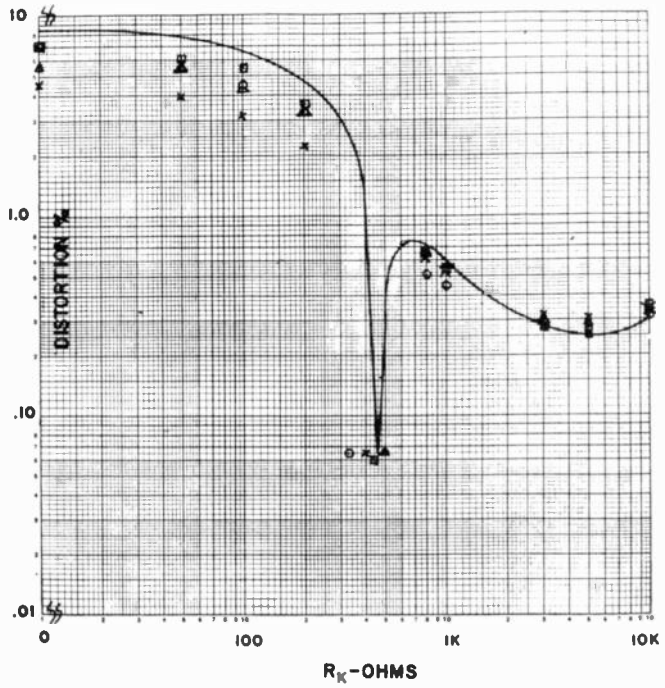

Fig. 16—Second harmonic distortion variation for five randomly-selected 12AU7 in schematic per Fig. 1. $R_{source}=50K$, $R_G=500K$, $R_L=50K$, $E_{bb}=250$.

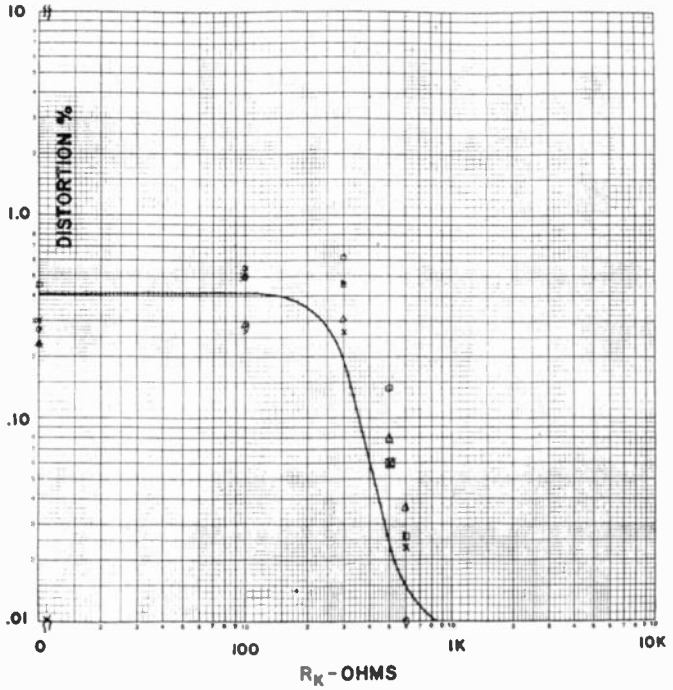

Fig. 17—Third harmonic distortion variation for five randomly-selected 12AU7 in schematic per Fig. 1. $R_{source}=50K$, $R_G=500K$, $R_L=50K$, $E_{bb}=250$.

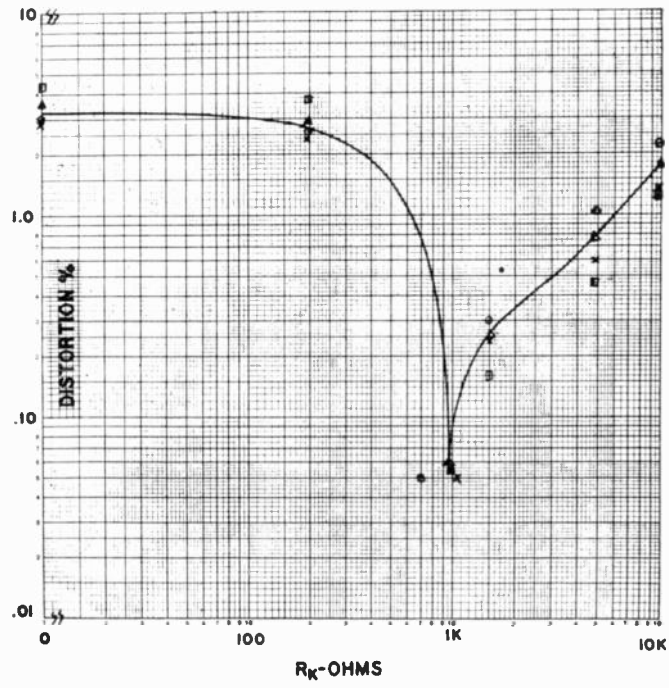

Fig. 18—Second harmonic distortion variation for five randomly-selected 12AX7 in schematic per Fig. 1. $R_{source}=50K$, $R_G=500K$, $R_L=50K$, $E_{bb}=250$.

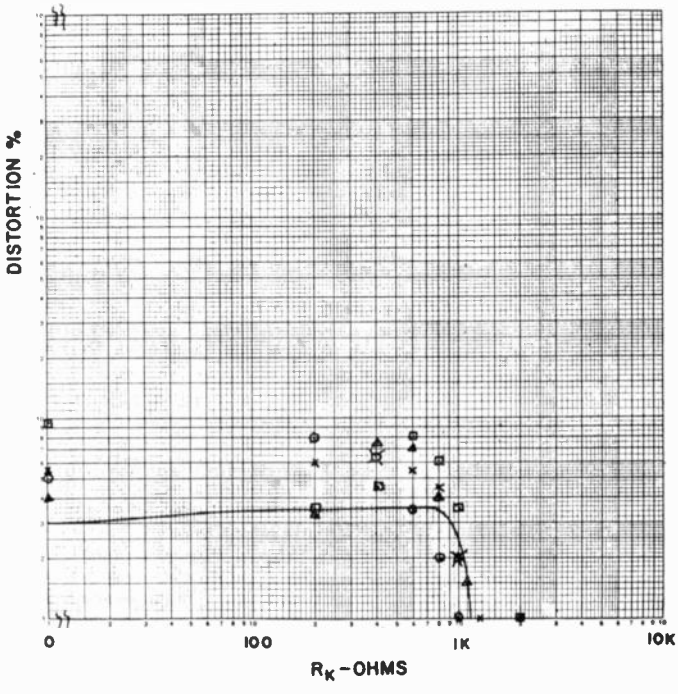

Fig. 19—Third harmonic distortion for five randomly-selected 12AX7 in schematic of figure. $R_{source}=50K$, $R_g=500K$, $R_L=50K$, $E_{bb}=250$.

Source impedance and nonlinear dynamic grid resistance are shown to be available parameters for the reduction of even harmonic distortion in low-level single-ended stages. The sharpness of the second harmonic null, demonstrated with a stage using a bypassed cathode, broadens considerably when moderate amounts of available local feedback are used. The null broadening is such that, with commercial grade components and commercial grade tubes burned-in past the 100-hour mark,[1] or with the more closely controlled premium variety tubes, the possibility for successful commercial use of this technique seems good.

[1] C. D. O'Neill, "The effects of grid contact potential and initial electron velocity on electron tube characteristics," *Sylvania Tech.*, p. 11; October, 1948.

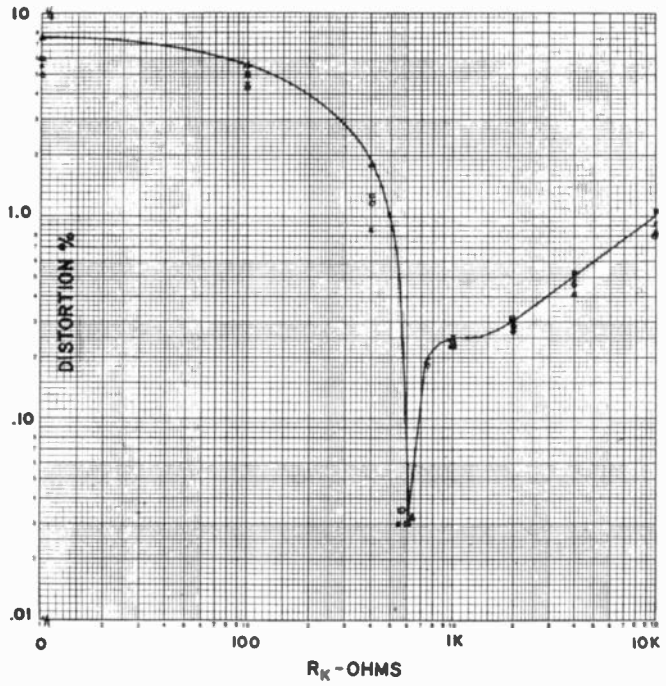

Fig. 20—Second harmonic distortion variation for five randomly-selected 12AY7 in schematic per Fig. 1. $R_{source}=50K$, $R_G=500K$, $R_L=50K$, $E_{bb}=250$.

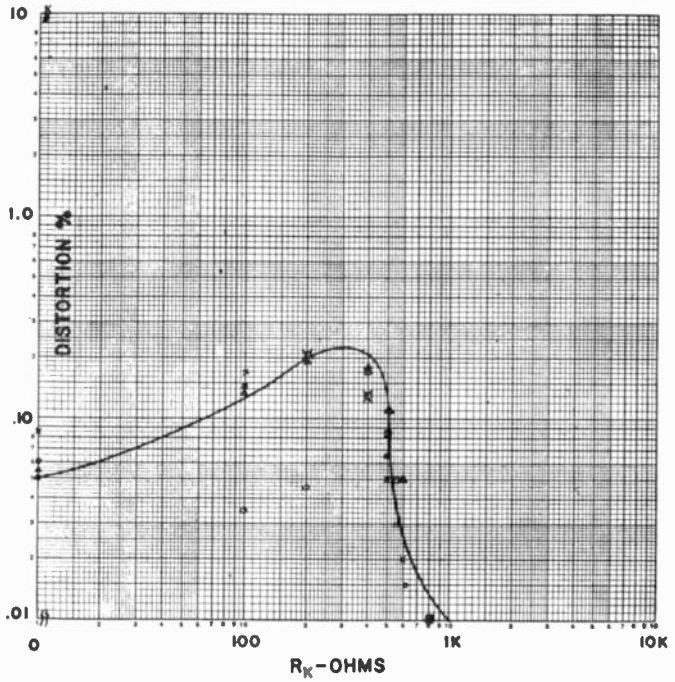

Fig. 21—Third harmonic distortion variation for randomly-selected 12AY7 in schematic per Fig. 1. $R_{source}=50K$, $R_G=500K$, $R_L=50K$, $E_{bb}=250$.

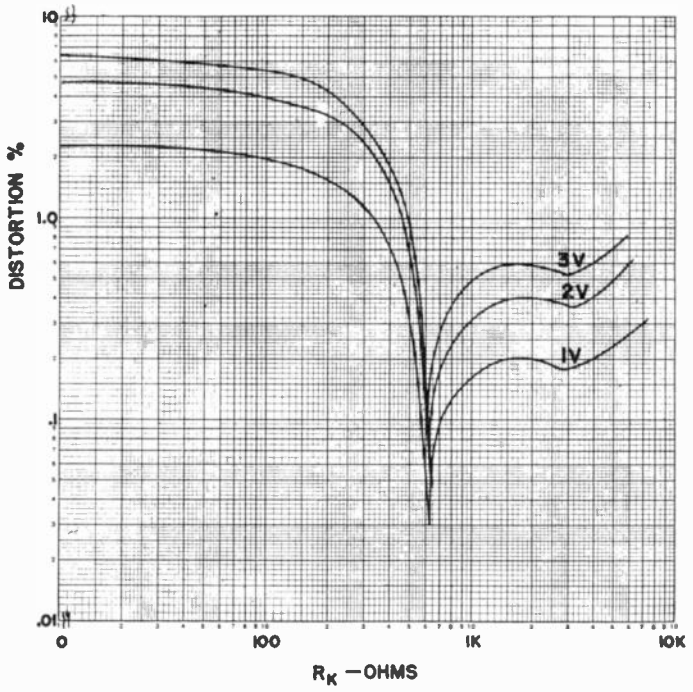

Fig. 22—Second harmonic distortion variation with signal level. Schematic per Fig. 1 with 12AT7. $R_{source}=50K$, $R_g=500K$, $R_L=100K$, $E_{bb}=250$.

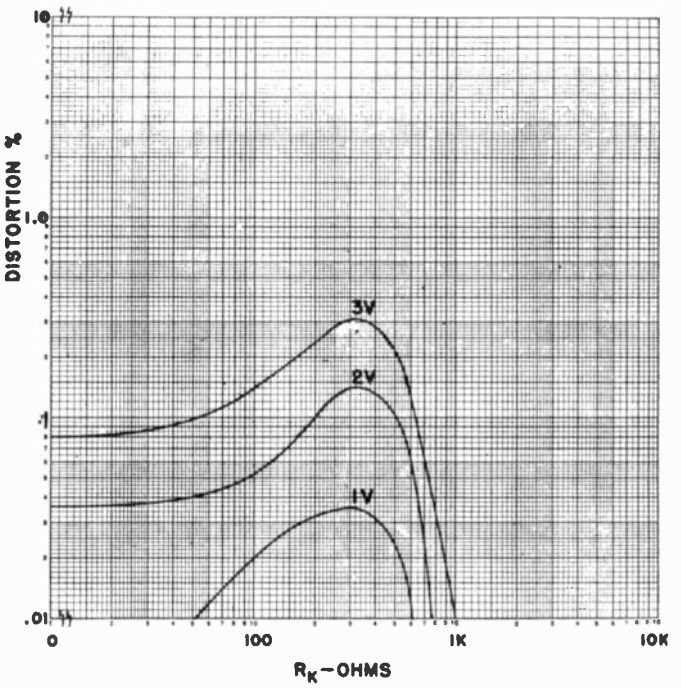

Fig. 23—Third harmonic distortion variation with signal level. Schematic per Fig. 1 with 12AT7. $R_{source}=50K$, $R_g=500K$, $R_L=100K$, $E_{bb}=250$.

Contributors

J. R. Macdonald (S'44–A'48–SM'54) was born in Savannah, Ga., on February 27, 1923. He received a B.A. degree in physics from Williams College and a S.B. degree in electrical engineering from M.I.T. in 1944. After a semester of teaching at the M.I.T. Army-Navy Technical Radar School, he was commissioned an ensign in the U. S. Naval Reserve in 1944. Upon completing radar courses at the Harvard and M.I.T. radar schools, he served as a technical radar officer. On release to inactive duty in 1946, he returned to M.I.T. and received the S.M. degree in electrical engineering in 1947. After a year's further graduate study in the M.I.T. Physics Department, he was awarded a Rhodes Scholarship for study at Oxford University. Dr. Macdonald received a D.Phil. degree in physics from Oxford in 1950 for theoretical and experimental work on ferromagnetic phenomena.

J. R. Macdonald

In 1950, Dr. Macdonald joined the Physics Department of the Armour Research Foundation and there carried out and directed work in theoretical and experimental physics until 1952. He then spent a year's leave of absence at the Argonne National Laboratory of the A.E.C. working on solid-state physics problems. He is presently Director of Solid State Physics Research at Texas Instruments Incorporated, Dallas, Texas. In addition, he also is serving as Clinical Associate Professor of Medical Electronics at Southwestern Medical School of the University of Texas in Dallas.

Dr. Macdonald is a member of Phi Beta Kappa, Sigma Xi and is a Fellow of the American Physical Society.

❖

R. J. Kircher (A'30–M'40–SM'43) was born in El Paso, Texas, on November 2, 1907. He received a B.S. degree in 1929 from California Institute of Technology and an M.S. degree from Stevens Institute of Technology in 1941.

R. J. Kircher

He joined Bell Telephone Laboratories in 1929, participating in the development of transoceanic radio transmitters and receivers, and multi-channel radio transmitter development. During the war he was engaged in radar and counter measures development work. In 1944 he transferred from radio research to electronic apparatus development, working on high frequency and ultra-high frequency power vacuum tubes. For four years he was associated with advanced development of transistor devices, and in 1952 joined a group working on transistor network development.

Mr. Kircher is a member of the New York Microscopical Society and Tau Beta Pi.

❖

J. Z. Knapp (S'49–A'50) was born on June 13, 1919, in New York, N. Y. He received the B.E.E. degree from the City College of the City of New York and the M.E.E. degree from New York University. During World War II he served as a communication officer with the rank of Major.

J. Z. Knapp

After the war he joined White Industries, Inc., as project engineer and assistant to the president. Since April, 1953 he has been associated with United Transformer Co. as development and audio application engineer.

INSTITUTIONAL LISTINGS (Continued)

ALLIED RADIO, 833 West Jackson Blvd., Chicago 7, Illinois
Everything in Radio, Television, and Industrial Electronics

ALTEC LANSING CORPORATION, 9356 Santa Monica Blvd., Beverly Hills, California
Microphones, Speakers, Amplifiers, Transformers, Speech Input

AMPEX CORPORATION, 934 Charter Street, Redwood City, California
Magnetic Tape Recorders for Audio and Test Data

AMPLIFIER CORPORATION OF AMERICA, 398 Broadway, New York 13, New York
Manufacturers of Magnetic Tape Recorders and Manufacturing Engineers

AUDIOPHILE RECORDS, Saukville, Wisconsin
High Quality Disc Recordings for Wide Range Equipment

BALLANTINE LABORATORIES, INC., Fanny Road, Boonton, New Jersey
Electronic Voltmeters, Decade Amplifiers, Voltage Calibrators, Multipliers, Shunts

CINEMA ENGINEERING CO., Division Aerovox Corp., 1100 Chestnut St., Burbank, California
Equalizers, Attenuators, Communication Equipment

THE DAVEN COMPANY, 191 Central Avenue, Newark 4, New Jersey
Attenuators, Potentiometers, Resistors, Rotary Switches, Test Equipment

Charge for listing in six consecutive issues of the TRANSACTIONS—$25.00. Application for listing may be made to the Chairman of the IRE-PGA Ways and Means Committee, Michel Copel, 156 Olive St., Huntington, Long Island, New York.

INSTITUTIONAL LISTINGS

The IRE Professional Group on Audio is grateful for the assistance given by the firms listed below, and invites application for Institutional Listing from other firms interested in Audio Technology.

ELECTRO-VOICE, INC., Buchanan, Michigan
Microphones, Pickups, Speakers, Television Boosters, Acoustic Devices

GENERAL CERAMICS CORPORATION, Keasbey, New Jersey
Technical Ceramics—Steatites and Aluminum, Ferramics, Solderseals

JENSEN MANUFACTURING COMPANY, 6601 South Laramie Avenue, Chicago 38, Illinois
Loudspeakers, Reproducer Systems, Enclosures

KLIPSCH AND ASSOCIATES, Box 64, Hope, Arkansas
Wide Range Corner Horn Loudspeaker Systems, Corner Horns

JAMES B. LANSING SOUND, INC., 2439 Fletcher Drive, Los Angeles 39, California
Loudspeakers and Transducers of All Types

MAGNECORD, INC., 360 North Michigan Avenue, Chicago 1, Illinois
Special & Professional Magnetic Tape Recording Equipment

PERMOFLUX CORPORATION, 4900 West Grand Avenue, Chicago 39, Illinois
Loudspeakers, Headphones, Cee-Cors (Hipersil Transformer Cores)

SHURE BROTHERS, INC., 225 West Huron Street, Chicago 10, Illinois
Microphones, Pickups, Recording Heads, Acoustic Devices

THE TURNER COMPANY, Cedar Rapids, Iowa
Microphones, Television Boosters, Acoustic Devices

UNITED TRANSFORMER COMPANY, 150 Varick Street, New York, New York
Transformers, Filters and Reactors

UNIVERSITY LOUDSPEAKERS, INC., 80 South Kenisco Avenue, White Plains, New York
Manufacturers of Public Address and High Fidelity Loudspeakers

(Please see inside back cover for additional listings.)